

Developing pre-industrial baselines from floodplain lake sediment cores
to quantify the extent of metals pollution within the Alberta Oil Sands
Region

by

Wynona Klemt

A thesis
presented to the University of Waterloo
in fulfillment of the
thesis requirement for the degree of
Master of Science
in
Biology (Water)

Waterloo, Ontario, Canada, 2018

© Wynona Hermine Klemt 2018

Author's Declaration

I hereby declare that I am the sole author of this thesis. This is a true copy of the thesis, including any required final revisions, as accepted by my examiners.

I understand that my thesis may be made electronically available to the public.

Abstract

Oil sands mining operations began in 1967, but the onset of a monitoring program to assess water and sediment quality in the Athabasca River watershed began 30 years later. Consequently, no knowledge of pre-industrial, baseline conditions exists upon which current river sediment quality can be compared. This has undermined an ability to determine the relative importance of contaminants supplied by natural processes versus pollution to the Athabasca River by rapid growth of oil sands development. In this study, a paleolimnological approach was used to analyze sediment cores from five flood-influenced lakes located upstream and downstream of oil sands operations within the Alberta Oil Sands Region (AOSR). Loss-on-ignition and organic carbon and nitrogen elemental analyses were used to differentiate periods of strong and weak Athabasca River flood influence. In addition, the temporal changes in concentrations of bitumen-associated metals vanadium (V) and nickel (Ni) were explored at each lake. A pre-industrial baseline was developed using pre-1967 sediment concentrations of V and Ni, normalized to aluminum concentration, from lakes in the AOSR to estimate the natural range of variability of these metals. When normalized metals concentrations in recently deposited flood-influenced sediment were compared to the pre-industrial baseline, no evidence of enrichment in the river-derived stratigraphic intervals was detected. However, significant enrichment of bitumen-related metals V and Ni (up to 2- and 1.6-fold above the baseline, respectively) was observed in weakly flood-influenced sediment in the two floodplain lakes located closest to the most active mining operations (< 10 km), indicating local atmospheric pollution. Athabasca River sediment data collected by regional monitoring programs RAMP (1997-2002) and JOSM (2012-2014) were examined in the context of the newly developed baselines and showed enrichment of V (1.2-1.7x baseline) and Ni (1.2-2.0x baseline) at some of the river monitoring sites, usually proximal to tributary outflows. This research indicates that sediment profiles from floodplain lakes along the lower Athabasca provide valuable information as pre-industrial depositional areas of natural sediment metals. Paleohydrological analyses, however, indicate that flood-influence at many of these lakes is declining, coincident with oil sands growth, and so many of the lakes no longer frequently capture flood sediments. Nonetheless, metal-specific baselines using the pre-1967 data can be used to detect enrichment in modern sediments of the floodplain lakes and in river sediment monitoring data, the latter previously criticized for inadequate baseline knowledge, and which also now serves as a foundation for ongoing river sediment monitoring.

Acknowledgements

This process has been a whirlwind and I am truly so thankful to everyone who has made such a positive impact on my life while completing this degree. So many wonderful people helped me over the past two years and I am very glad I kept a running list of everyone as this progressed. I could not believe how many people ended up on that list at the end, which is a testament to the fact that producing this document was most certainly not a solitary task.

I would like to first and foremost thank my supervisors Dr. Roland Hall and Dr. Brent Wolfe for their wonderful support and guidance throughout this process. Your invaluable expertise in paleolimnology and hydrology guided me throughout this project. As supervisors you have both been incredibly supportive and understanding. You always endeavour to give your students amazing opportunities and I am so grateful for every experience I have had in this lab. (Shout-out to Dr. Bronwyn Hancock at Yukon College for guiding me to this lab group in the first place!). I would like to acknowledge that funding for this project came from an NSERC Discovery grant to Dr. Hall. Field work was made possible through Northern Scientific Training Program funding that I received, as well as funding to Dr. Hall and Dr. Wolfe from the Polar Continental Shelf Program.

Many thanks to my committee members Dr. Heidi Swanson and Dr. Rebecca Rooney. You both have given me valuable feedback, guidance, and advice throughout this whole process. I learned a lot from you both and I am grateful to have had you both on my committee. As well, your stats course was a highlight of my graduate degree.

Thank you so much to Dr. Johan Wiklund for teaching me lab skills, providing much needed advice and counsel, and of course for running the gamma spec! I am eternally grateful for your desire to help and for your patience in explaining complicated concepts.

I am also indebted to so many people outside the university who greatly helped me progress this project. First, thanks to Dr. Colin Cooke at Alberta Environment and Parks for providing me with your sediment core data. Your willing correspondence and helpfulness allowed me to incorporate new data and analyses into my project for which I am extremely grateful. Thanks as well to Dr. Jane Kirk and Dr. Yamini Gopalapillai at Environment and Climate Change Canada for meeting with me and providing guidance. Big thanks to Dr. Joseph Culp (ECCC / Wilfrid

Laurier University) for providing me with sediment data and methods information that I was unable to retrieve on my own. Lastly, thank you to Dr. Kelly Munkittrick at Wilfrid Laurier University for meeting with me, and giving me valuable insight into the “behind the scenes” of oil sands intrigue.

Huge hugs and thanks to my lab mentors, friends, and confidants: Casey Remmer and James Telford. Casey - you have always been there to support, listen, and encourage. From co-organizing Women in Science events to embarking on fun adventures, I cannot imagine grad school without you. James - you helped me learn and apply so many new lab techniques, often taking time out of your own work to explain things. Your patience and ability to make everything fun made long hours in the lab significantly better. To the rest of my friends in the Hall Lab/Wolfe Pack: Mitch Kay, Jelle Faber, Eva Mehler, Tanner Owca, and Laura Neary – you not only helped me in the lab and in the field, but you also made me laugh until I cried and that is just as important. I am really going to miss being a part of this lab group. Big thanks to all the undergraduate students to whom I am indebted and without whom I would probably still be doing lab work: u/g thesis students Ashley Grant and Rebecca Osborne who did outstanding work during their 499s, and lab volunteers Mia Stratton, Emily Lau, and Josh Deane.

Thanks to all the friends I made in the Waterloo Biology department in the past two years. You’re a lovely, open, and welcoming group of peers and I am so grateful this is where I ended up. Thanks as well to my wonderful cohort in the Collaborative Water Program, and my fellow coordinators in SWIGS – Amy D., Amy Y., Erin, Fred, and Steph – you were such a fun and enthusiastic group and I’m very happy the CWP brought us all together.

Thank you to my environmental science BFFs and roommates Rachel Henderson and Steph Slowinski. You have been with me through thick and thin and I can’t imagine how this process would have gone if I hadn’t met you both 7 years ago. Thank you to Kate Hamilton, Vera Kazakova, Simon Baer, and Linda Fan for being amazing friends and supportive when I needed distractions and time away, and to Cody Shirriff – I do not have enough words to describe how sane you have kept me in this whole endeavour.

Finally, the biggest thanks go to my Mum and Gabrielle. You are my loudest cheerleaders and best support system and I could not have gotten to this point without your continuous and unconditional love and support.

Dedication

This thesis is dedicated to my father, Christian Klemt. I always strive to be as strong, intelligent, creative, and loving as you were. Although you have not been here to see most of my academic achievements, I know you have been with me through every milestone, including this one.

Table of Contents

Author’s Declaration.....	ii
Abstract.....	iii
Acknowledgements.....	iv
Dedication.....	vi
Table of Contents.....	vii
List of Figures.....	ix
List of Tables.....	xi
Chapter 1 – Introduction.....	1
1.1 Background.....	1
1.2 Environmental monitoring in the Alberta oil sands region.....	2
1.3 River sediment quality monitoring.....	6
1.4 Paleolimnological applications in assessing pollution.....	8
1.5 Paleolimnology in the AOSR.....	9
1.6 Paleolimnology in floodplains.....	10
1.7 Metals of concern.....	13
1.8 Study Objectives.....	15
Chapter 2 – Methods.....	18
2.1 Site descriptions: Alberta oil sands region.....	18
2.2 Field methods.....	24
2.2.1 Sediment core collection.....	24
2.2.2 RAMP & JOSM Athabasca River sediment collection.....	24
2.2.3 Additional Athabasca River sediment collection.....	26
2.2.4 JOSM sediment core collection.....	26
2.3 Sediment core analyses (Physical and geochemical proxies).....	27
2.3.1 Loss-on-ignition.....	27
2.3.2 Organic carbon and nitrogen elemental and isotope analysis.....	28
2.3.3 Sediment metals concentrations.....	29
2.3.4 Sediment core chronologies.....	31
2.4 Data analysis (numerical & statistical).....	32
Chapter 3 – Results and Interpretation.....	36

3.1 Sediment core chronologies & paleohydrology	36
3.2 Temporal trends in sediment composition and inferred paleohydrology	41
3.3 Temporal variations in metals concentrations	42
3.4 Developing a regional pre-industrial baseline	46
3.5 Assessment for V and Ni pollution	51
3.6 Evaluation regional river sediment monitoring data for evidence of pollution	56
3.7 Enrichment factor and excess flux analyses	58
Chapter 4 – Discussion	64
4.1 Use of floodplain lake sediment cores to develop baseline metal concentrations	64
4.2 Evaluating the extent of pollution to the Athabasca River	70
4.3 Atmospheric signals of pollution at floodplain lakes	74
4.4 EF development for establishing a foundation for ongoing monitoring	76
Chapter 5 – Conclusions, Implications and Recommendations	78
5.1 Summary of findings	78
5.2 Research significance and implications	79
5.3 Future recommendations	81
References	85
Appendix A: Study site information	96
Appendix B: Compiled loss-on-ignition & organic carbon and nitrogen elemental and isotope composition data and graphs	100
Appendix C: Compiled metals data	115
Appendix D: Chronology information (for developing age-depth models)	127
Appendix E: Statistical analyses	132

List of Figures

- Figure 1. Site map of the Athabasca oil sands region with floodplain study lakes Up 17, Up 10, Down 1, Down 26, and Down 58, as well as select JOSM monitoring lakes NE 13, NE20, and RAMP 418/Kearle. The oil sands land cover as of 2014 (source: RAMP) is outlined in orange, and waterbodies are blue. The blue star denotes location of AR6.....21
- Figure 2. Photographs of the floodplain study lakes taken in October 2016 (Up 17, Down 1, Down 26, Down 58) and in July 2017 (Up 10). The pink diamond indicates the approximate coring location at each of the floodplain lakes22
- Figure 3. Site map of the RAMP and JOSM sediment monitoring locations in the Athabasca oil sands region. RAMP sites begin with the signifier ATR (for Athabasca River) and the JOSM sites begin with the signifier M (for Mainstem) (see Table A3). JOSM suspended sediment sites are indicated by SS after the site name. Site M0 is not shown as it is > 50 km kilometers upstream of Fort McMurray. The oil sands land cover as of 2014 is outlined in orange (source: RAMP), and waterbodies are blue23
- Figure 4. Activities profiles of radioisotopes ^{210}Pb (black circles), ^{137}Cs (open circles), and ^{226}Ra (dark grey circles) in Bq/kg for sediment cores from lakes Up 17, Up 10, Down 1, and Down 26. The age-depth relationship is also plotted for each graph, with extrapolation using the CRS model (light grey circles) and the ^{137}Cs peak indicated by a yellow star. Sedimentation rate is presented in the right panels. Error bars represent 1 standard deviation. Note: low ^{210}Pb values at Down 26 prevented the calculation of varying sedimentation rate ($0.1666 \text{ g cm}^{-2} \text{ year}^{-1}$).....40
- Figure 5. Stratigraphic profiles of organic matter (black circles), mineral matter (white circles), and organic carbon (dark grey circles) content in sediment cores from lakes Up 17, Up 10, Down 1, Down 26, and Down 58. Lakes are arranged in sequence from upstream to downstream. Shaded areas represent strongly flood-influenced sediment intervals44
- Figure 6. Stratigraphic profiles of concentrations (ug/g) of metals aluminum (Al), vanadium (V), and nickel (Ni) in sediment cores from the study lakes, with lakes arranged from upstream to downstream. Shaded areas are interpreted to represent intervals of stronger flood-influence45
- Figure 7. Crossplots showing the relations between sedimentary concentrations of Al and V (left column, A & C) and Al and Ni (right column, B & D) in pre-1967 floodplain lake sediment from lakes Up 17 (light blue), Up 10 (green), Down 1 (dark blue), Down 26 (purple), with the open circles denoting less-flood-influenced sediment from Down 1. Pre-1967 headwater lake sediment from lakes NE13 (dark red), NE20 (orange), and RAMP418/ Kearle (yellow) were added to the floodplain lake data (C: V/Al, D: Ni/Al). The linear regression line (black line) and the 95% prediction intervals (red) are based on pre-1967 sediments from all the lakes listed.....50

Figure 8. Crossplots assessing Al-normalized V concentrations in sediments deposited in the study lakes since 1967-onset of oil sands development (circles) relative to the pre-industrial baseline (black line) and 95% prediction intervals (red lines). Closed circles: flood-influenced sediment intervals; Open circles: less-flood-influenced sediment intervals. Error bars are from the mean % precision of V calculated from ALS-analyzed duplicate lake sediment samples 200 km downstream (Wiklund et al., 2014)53

Figure 9. Map of the AOSR mining region showing locations of the study floodplain lakes Up 17, Up 10, Down 1, Down 26, and Down 58, superimposed on a vanadium net loading map to the snowpack in winter of 2012 (adapted from Figure S6: Kirk et al., 2014)54

Figure 10. Crossplots assessing Al-normalized Ni concentrations in sediments deposited in the study lakes since 1967-onset of oil sands development (circles) relative to the pre-industrial baseline (black line) and 95% prediction intervals (red lines). Closed circles: flood-influenced sediment intervals; Open circles: less-flood-influenced sediment intervals. Error bars are from the mean % precision of Ni calculated from ALS-analyzed duplicate lake sediment samples 200 km downstream (Wiklund et al., 2014)55

Figure 11. Scatterplot of post-1967 Athabasca River sediment vanadium (A) and nickel (B) concentrations versus aluminum concentrations in the Athabasca River sediment samples collected by the Regional Aquatics Monitoring Program (RAMP) and the Joint Oil Sands Monitoring Program (JOSM). Exposed river-bottom sediment and a flood deposit sample collected during this study (2016, 2017) are also shown. Samples are plotted relative to the V/Al and Ni/Al linear regressions (black line) and 95% prediction intervals (red lines) from Figure 757

Figure 12. Enrichment factors for V and Ni at lakes Up 17 (pink), Up 10 (green), Down 1 (red), and Down 26 (purple) in the two left-hand panels. In the right-hand panels, enrichment factors for Athabasca River-bottom sediment monitoring data from RAMP (dark green circles) and JOSM (purple triangles) are plotted beside JOSM suspended sediment data (grey squares), exposed river-bottom samples collected during this study (light green triangles), and a flood deposit sample (light blue triangle). The dashed line at an EF = 1 represents the baseline, and the grey dashed-and-dotted line above it represents the upper 95% prediction interval EF. A dotted line at 1967 represents the start of AOSR development62

Figure 13. Adjusted excess flux (ΔF_{adj}) of V (plot A) for lakes Up 10 (green) and Down 1 (red) and Ni (plot B) for lakes Up 17 (pink) and Down 1 (red), from 1960-2017. The solid line connects intervals that are enriched above the upper 95% P.I. on the V/Al baseline. The dashed line represents points that do not display enrichment above the baseline63

List of Tables

Table 1. Lake and sediment core information for Athabasca River floodplain lakes located upstream (Up 17, Up 10) and downstream (Down 1, Down 26, Down 58) of central oil sands operations (AR6) in Alberta, Canada. (*) denotes the core chosen for analyses18

Table 2. Results of Mann-Kendall trend tests on the vanadium EF values from sediment cores from lakes Up 17, Up 10, Down 1, and Down 26. The symbols (*) = denotes stat. significance, $p < 0.05$; (+) = upwards trend; (-) = downwards trend60

Table 3. Results of Mann-Kendall trend tests on the nickel EF values from sediment cores from lakes Up 17, Up 10, Down 1, and Down 26. The symbols (*) = denotes stat. significance, $p < 0.05$; (+) = upwards trend; (-) = downwards trend60

Chapter 1 – Introduction

1.1 Background

The Alberta Oil Sands Region (AOSR) in northern Alberta, Canada, holds the third largest oil reserves in the world and is believed to contain 164 billion barrels of recoverable oil under an area of 142,000 km² in the Athabasca River, Peace River, and Cold Lake watersheds (CAPP, 2018a). Commercial production in the Alberta oil sands began in 1967 at the Great Canadian Oil Sands plant (Suncor Inc.) and produced 32,000 barrels/day (CAPP, 2018b). Today, production has grown to around 2.8 million barrels of oil per day and is mined via both surface (43%) and in situ (57%) extraction techniques (CAPP, 2018a). These mining activities have a large environmental footprint, covering around 1670 km² of land in northern Alberta, mostly within the Athabasca River basin (Rooney *et al.*, 2012).

Increased oil production in the region has led to concerns surrounding negative effects of mining operations to nearby lake, wetland, and river ecosystems, by processes such as the atmospheric release and deposition of contaminants, which include polycyclic aromatic hydrocarbons (PAHs; Kelly *et al.*, 2009, 2010; Kirk *et al.*, 2014; Manzano *et al.*, 2016) and metals of concern (Cooke *et al.*, 2017), nutrient delivery (Hazewinkel *et al.*, 2008; Summers *et al.*, 2016, 2017), acidification (Hazewinkel *et al.*, 2008; Curtis *et al.*, 2010), as well as land disturbance and peatland loss by expansion of the mining activities and related infrastructure (Timoney & Lee, 2009; Schindler, 2010; Rooney *et al.*, 2012). Studies that have evaluated atmospheric contaminant deposition in the AOSR have shown elevated deposition of PAHs and metals of concern to the landscape within a 50 km radius of the centre of Athabasca oil sands development at Syncrude's Mildred Lake mine (denoted as AR6 in Kelly *et al.*, 2009, 2010),

with the deposition footprint largely following the Athabasca River valley corridor (Kirk *et al.*, 2014). This has been demonstrated by several years of measurements made on snowpack investigating the amount of deposition that accumulates on the environment during the winter (Kelly *et al.*, 2010; Kirk *et al.*, 2014; Manzano *et al.*, 2016), and measurements made on lake sediment and peat core samples that capture the ice-free season when these contaminants are deposited directly on the waterbodies within the AOSR (Jautzy *et al.*, 2013; Kurek *et al.*, 2013; Cooke *et al.*, 2017; Shotyky *et al.*, 2016b; Zhang *et al.*, 2016). During spring snowmelt and rain events, contaminants are moved through the landscape and are eventually deposited in the Athabasca River as well as smaller water bodies and tributaries.

Concerns have been expressed about the effects of mining activities on human and ecosystem health in downstream environments along the Athabasca River (Timoney & Lee, 2009; Schindler, 2010). People in the downstream community of Fort Chipewyan, in the Peace-Athabasca Delta (PAD) - a Ramsar Wetland of International Importance and a UNESCO World Heritage Site - have reported higher than average rates of cancer in recent decades, as well as perceived increased incidence of deformed fish from the Athabasca River (Schindler, 2010; McLachlan, 2014). Clearly, there is a need for improved understanding of the influences of industry on the Athabasca River system.

1.2 Environmental monitoring in the Alberta oil sands region

Monitoring is a systematic process which involves the consistent, repeated observation of a system at set locations and at regular intervals over time to assess current conditions and evaluate trends (Chapman, 1991). Systematic monitoring of surface water and sediment in the AOSR for contaminants first began in 1997 with the incorporation of the industry-funded Regional Aquatics Monitoring Program (RAMP) (Cronmiller & Noble, 2018). This program

involved a multiple-stakeholder Technical Program Committee which included industry partners, local, provincial, and federal government groups, consultants (e.g., Hatfield), environmental groups (e.g., Cumulative Environmental Management Association (CEMA), Wood Buffalo Environmental Association (WBEA)), and First Nations communities along the lower Athabasca River (Cronmiller & Noble, 2018). Monitoring for RAMP included the collection of environmental data from the Athabasca River, its tributaries, the downstream delta, and some ecologically-important lakes and wetlands in the watershed. Environmental data included the collection of water, surface sediment, benthic invertebrates, fish, and climate and hydrologic measurements (Cronmiller & Noble, 2018). Unfortunately, the RAMP program was highly controversial, and criticized for inconsistent sampling and methodology, an inability to detect trends of pollution, and lack of accessibility to their data (Schindler, 2010). In his 2010 critique, Schindler highlighted the need to design a sampling program that can separate industrial from natural sources, while monitoring the various pathways of contaminant deposition. As well, seasonal changes must be addressed to account for increases in delivery of pollutants to aquatic systems from contaminated snow during the spring melt (Schindler, 2010).

Following these criticisms, an oil sands Expert Advisory Panel was established by the federal Minister of the Environment in 2010 to assess the state of monitoring and scientific research in the oil sands region and determine the strengths and weaknesses of the current environmental monitoring program. The Expert Panel identified key weaknesses including the lack of pre-industrial baseline data, lack of transparency, and sporadic and inconsistent sampling methodology, and provided recommendations on how to improve monitoring in the AOSR (Dowdeswell *et al.*, 2010). In 2012, the Joint Canada-Alberta Implementation Plan for Oil Sands Monitoring was developed to expand and improve current environmental monitoring programs

in the AOSR, including RAMP. As part of this implementation plan, the Joint Oil Sands Monitoring Program (JOSM) was initiated to characterize the state of the environment in the AOSR, assess cumulative effects to the watershed, and develop recommendations for an integrated environmental monitoring program (Cronmiller & Noble, 2018). Working with federal and provincial government groups, RAMP's environmental monitoring activities were fully transitioned to JOSM in 2012 (Cronmiller & Noble, 2018). JOSM continues to work closely with both governments, as well as with industry groups and local stakeholders, to improve communication and provide open and transparent collection and reporting of environmental data across the AOSR.

One of the key recommendations mentioned in reports such as the Oil Sands Advisory Panel Report to the Minister of the Environment (Dowdeswell *et al.*, 2010) and the Final Program Report by RAMP in support of JOSM (Hatfield Consultants, 2016) is the need for baseline data that underpins an ability of monitoring programs to quantify the extent of industrial pollution. The 2010 report states that “it is important to establish as rigorously as possible the background or baseline level of pollution, against which any future trends can be assessed” (Dowdeswell *et al.*, 2010, p.31). Since RAMP was initiated 30 years after oil sands development began in 1967, no pre-oil sands development environmental baseline exists upon which current river sediment and water quality monitoring data can be compared. Studies and environmental monitoring programs have attempted to address the lack of baseline in various ways. RAMP states on its website that it compared sediment and water quality measurements to “historical, pre-development, and regional baseline values”, but no details are provided to what those data are. Most recently in the Final Program Report (Hatfield Consultants, 2016), “baseline” for the Athabasca River was defined as any data collected from locations upstream of oil sands

development as of, or prior to, 2015. Pre-industrial baseline data are crucial to interpreting any environmental monitoring data collected, as increased industrial activity during 1997-2015 renders data from this period inappropriate for use as baseline. This situation is further confounded for the Athabasca River, because the river flows through the naturally bitumen-rich McMurray Formation (McMF) where riverbank erosion, groundwater mixing, natural runoff, and aerial transport provide natural inputs of contaminants to the Athabasca River and surrounding watershed (Headley & McMartin, 2004). To date, only a few studies have attempted to use the RAMP monitoring database to evaluate trends (Evans *et al.*, 2016), or to evaluate for evidence of downstream pollution (Wiklund *et al.*, 2014), in water and sediment data since monitoring of the Athabasca River and surrounding water bodies began. The inability to distinguish natural from industrial sources of heavy metals continues to undermine our ability to track industry-related change across the AOSR. This study aims to use paleolimnological techniques to generate pre-industrial baseline data on river sediment-metals concentrations and lend insight to the interpretation of Athabasca River-monitoring data. Paleolimnology, the study of physical, chemical, and biological information preserved in lake sediments over time, provides a scientific approach for reconstructing past changes in environmental conditions of lakes (Smol, 1992; Cohen, 2003; Smol, 2009). Analysis of lake sediments can aid in the evaluation of aquatic systems where little to no monitoring data are available, and in areas where levels of contaminants are naturally high, to develop knowledge of pre-industrial baseline conditions (Smol, 1992).

Given the short-term data records in the region, paleolimnological studies can provide means to evaluate long-term trends in contaminant deposition and accumulation in the AOSR. In fact, when developing the new water quality monitoring plan for JOSM in 2011, the report's

authors recognized the importance of paleoenvironmental analyses in the AOSR and stated that “careful paleolimnological sampling and analysis could provide essential information on natural background levels (baseline or reference conditions) of sediment and contaminants transported via the rivers and atmosphere, and to quantify trends over time since the onset of industrial activities” (Wrona & di Cenzo, 2011, p. 65). Previous studies have evaluated regional atmospheric trends in contaminant deposition from paleolimnological analyses conducted at small headwater lakes in the AOSR, but have yet to apply these techniques to river-influenced lakes to determine the extent of river pollution (Jautzy *et al.*, 2013; Kurek *et al.*, 2013; Cooke *et al.*, 2017).

1.3 *River sediment quality monitoring*

Monitoring of sediment quality in aquatic systems has been highlighted as one of the best ways to assess for evidence of aquatic pollution (Reuther, 2009). Sediment quality influences benthic communities and the chemistry of overlying waters (Peeters *et al.*, 2004). Thus, sediment quality is directly linked to the health of aquatic systems. Metals can be released to the environment in both particulate and dissolved form. In rivers, dissolved and particulate metals form complexes with sediment and organic matter in the water due to their low solubility, eventually being deposited in river-bottom sediment (Förstner & Müller, 1981; Reuther, 2009). Depositional areas along the river, such as slow-moving sections of the river or lakes that receive floodwaters, can accumulate the sediments carried by the river over time (Audry *et al.*, 2004). The method by which benthic and other aquatic organisms interact with heavy metals in sediments is highly dependant on interactions with sediment and organic matter, which ultimately affects the mobility and bioavailability of the metal (Barton & Wallace, 1979; Peeters *et al.*, 2004; Parsons *et al.*, 2010).

Sediment sampling as part of the RAMP/JOSM monitoring programs has generally focused on areas of deposition within the Athabasca River and its tributaries, where collected sediments consist mostly of sands, silts, and clays, as opposed to gravels and coarser-grained sediment. Sampling of the mainstem of the Athabasca River as a part of RAMP was discontinued in 2005, as it was not considered representative of a depositional environment where temporal changes could be evaluated (Hatfield Consultants, 2009). It was decided by the RAMP Technical Program Committee that efforts should instead be focused on further depositional reaches of the Athabasca Delta (Conly *et al.*, 2002; Hatfield Consultants, 2009). In 2006, RAMP began to collect river sediment samples primarily in conjunction with benthic invertebrate and fish monitoring data, and sampling locations were shifted to the lower end of 'depositional reaches' of the river (i.e., near the Embarras River tributary). In the development of the new water quality monitoring plan for JOSM, focus on sediment sampling in the Athabasca River was transitioned to suspended sediments, tied in with understanding hydraulic behaviour of the river and how that can play a role in the transport of contaminants (Wrona & di Cenzo, 2011). River-bottom sediment in depositional areas continues to be collected as a part of JOSM in conjunction with benthic invertebrate monitoring.

The Athabasca River floods most often in the spring, when water levels are highest and erosional events transport natural bitumen downstream (Conly *et al.*, 2002). As well, a large influx of contaminants to the river from polluted snowmelt occurs. Studies of particulate and dissolved metals and PAHs in the Athabasca River by Kelly *et al.* (2009, 2010) show highest dissolved concentrations in river water near, and immediately downstream of, oil sands development, which has been interpreted as a consequence of oil sands pollution. But, since metals and PAHs preferentially adsorb onto particles, measurements of particulate and sediment

metals concentrations are needed to improve assessment of river pollution. Recently, the new JOSM monitoring plan suggested paleolimnological sampling of floodplain lakes, back-eddy zones, and deltaic sediments as a method to target depositional areas for pre-industrial river sediment and contaminant levels (Wrona & di Cenzo, 2011).

1.4 *Paleolimnological applications in assessing pollution*

Many approaches have been developed to assess the anthropogenic contribution of metal accumulation in lacustrine systems using sediment cores. Most commonly used approaches include the calculation of an enrichment factor (EF), excess flux, also known as anthropogenic flux (ΔF), and/or a geoaccumulation index (I_{geo}) (e.g., Müller, 1969; Audry *et al.*, 2004; Balogh *et al.*, 2009; Boës *et al.*, 2011; Kurek *et al.*, 2013; Wiklund *et al.*, 2014; Wang *et al.*, 2015; Cooke *et al.*, 2017). An enrichment factor quantifies the ratio of the normalized concentration or flux of an element of interest in samples deposited since development relative to values before development (e.g., Audry *et al.*, 2004; Boës *et al.*, 2011), and has been used to assess enrichment above pre-industrial levels in the AOSR (Kurek *et al.*, 2013; Wiklund *et al.*, 2014; Cooke *et al.*, 2017). Flux measurements evaluate the product of elemental concentration to the sedimentation rate and have been applied to lake systems in the AOSR to evaluate anthropogenic excess flux of PAHs and metals (Kurek *et al.*, 2013; Cooke *et al.*, 2017). Measurements of flux are beneficial when evaluating flood-influenced systems as they account for the sedimentation rate. Other common methods that have not yet been applied to lakes in the AOSR include the geoaccumulation index (I_{geo}), which is a method of determining qualitatively the scale of pollution intensity to determine the degree of anthropogenic influence (e.g., Müller, 1969; Audry *et al.*, 2004; Wang *et al.*, 2015). I_{geo} values are calculated using pre- and post-contaminant concentrations and compared to the I_{geo} table, where a value of > 5 indicates the site is “very

strongly polluted” and a value < 0 is “unpolluted.” As well, some evaluations of anthropogenic metal enrichment in lakes have used stable isotopes of metals (i.e., Pb) to evaluate the anthropogenic enrichment factor, using a two-component isotope mixing model to differentiate sources of natural and atmospherically deposited metals (Boës *et al.*, 2011).

1.5 Paleolimnology in the AOSR

Paleolimnological assessments of spatial and temporal patterns of change in PAH and heavy metal deposition have been performed at several lakes within the AOSR (Hazewinkel *et al.*, 2008; Curtis *et al.*, 2010; Jautzy *et al.*, 2013; Kurek *et al.*, 2013; Summers *et al.*, 2016, 2017; Cooke *et al.*, 2017). These studies all focused on elevated, headwater lakes that do not flood by the Athabasca River and so were used to track changes in deposition via the atmosphere. A study by Kurek *et al.* (2013) showed increased deposition of PAHs via the air since the 1980s within the 50 km radius defined by the Kelly *et al.* studies (2009, 2010), coincident with increases in oil sands development. Analyses of the $\delta^{13}\text{C}$ signatures of PAHs in sediment cores from lakes within the 50 km radius have demonstrated a shift away from petroleum-derived PAHs to those associated with unprocessed bitumen, aiding our understanding of modern source pollution in the AOSR (Jautzy *et al.*, 2013). Analysis of temporal trends in airborne metal deposition to near-, mid-, and far-field lakes in the AOSR by Cooke *et al.* (2017) reported no metal enrichment beyond 50 km, and a recent decrease in V and Pb, attributed to improvements in mining technologies. This study combined data across lakes, using decadal periods to better analyze spatial differences across the landscape (Cooke *et al.*, 2017).

Paleolimnological studies that tackle multiple-stressors on lakes in the AOSR have been increasing in prevalence in recent years, due to the recognition that understanding additive effects of stressors is needed to determine effects on biological endpoints (Lima & Wrona,

2018). Using food-web bioindicator taxa, a study looked at the relative influences of atmospheric deposition and climate change trends in increased primary production, and demonstrated high vulnerability of these shallow, boreal lakes are to the combined effects of warming and industrial activities (Summers *et al.*, 2017). The research that has been conducted in the AOSR shows that paleolimnological studies have been quite successful in identifying large-scale anthropogenic influences, atmospheric pollution, ecological response to industrial activity and spatial patterns of deposition in the AOSR. These types of studies, however, have generally avoided using floodplain systems due to the added complications of riverine additions to interpreting the atmospheric signal. As well, because the sedimentation rate in these systems is variable, and there is very little organic matter present in the lakes, conventional radioisotope dating techniques can be difficult to apply and interpret, which is why multiple lines of evidence (i.e., ^{137}Cs and ^{210}Pb) are needed. Floodplain lakes, however, provide a unique opportunity to investigate temporal trends in Athabasca River sediment quality and potentially disentangle natural and anthropogenic sources of contaminants in the river. Indeed, a key research opportunity lies in the application of paleolimnology at flood-influenced lakes along the Athabasca River to address concerns over river pollution that is missing from the literature. There has been much speculation about what gets deposited in the Athabasca River, but there has yet to be a systematic study that incorporates baseline knowledge to identify the extent of industrial pollution of the river.

1.6 *Paleolimnology in floodplains*

Paleolimnological studies analyzing metals have successfully been conducted in river-influenced systems in northern Canada and around the world (e.g., Balogh *et al.*, 1999, 2009; Audry *et al.*, 2004; Brock *et al.*, 2010; Wiklund *et al.*, 2014; MacDonald *et al.*, 2016; Lintern *et*

al., 2016b; Ota *et al.*, 2017). Paleolimnological assessment of river-transported sediment deposits allows for time-trend analysis of metals and identification of concentrations elevated above pre-industrial background levels that may be attributable to river pollution. This approach has proven to be effective in assessing river pollution using sediment cores from floodplain lakes (e.g., Audry *et al.*, 2004; Wiklund *et al.*, 2014; MacDonald *et al.*, 2016), billabongs/oxbow lakes (e.g., Lintern *et al.*, 2016b), and reservoirs (e.g., Balogh *et al.*, 1999, 2009) in areas outside the AOSR. This approach was used downstream of the AOSR, in floodplain lakes in the Peace-Athabasca Delta at the terminus of the Athabasca River (Wiklund *et al.*, 2014). Pre-industrial baselines were developed from metals analyses of river-supplied sediments deposited before onset of industrial development. Surface sediments collected by RAMP from 2001-2013 were assessed for pollution relative to the baselines and no enrichment was detected (Wiklund *et al.*, 2014). Similar research in the Slave River Delta used sediment cores to analyze the various pathways and sources of heavy metals to a flood-influenced lake (MacDonald *et al.*, 2016). Researchers found an increase in arsenic concentration coinciding with the onset of gold processing at Giant Mine in Yellowknife, NWT, indicating that this technique can be useful in detecting airborne pollution from industrial sources when the paleohydrological conditions are taken into consideration.

Sedimentary environments of flood-influenced lakes are more complicated than those of isolated lakes because contaminants may be supplied by both river flood-waters and atmospheric pathways. River flood events influence the relative contributions of allochthonous (river-derived inorganic sediment, typically organic matter-poor and metal-enriched), and autochthonous (lake-derived sediment, typically organic matter-rich and metal-poor), sediment present in a floodplain lake at a given time. As well, it is more difficult to date cores accurately by ^{210}Pb methods, as

rapid deposition of river-borne sediments can depress ^{210}Pb activity in sediment core intervals and make it difficult to identify the depth at which background (or supported) ^{210}Pb activity is reached. A key component in analyzing flood-influenced systems is to distinguish river-derived / allochthonous sediment from lake-derived / autochthonous sediment to draw conclusions about what the river has contributed to the lake system. For example, Lintern *et al.* (2016a,b) studied a contaminated billabong (oxbow lake) in Australia and identified flood deposits by two methods. The first assessed changes in sediment characteristics within the core using four common characteristics of flood sediments: presence of laminations, high magnetic susceptibility, smaller particle size, and low occurrence of organic matter (Lintern *et al.*, 2016a). The second method is a calculation of Flood Signal Strength (FSS), which quantifies the likelihood that a sample is fluvial in origin using the number of flood-characteristics that are met as well as the magnitude of these properties: high magnetic susceptibility and inorganic matter, sediment particle size, and enrichment of elements more common in the catchment as opposed to local soils (Lintern *et al.*, 2016a). In assessing the hydrologic history of a flood-influenced lake in the Slave River Delta, NWT, Brock *et al.* (2010) used a combination of physical, geochemical, and biological proxies to assess flood periods by comparing measured values to the characteristics of a flood deposit sample collected near the lake from a flood event in 2005. Bulk organic carbon (C_{org}) and nitrogen (N) elemental content and isotopic signatures ($\delta^{13}\text{C}_{\text{org}}$, $\delta^{15}\text{N}$), carbon-to-nitrogen ratios (C/N), as well as moisture and organic matter contents were measured. These were compared to diatom assemblages, including those indicative of high (*Navicula libonensis*, *Rhopalodia gibba*) and low (*Achnanthes lanceolata* var. *frequentissima*, *Achnanthes minutissima*, *Navicula pupula*, *Nitzschia amphibia*) river influence. Most studies analyzing floodplain lakes have additionally validated their reconstructed flood history by comparing it to historical records captured by river

discharge gauges upstream of the floodplain lake (Wolfe *et al.*, 2008a,b; Lintern *et al.*, 2016a; Brock *et al.*, 2010; Ota *et al.*, 2017).

One main factor, especially when considering river-influenced systems, is the need to account for the influence of variations in grain size on sediment metals concentrations, as metals preferentially partition onto fine-grained sediments like silt and clays (Wiklund *et al.*, 2014). One way to do this is by normalizing metal concentrations to a lithogenic element. Geochemical normalization is important for flood-influenced systems due to the fluctuations in energy of the river, which generates variations in grain-size of the sediment being carried (Wang *et al.*, 2015). Floodplain lakes generally receive a primarily fine-grained fraction from the river, as the river water must travel a distance across the land and the energy of the river dissipates when flooding these systems (Wiklund *et al.*, 2014). Common lithogenic elements used in geochemical normalization include aluminum, lithium, rubidium, scandium, titanium, and zirconium (Audry *et al.*, 2004; Boës *et al.*, 2011; Wiklund *et al.*, 2014; Wang *et al.*, 2015). The normalizing agent chosen usually reflects the local geology, to best represent the “natural” geogenic level of a metal of interest (Audry *et al.*, 2004; Boës *et al.*, 2011; Wiklund *et al.*, 2014).

1.7 *Metals of concern*

Accumulation of metals of concern in the environment from anthropogenic sources (mining, smelting, etc.) has historically been a key consideration for monitoring mining-impacted areas around the world (e.g., Davis *et al.*, 1983; Renberg, 1987; Ek & Renberg, 2001; Salonen *et al.*, 2006; Jernström *et al.*, 2010). Heavy metals are classified as elements that possess a high density and atomic weight (Tchounwou *et al.*, 2012). The toxicity of heavy metals depends on factors such as dose, method of exposure, and chemical species, as well as the characteristics (e.g., age, genetics, etc.) of specific individuals (Tchounwou *et al.*, 2012). Due to

their high degree of toxicity, heavy metals such as arsenic, cadmium, chromium, lead, and mercury have been classified by the United States Environmental Protection Agency (US EPA) as some of the most dangerous for human health, as some bioaccumulate (e.g., mercury), are toxic even at extremely low concentrations (e.g., arsenic), and can be classified as carcinogenic (Tchounwou *et al.*, 2012).

The US EPA lists priority pollutants in the Clean Water Act (2014) that includes many contaminants particularly toxic to aquatic organisms and humans, including many organic compounds, as well as heavy metals such as antimony (Sb), arsenic (As), beryllium (Be), cadmium (Cd), chromium (Cr), copper (Cu), lead (Pb), mercury (Hg), nickel (Ni), selenium (Se), silver (Ag), thallium (Tl), and zinc (Zn). Kelly *et al.* (2010) detected elevated levels of the above 13 elements in snowpack within 50 km of a central location within the AOSR. A similar spatial extent was determined by Kirk *et al.* (2014) for mercury in snowpack within the AOSR. Based on the spatial pattern of contaminant deposition, it has been suggested that longitudinal patterns of priority pollutant concentrations in the Athabasca River are a result of aerial deposition of metals from industry and subsequent transport during snowmelt and rain events (Kelly *et al.*, 2009, 2010). A few studies have even linked a large portion of airborne pollution to airborne petroleum coke (petcoke) dust and unprocessed bitumen, by analyzing lake sediment cores and living moss and peat cores in the AOSR (Jautzy *et al.*, 2015; Shotyk *et al.*, 2016b; Zhang *et al.*, 2016). Currently, oil sands companies store vast quantities of petcoke on site in large piles, making it susceptible to re-distribution by winds (Alberta Energy Regulator, 2014).

Bitumen in the AOSR is highly enriched in metals like vanadium (V), nickel (Ni), iron (Fe), and titanium (Ti), which make them good geochemical tracers of oil sands contamination (Hodgson, 1954; Jack *et al.*, 1979; Jacobs & Filby, 1983). Vanadium is a common transition

metal, usually found at low concentrations in the environment, however it is elevated in carbonaceous sediments such as those found in the Alberta oil sands McMF (Schiffer & Liber, 2017). In fact, V concentrations in crude oil can range from 150-290 mg/kg. Following the bitumen upgrading process, V is removed and concentrated in petcoke, a by-product of this process, reaching concentrations of 1,000 mg/kg or higher (Schiffer & Liber, 2017). The most mobile and bioavailable form of the V ion is V(V), which forms oxyanions (H_2VO_4^- and HVO_4^{2-}). These oxyanions mimic phosphate anions (H_2PO_4^- and HPO_4^{2-}) in the environment due to their structural similarities and compete for uptake in plant and animal cells (Schiffer & Liber, 2017). This also makes V(V) the more toxic ionic form of V as it can inhibit phosphate-metabolising enzymes (Schiffer & Liber, 2017). Until as recently as May 2016, no federal water quality guidelines existed for V for the protection of aquatic life, despite being highly enriched in bitumen and bitumen by-products (Schiffer & Liber, 2017). Currently, the federal freshwater guideline is 0.12 mg V/L for freshwater, but no AOSR or province-specific guidelines exist for acute and chronic exposure for multiple species (ECCC, 2016). A more thorough investigation in V toxicity on four model organisms led by Schiffer & Liber (2017) found that the chronic HC5 toxicity level, which is the hazardous concentration to the most sensitive 5% of species tested, should be 0.05 mg V/L. Leaching of V from petroleum coke, which can exceed 1 mg/L, can have a detrimental effect on the more sensitive cladoceran and diatom species that are prevalent in northern Alberta freshwater systems, and can affect the survivability of regionally important fish species such as *Pimephales promelas* (Schiffer & Liber, 2017).

1.8 Study Objectives

The lack of pre-industrial, baseline, sediment metals data for the Athabasca River in the AOSR impedes ability to detect and quantify the magnitude of river pollution, since the natural

range of variation is unknown. Studies of contaminants in the regional snowpack show clear evidence of atmospheric pollution at least within a 50 km radius of AR6, but we do not know if this leads to discernable pollution of the Athabasca River (Kelly *et al.*, 2009, 2010; Kirk *et al.*, 2014). Despite monitoring of river-bottom and suspended sediment metals in the Athabasca River by programs like RAMP and JOSM since 1997, these data have yet to be used successfully to evaluate origin or trends in river contaminant concentrations. To address these knowledge gaps, we require both pre- and post-industrial measurements of river contaminant concentrations. The upstream-downstream study design in Kelly *et al.* (2009, 2010) showed that contaminant concentrations are higher within and downstream of oil sands development compared to upstream locations, but without pre-industrial baseline information we cannot know for sure if this spatial pattern has long existed due to erosion of bitumen in shoreline exposures, or has arisen as a result of the release of contaminants by industry via air, surface water, and groundwater.

I hypothesize that this critically missing knowledge can be investigated through the establishment of metal baselines from sediment profiles of flood-influenced, river-proximal lakes in the AOSR using paleolimnological approaches. Paleolimnological work can extend and enhance current monitoring records to develop much needed baselines to adequately assess the extent of industrial pollution. Thus, the objectives of this study are 1) to establish pre-1967 Athabasca River baseline concentrations of bitumen-indicator metals V and Ni using lakes that have historically received river floodwaters in the AOSR; 2) to assess if temporal changes in deposition of these metals have occurred at the study lakes coincident with oil sands development; and 3) to use the V/Al and Ni/Al baselines to evaluate and interpret post-industrial RAMP/JOSM river-bottom and suspended sediment monitoring data for evidence of pollution.

Results from this study will lend insight into future applications of this model to place modern river sediment monitoring data in a long-term context.

Chapter 2 – Methods

2.1 Site descriptions: Alberta oil sands region

In the Athabasca River watershed, most of the bitumen is located within the McMurray Formation (McMF; Conly *et al.*, 2002). The McMF is a natural and diffuse source of metals and PAHs to the river, with several outcrops visible along the banks of the Athabasca River and the Clearwater River, a major tributary upstream of the oil sands (Conly *et al.*, 2002). Downstream of Fort McMurray, the steep banks along the Athabasca River gradually begin to open and flatten into a floodplain. Floodplain lakes were chosen based on their proximity to the river and by assessing the extent of the floodplain on Google Earth imagery. Five floodplain lakes were used in this study, two located upstream and three located downstream of major oil sands mining operations (Figure 1). Lake IDs were developed using the lakes' river distances (in km) upstream (Up) or downstream (Down) from AR6 along the Athabasca River, the central location within the AOSR used by Kelly *et al.* (2009, 2010) (Table 1).

Table 1. Lake and sediment core information for Athabasca River floodplain lakes located upstream (Up 17, Up 10) and downstream (Down 1, Down 26, Down 58) of central oil sands operations (AR6) in Alberta, Canada. (*) denotes the core chosen for analyses.

Lake ID	Distance from central oil sands activities (river km)	Distance from lake to river (m)	Lake Depth (m)	Difference in elevation river to lake (m)	Core lengths (cm)
AR Up 17	17	140	1.4	4	HC1: 43 * HC2: 30
AR Up 10	10	730	4.7	4	HC1: 61 HC2: 62 *
AR Down 1	1	140	0.6	3	HC1: 55 HC2: 54 *
AR Down 26	26	72	N/A	2	HC1: 42 * HC2: 39
AR Down 58	58	87	1.3	1	HC1: 38 HC2: 45 *

N/A = shallower than the probe detection limit of 0.5 m

The floodplain lakes vary considerably in dimension (Table 1). Lake Up 17 is a relatively long (1,339.5 m), narrow (48.5 m), shallow (1.4 m) lake that appears to be part of a former river channel (Figure 2). Former river scars around Up 17 also show the pathway where river floodwaters likely enter the lake, washing in from the southern tip of the old meander. Lake Up 17 is beside some reservoirs adjacent to Highway 63, which appear to have been constructed in 2010 (Google Earth). The lake is situated ~140 m from the river's edge and is elevated ~4 m above the Athabasca River. In comparison, lake Up 10 is larger (approx. 1,810.4 m long x 138.8 m wide), deeper (4.7 m), and is located directly across the river from the Millennium Mine (Figure 2). Although upstream of AR6, the lake sits at the bottom of an incline, atop of which the Mildred Lake Mine is located. Lake Up 10 is farther inland, ~730 m from the river, with a ~4 m difference in elevation.

Lake Down 1 is a small (approx. 1,024.6 m long x 98.3 m wide), shallow lake (0.6 m) (Figure 2). This first downstream lake is located directly across from the Mildred Lake mine and ~600 m downstream of the outlet from the Steepbank River tributary, which cuts through exposures of bitumen from the McMF in a highly altered landscape. There is a ~3 m elevation difference between lake Down 1 and the Athabasca River. Lake Down 26 is a very small (approx. 78.4 m long x 24.2 m wide), shallow (<0.5 m) pond (Figure 2). This downstream lake is located very close to the river (~72 m), with a difference in elevation of ~2 m, indicating that this lake system is highly susceptible to receiving river floodwaters. Down 26 is ~9.93 km and ~5.93 km downstream of the Muskeg and MacKay River tributaries respectively, of which the Muskeg cuts through the industrialized Muskeg River Mine area. The farthest downstream lake, Down 58, is also a small (approx. 484 m long x 55.0 m wide), shallow (1.3 m) lake (Figure 2). With a distance from the river of ~87 m and a difference in elevation of ~1 m, this lake is highly flood-

influenced. Photographs of the study lakes show that the surface areas have shrunk, and water levels have declined in most of the lakes over time (Figure 2). Shrubs and macrophytes are abundant along the shoreline and extend across the bottom of most of the shallower lakes.

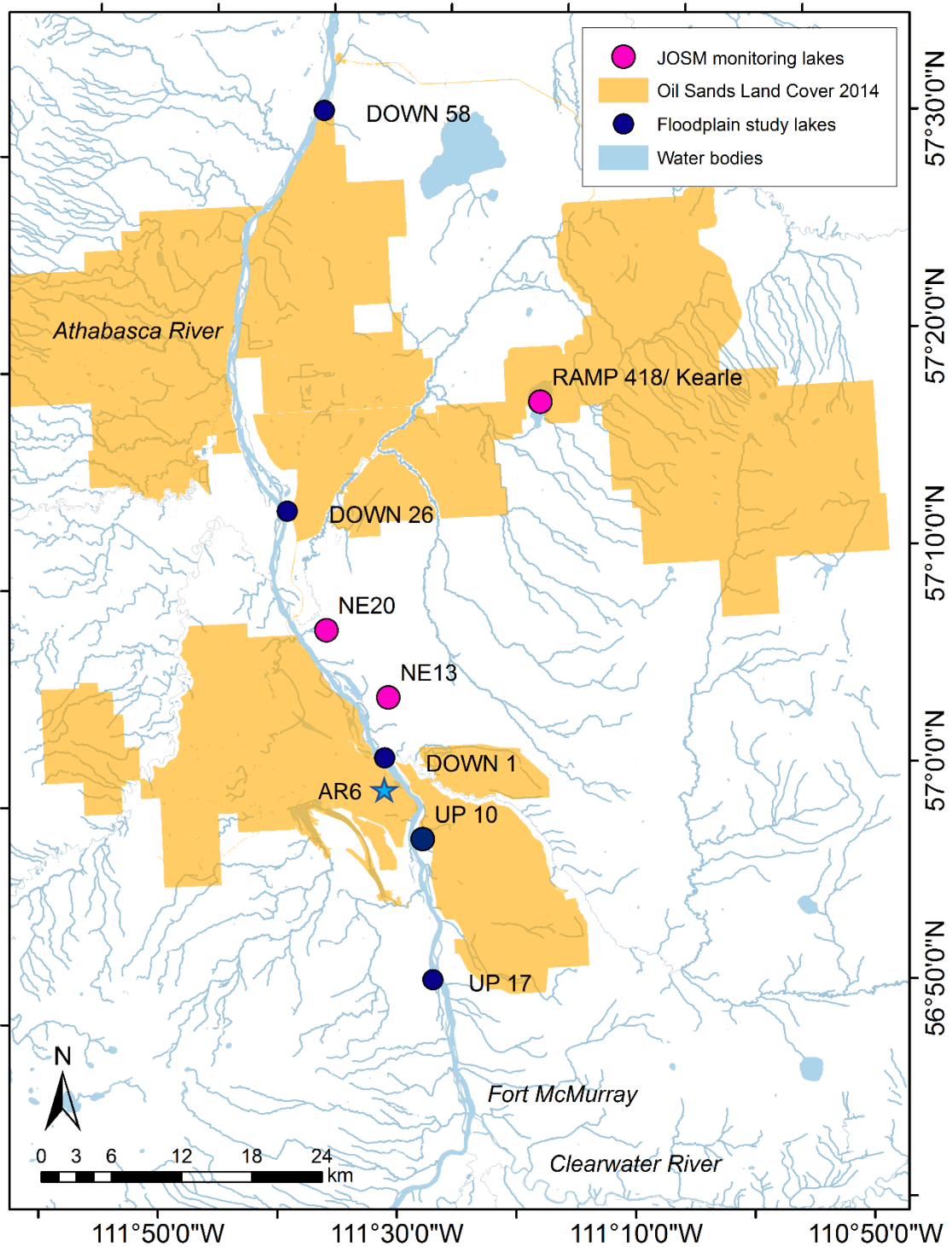


Figure 1. Site map of the Athabasca oil sands region with floodplain study lakes Up 17, Up 10, Down 1, Down 26, and Down 58, as well as select JOSM monitoring lakes NE 13, NE20, and RAMP 418/Kearle. The oil sands land cover as of 2014 (source: RAMP) is outlined in orange, and waterbodies are blue. The blue star denotes location of AR6 (Kelly *et al.*, 2009, 2010). Map courtesy of Casey Remmer, 2018.



Figure 2. Photographs of the floodplain study lakes taken in October 2016 (Up 17, Down 1, Down 26, Down 58) and in July 2017 (Up 10). The pink diamond indicates the approximate coring location at each of the floodplain lakes.

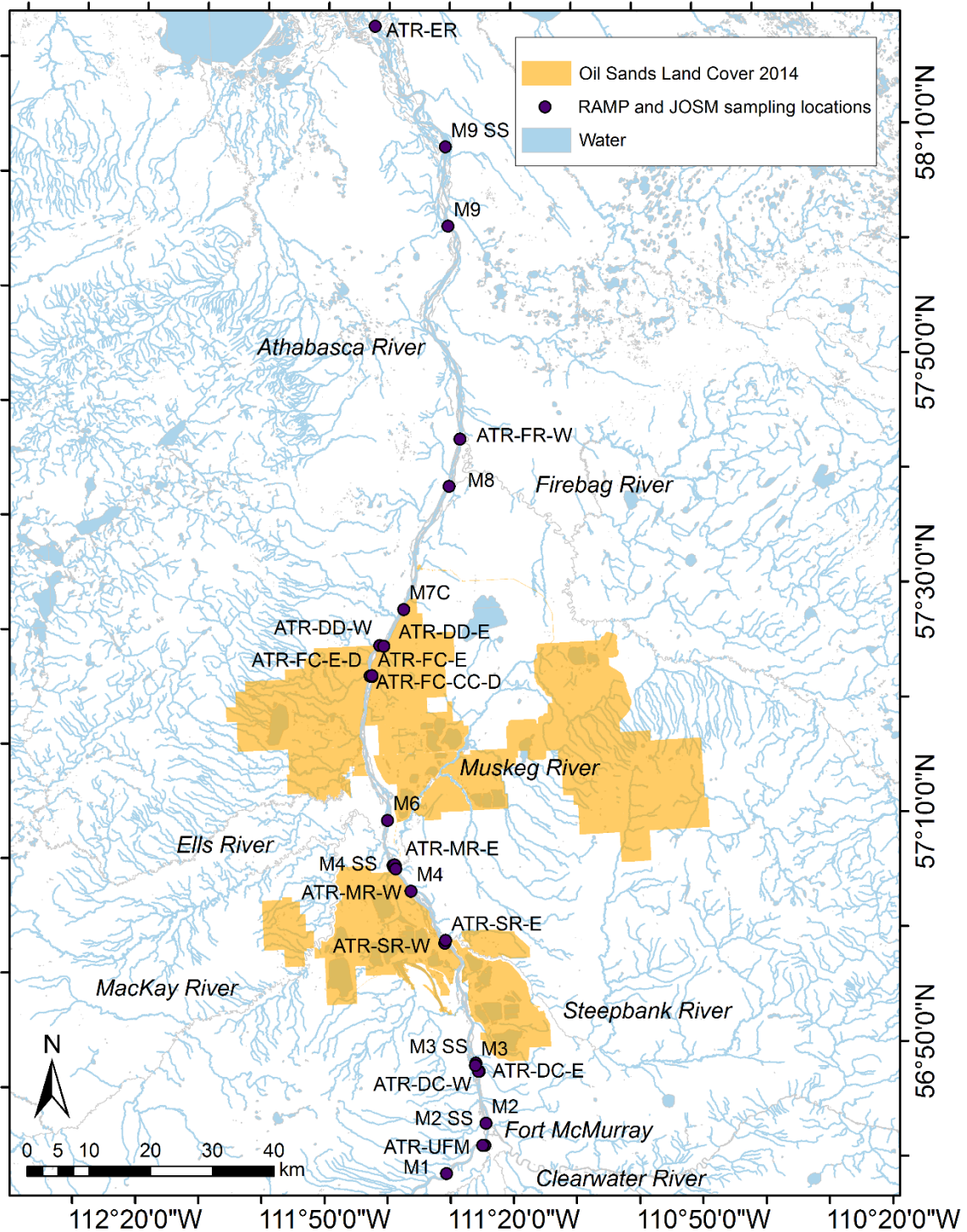


Figure 3. Site map of the RAMP and JOSM sediment monitoring locations in the Athabasca oil sands region. RAMP sites begin with the signifier ATR (for Athabasca River) and the JOSM sites begin with the signifier M (for Mainstem) (see Table A3). JOSM suspended sediment sites are indicated by SS after the site name. Site M0 is not shown as it is > 50 km kilometers upstream of Fort McMurray. The oil sands land cover as of 2014 is outlined in orange (source: RAMP), and waterbodies are blue. Map courtesy of Casey Remmer, 2018.

2.2 *Field methods*

2.2.1 *Sediment core collection*

Sediment cores were collected from lakes Up 17, Down 1, Down 26, and Down 58 in October 2016, and from lake Up 10 in July 2017. Two sediment cores were collected from each lake using a hammer-driven gravity corer (Glew, 2002). Sediment coring was performed from a helicopter on floats, and the cores were taken from a central deep-water location within each lake. Cores were transported to a field base in Fort McMurray where they were sectioned within 24 hours of collection into 1.0-cm intervals using a vertical extruder (Glew, 1988). Samples were stored in Whirl-Pak® bags, kept in the dark, and refrigerated at 2-4°C.

Limnological measurements were taken to assess the depth, temperature (°C), pH, dissolved oxygen concentration (%), turbidity (FNU), and specific conductivity (µS/cm) of water at each lake using a YSI probe (YSI ProDSS) (Table A3, Appendix A). The longitude and latitude of the sampling locations were recorded using a GPS device (Table A1, Appendix A).

2.2.2 *RAMP & JOSM Athabasca River sediment collection*

Metals concentrations data collected by the RAMP and JOSM monitoring programs were used in this study to evaluate post-development river bottom and suspended sediment for evidence of pollution above pre-1967 V/Al and Ni/Al baselines generated from floodplain lake sediment cores. From 1997-2002, river-bottom sediment was collected by RAMP monitoring agencies using 2-4 grabs from a 6" x 6" Ekman dredge and homogenized in a pan before sampling to ensure a representative sample (Hatfield Consultants, 2009). Sediment was collected from various locations along the Athabasca River, usually from depositional areas near the

mouth of major tributaries to the river in conjunction with water quality sampling locations on the east and west banks of the river (Figure 3) (Hatfield Consultants, 2009).

JOSM river-bottom samples were collected as a grab sample from near-shore gravel and sand habitats (Wrona & di Cenzo, 2011). River-bottom sediment for RAMP and JOSM were both collected in autumn in conjunction with benthic invertebrate sampling, as that is considered the period of highest macroinvertebrate abundance and diversity. Bulk suspended sediment samples were collected for JOSM with a passive sampler via continuous flow centrifugation (Wrona & di Cenzo, 2011). River-bottom surficial samples provide information on sediment conditions at the bed-water interface, which are of relevance to benthic organisms and fish during early life stages (Wrona & di Cenzo, 2011). Information on suspended sediment is essential in understanding river contaminant loadings, as many contaminants, such as metals, partition strongly to the fine fraction of sediments, with resulting effects on the health of aquatic and benthic species in the river (Wrona & di Cenzo, 2011). These river-bottom and suspended-sediment samples were evaluated for metals enrichment using the V/Al and Ni/Al baselines developed in this study.

Sediment metals concentrations data from river-bottom samples (RAMP) and river-suspended sediment samples (JOSM) were downloaded from their respective online databases (“Sediment Quality”, 2015; “Sediment Quality Mainstem”, 2016). River-bottom sediment metals concentrations data collected for JOSM were received from Dr. Joseph Culp (Environment & Climate Change Canada / Wilfrid Laurier University) who is affiliated with the JOSM benthic invertebrate sampling program in the AOSR. Available RAMP data span from 1997 – 2002, and JOSM data from 2012 – 2014. Additional information on the RAMP and JOSM sampling programs, including the study design, sample locations, and lab processing procedures can be

found in the RAMP Technical Design and Rationale report (Hatfield Consultants, 2009) and the Phase 1 Lower Athabasca Water Quality Monitoring Plan (Wrona & di Cenzo, 2011), or the annual RAMP and JOSM monitoring reports (e.g. “Joint Canada/Alberta”, 2015; Hatfield Consultants, 2016).

2.2.3 Additional Athabasca River sediment collection

To supplement the river monitoring data collected by RAMP and JOSM with additional data from recent years, river sediment samples were collected during lake coring trips in 2016 and 2017. Samples of recently deposited surficial river sediment were collected from exposed sandbars and shorelines of the Athabasca River at two locations downstream of oil sands activities and one location upstream (October 2016 and July 2017). Following the spring flood in 2017, a sediment sample was also collected from an inland deposit of flood-transported sediment at a location upstream of AR6, in a known area of flooding based on flood maps generated by Alberta Environment & Parks (2017). This sample was collected to evaluate the sediment characteristics of Athabasca River “flood sediment,” as it could be indicative of the type of sediment deposited in AOSR floodplain lakes.

2.2.4 JOSM sediment core collection

Sediment core metals concentrations data collected from small, headwater AOSR lakes NE13, NE20, and RAMP 418/Kearle as a part of the JOSM monitoring program, and published in Kurek *et al.* (2013), Summers *et al.* (2016), and Cooke *et al.* (2017), were used in conjunction with data from this study’s floodplain lakes to construct the pre-industrial baselines (Table A1). The floodplain lake data captures metals concentrations at the high end of the range (> 10,000 ug/g Al), but does not overlap with lower concentrations in coarser surficial river bottom

sediments of the RAMP and JOSM programs. The AOSR headwater lake sediment data were explored and found to be useful in extending the range of metals concentrations at the low end (< 10,000 ug/g Al) since the lakes appear to share a common geological source of V, Ni, and Al (see Chapter 3).

The headwater lake sediment cores used in the Cooke *et al.* (2017) AOSR paleolimnology metals study were collected as part of the JOSM program between 2011-2014. Cores were sectioned at 0.5-cm intervals for the first 20 cm, below which they were sectioned at 2-cm intervals. Metals were analyzed at the National Laboratory for Environmental Testing (Burlington, Canada) using the aqua-regia method of sediment-metal extraction (Cooke *et al.*, 2017). Further information on sediment metals analysis can be found in Cooke *et al.* (2017). Additionally, detailed information on JOSM sediment core collection and dating can be found in Summers *et al.* (2016) and Kurek *et al.* (2013).

2.3 *Sediment core analyses (Physical and geochemical proxies)*

2.3.1 *Loss-on-ignition*

Loss-on-ignition (LOI) analysis is a method used to sequentially measure the content of water, organic matter, carbonate (CaCO₃), and mineral matter in lake sediments (Heiri *et al.*, 2001). LOI analyses were performed on every 1.0-cm section of sediment from each core from the floodplain lakes using ~0.5 g of wet sediment. Sediment samples were first placed in pre-weighed porcelain crucibles and heated in an oven at 90°C for 24 hours, after which they were removed and placed in a desiccator for no less than 2 hours, and then weighed to determine the water content (% wet weight). Samples were then placed in a furnace at 550°C for 2 hours, then removed and placed in a desiccator for 24 hours, following which they were weighed to analyze for the organic matter content in the sediment (% dry weight). Lastly, the samples were once

again placed in the furnace, this time at 950°C for 2 hours, after which they were placed in a desiccator for 24 hours, and then weighed to determine the amount of carbonate (% dry weight) present in the sample. Mineral matter content (% dry weight) was calculated by dividing the post-950°C sediment weight by the post-90°C sediment weight. Following LOI analysis on both cores from each lake, one core was selected for further analyses (Table 1).

2.3.2 *Organic carbon and nitrogen elemental and isotope analysis*

Organic carbon and nitrogen elemental content and stable isotope ratios of $^{13}\text{C}/^{12}\text{C}$ and $^{15}\text{N}/^{14}\text{N}$ can aid in differentiating lake-derived from river-derived sediment (Meyers & Teranes, 2002). Higher C/N ratios are generally associated with flood events, as they bring in more terrestrial-derived organic matter (vascular plants), whereas lower C/N ratios are associated with lake-derived organic matter (algae and aquatic plants) (Meyers & Teranes, 2002).

The carbon isotope composition of sediment is a valuable proxy for determining organic matter sources, as well as changes in lake productivity and nutrient availability over time (Meyers & Teranes, 2002). The ratio of $^{13}\text{C}/^{12}\text{C}$ can help determine lake productivity, as algae (C_3 plants) preferentially take up ^{12}C , which reduces the amount of ^{12}C in the dissolved inorganic carbon (DIC) and provides a signature in algal-derived organic matter that is around 20‰ lighter than the original DIC (Meyers & Teranes, 2002). Algal organic matter can have a very similar carbon isotopic signature to other C_3 plants in the surrounding watershed, but has a distinct isotopic signature compared to C_4 land or water plants (Meyers & Teranes, 2002). Nitrogen isotope composition of sediment is another proxy for past changes in lake productivity, as well as to differentiate organic matter sources (Meyers & Teranes, 2002). The $\delta^{15}\text{N}$ value of dissolved NO_3^- , the most readily available form of dissolved inorganic nitrogen for plants and algae, is

more enriched relative to the dissolved inorganic nitrogen that most land plants utilize (Meyers & Teranes, 2002).

Carbon and nitrogen elemental and stable isotope compositions were measured on one core from each floodplain lake at each 1.0-cm interval. A representative sediment sample (~5 g) was placed into 50 mL test tubes. Samples were then acidified with ~45 mL of 10% hydrochloric acid (HCl) for 24 hours to remove carbonate carbon from the sample, with the first two hours spent in a 60 °C water bath to accelerate the reaction. After 24 hours, once the sediment had settled, the acid was aspirated off from above the sediment and the samples were rinsed with deionized (DI) water. Samples were repeatedly allowed to settle, aspirated, and rinsed until the pH became equivalent to that of the DI water being used. The samples were then freeze dried and sieved at 500 µm to obtain the fine fraction of the sediment and eliminate any coarse debris. Subsamples of the fine fraction (~1-20 mg) were analysed at the University of Waterloo Environmental Isotope Laboratory (UW-EIL) using an elemental analyzer interfaced with a continuous-flow isotope-ratio mass spectrometer (CF-IRMS). This device produces CO₂ through an on-line connection, which it delivers to the detector for analysis (Teffera *et al.*, 1996).

2.3.3 *Sediment metals concentrations*

Metals analyses were completed on every 1.0-cm sub-section of a sediment core from each floodplain lake. For each sample, ~1.0 g of freeze-dried sediment was sent to ALS Canada Ltd. (Waterloo, Ontario), a Standards Council of Canada (SCC) accredited laboratory, for analysis of a suite of metals. Sediments were acid digested using HNO₃ and HCl prior to sample analysis by inductively coupled plasma mass spectrometry (ICP-MS) following method 200.2/6020A outlined by the United States Environmental Protection Agency (US EPA, 1998). This method is only a partial digest, to dissolve all environmentally available metals, but not

those that are bound within the crystal structure of the sediment, as is recommended by the Canadian Interim Sediment Quality Guidelines (CCME, 2001). This is the same method of analysis used in determining sediment-metals concentrations in the AOSR headwater lakes analyzed by Cooke *et al.* (2017). Quality assurance and control involved the analysis of blank and duplicate samples every 20 cm, and for duplicate measurements of a sample, the average value was used for further analyses. A suite of 34 metals were analyzed by ALS, however metals targeted for interpretation were V, Ni, and Al. In Alberta oil sands bitumen and petroleum coke, V and Ni are enriched relative to other geological sources of river sediment and are therefore considered oil sands indicator metals (Gosselin *et al.*, 2010; Wiklund *et al.*, 2014). These elements have also been found to be more elevated in snowpack near oil sands operations (Kelly *et al.*, 2010; Kirk *et al.* 2014). Additionally, Ni is considered a priority pollutant by the EPA's Clean Water Act (US EPA, 2014).

To assess for evidence of metal enrichment in the sediment cores, a geochemical normalization procedure was used to account for the influence of variation in grain size in the sediment (Loring, 1991). During the time captured by a lake sediment core, floods can introduce variation in the grain size of sediment deposited (Kersten & Smedes, 2002; Wiklund *et al.*, 2014). Metals have low solubility in water and therefore adsorb to (or partition onto) particle surfaces. Since smaller grain sizes have a higher surface to mass ratio, they also possess a higher concentration of metals. Due to these processes, normalization is needed to compare among samples within a lake sediment core and among sites. Metals were normalized to aluminum (Al) concentrations, a common lithogenic element used in sediment normalization (Cooke *et al.*, 2017; Wiklund *et al.*, 2018). Previous studies in the AOSR have used geochemical normalizers Al (Cooke *et al.*, 2017), Li (Wiklund *et al.*, 2014), and Th (Shotyk *et al.*, 2014, 2016a, 2016b).

The use of Al as a lithogenic normalizer within the zone of aerial deposition in the AOSR does present a challenge, as it too becomes enriched in the environment due to oil sands activities (Kelly *et al.*, 2010; Kirk *et al.*, 2014; Blais & Donahue, 2015; Cooke *et al.*, 2017). Due to this, a normalizing agent such as Li or Th, which may be less mobilized by dust would normally be a better alternative. In this study, Al was primarily chosen to explore the RAMP dataset, which did not analyze a complete suite of metals, and therefore lacked an alternative normalizer. Increased Al in post-industrial samples can result in a reduced ability to detect contamination by V and Ni and could lead to errors of omission when concluding there is no contamination when, in fact, V and Ni are elevated. Therefore these consequences were considered when analyzing post-industrial V:Al and Ni:Al concentrations.

2.3.4 *Sediment core chronologies*

The sediment age-depth relationship for lakes Up 17, Up 10, Down 1, and Down 26 were developed for one core from each lake using gamma ray spectrometric determination of ^{210}Pb and ^{137}Cs activity. For each sample analyzed, ~3-4 g of freeze-dried sediment was tightly packed into pre-weighed, plastic SARSTEDT polypropylene tubes to a standard height of 3.5 cm. A thin silicone disc (Supelco®) was placed on top of the sediment, followed by 2 Ton Clear Epoxy resin (Devcon®) to a height of 1 cm. Samples were then left for a minimum of 14 days to allow ^{222}Rn and its decay products in the sample to equilibrate with ^{226}Ra prior to analysis of ^{210}Pb , ^{214}Bi , and ^{214}Pb activity. Samples were analyzed for radioisotope activity using the WATER lab's Ortec co-axial HPGe Digital Gamma Ray Spectrometer (Ortec GWL-120-15). ^{210}Pb activities measured were decay-corrected to the coring date for the core taken at each lake, as well as corrected for density (total sediment and bag weights for each sample) (Schelske *et al.*, 1994). Chronologies were developed using a Constant Rate of Supply (CRS) model, where the

activities of ^{214}Pb and ^{214}Bi were used to estimate the level of supported ^{210}Pb activity in the sediment (Robbins, 1978; Appleby, 2001). Standard methods were used to determine the depth of the core where total ^{210}Pb activity is equal to the supported activity (Binford, 1990). ^{137}Cs activity was also measured throughout the cores to validate the ^{210}Pb CRS chronology, or in the case of limited ^{210}Pb data, to develop the chronology (i.e., at Down 26). For lake Down 58, a chronology was not developed but the depth of maximum measurable ^{137}Cs was used to estimate the age at that depth. This was determined by relating the peak ^{137}Cs activity to be the maximum fallout of nuclear testing in the northern hemisphere, which occurred around 1963 (Appleby, 2001).

2.4 *Data analysis (numerical & statistical)*

To interpret past variations in V and Ni concentrations in the sediment cores, pre-industrial baselines were developed. The pre-industrial period was set as the time prior to 1967, when major oil sands operations began in the AOSR (Gosselin *et al.*, 2010). AICc model selection was used to test whether a linear or log-linear relationship would provide a significantly better fit for the data, due to potentially different binding affinities of Al, V, and Ni for different particle sizes of sediment. AICc values were calculated using the AICcmodavg (Mazerolle, 2016) and MASS packages (Ripley, 2018) in 'R' software, version 3.5.1. Pre-industrial baselines were established using linear relations between pre-1967 metal concentrations and the normalizing metal (Al). Data used in baseline development were from floodplain lakes Up 17, Up 10, Down 1, and Down 26, and headwater lakes NE13, NE20, and RAMP 418/Kearle lake (see Chapter 3). 95% prediction intervals (P.I.) were determined and plotted about the linear regressions to define the natural range of variation of individual sediment samples. Post-1967 floodplain lake sediment and RAMP and JOSM river-monitoring metals concentrations data

were evaluated relative to this baseline. If greater than 2.5% of the data points deposited after 1967 plot above the 95% P.I., this was deemed as indicative of pollution (Loring, 1991; Kirsten & Smedes, 2002; Wiklund *et al.*, 2014; MacDonald *et al.*, 2016). Error bars using the mean precision calculated for replicate sediment samples in PAD lakes, and processed by ALS Canada (Edmonton) for Wiklund *et al.* (2014), were applied to the post-industrial data to evaluate the range of variability that might be expected.

Enrichment factors (EF) were used to assess the magnitude of regional anthropogenic pollution of metals in sediments deposited after 1967 (in the study lakes and RAMP/JOSM river-bottom surficial sediments and river suspended sediments), following methods widely employed by other studies in the AOSR (Wiklund *et al.*, 2012; Kurek *et al.*, 2013; Cooke *et al.*, 2017) and elsewhere (e.g., Müller, 1969; Audry *et al.*, 2004; Balogh *et al.*, 2009; Boës *et al.*, 2011). The EF is generally expressed as a ratio of the measured normalized concentration of a metal at a specific sediment depth (X_i) to the concentration that is expected based on its relationship with the normalizing metal, in this case aluminum (Al_i), prior to industrial activity (Equation 1). This relationship was evaluated using the pre-industrial V/Al and Ni/Al baselines developed in the previous section. Values of EF above 1 identify enrichment of the metal concentration above values expected from the pre-industrial relationship.

$$EF = (X_i/Al_i)/(X_{pre-1967}/Al_{pre-1967}) \quad (\text{Equation 1})$$

For the EFs, an upper 95% EF P.I. was calculated for each metal of concern using the average of three points from the V/Al and Ni/Al baseline upper P.I. and following Equation 1. Statistical analyses on the trends observed in the enrichment factors over time were conducted using 'R' software, version 3.5.1.

The nonparametric Mann-Kendall trend test was used to assess the strength and direction of association between metals concentrations and time in floodplain lakes Up 17, Up 10, Down 1, and Down 26 (Ho: no trend; Ha: monotonic trend (upward or downward)), with the ‘Kendall’ package (v.2.2) (McLeod, 2011). Time series of the lakes’ temporal enrichment factors were configured using the ‘zoo’ package (v.1.8-3) (Zeileis *et al.*, 2018). The Mann-Kendall trend test assessed if there were statistically significant increasing or decreasing monotonic trends of metal enrichment in the time series defined by a core from these lakes. To evaluate the occurrence of directional trends in the metals concentrations over time, breakpoint linear regressions were used. The ‘segmented’ package (v.0.5-3.0) was used to determine if and when breakpoints occur in normalized V and Ni concentrations (Muggeo, 2017). Two breakpoints were assumed for the linear relationships and a three-segmented model was used. This assumption was based on observations of the EF graphs for lakes with significant increasing trends over time, where an increase was observed (breakpoint 1) followed by a plateau or decrease (breakpoint 2).

Excess flux (also known as anthropogenic flux, ΔF) can be used to detect the extent to which the supply rate of the metal of interest to the floodplain lake has become elevated above the pre-industrial baseline. Therefore, excess flux measurements were only calculated for lakes where there was significant “excess” observed above the V/Al and Ni/Al baselines. To calculate the flux of anthropogenically-enriched metals to the lake, the calculated enrichment factor (X_{EF}) is multiplied by the dry mass sedimentation rate ($\text{g cm}^{-2} \text{ yr}^{-1}$) and the raw concentration of the metal measured at a specific interval depth (X_i). Excess flux measurements were also corrected for sediment focusing, to allow for the quantification of the atmospheric deposition of anthropogenically-derived metals. The ‘adjusted excess flux’ (ΔF_{adj}) is developed using the sediment focus factor (FF), following Muir *et al.* (2009). FF is calculated for all ^{210}Pb dated

cores by dividing the measured ^{210}Pb flux to the ^{210}Pb flux predicted for the core based on the latitude of the lake site and therefore varies for each core (Table E6).

$$\Delta F = ((X_{\text{EF}}-1)/(X_{\text{EF}}))*(\text{dry mass sedimentation rate} * 10) * (X_i) \quad (\text{Equation 2})$$

$$\Delta F_{\text{adj}} = \Delta F / FF \quad (\text{Equation 3})$$

Chapter 3 - Results and Interpretation

3.1 *Sediment core chronologies & paleohydrology*

The ^{210}Pb activities in the sediment cores from lakes Up 17, Up 10, Down 1, and Down 26 decline downcore, but with marked variability (Figure 4). This is typical of flood-influenced lakes, where episodic influxes of river-supplied sediment with low ^{210}Pb activity depress activities of atmospheric deposition of ^{210}Pb to the lake bottom. At lake Up 17, total ^{210}Pb activity is relatively constant in the upper 4 cm, rises to a peak at 10 cm (137.68 Bq/kg) and declines markedly between 10 and 18 cm depth, after which values continue to decline more gradually to background (or the supported ^{210}Pb value = $33.37 \text{ Bq/kg} \pm 4.16$, 1 SD) at 40-41 cm ($34.86 \text{ Bq/kg} \pm 5.70$, 1 SD) (Figure 4). The sedimentation rate is relatively rapid (avg. = $0.2356 \text{ g cm}^{-2} \text{ year}^{-1}$). Periods of lower radioisotope activity and high mineral matter content in the sediment core from lake Up 17 correspond to periods of rapid sedimentation, and likely represent periods of strong flood influence (Figure 5). The highest peak in sedimentation dates to 1944 ± 20 years, which corresponds to the highest flood recorded in Fort McMurray in 1936 (Winhold & Bothe, 1993). Other spikes in sedimentation rate date to 1976 ± 9 years, 2013 ± 0.9 years, and 2016 ± 0.3 years, and likely correspond to the Fort McMurray floods in 1977, 2013, and 2016, respectively (Winhold & Bothe, 1993; Sturgess, 2014; Giovannetti, 2016) (Figure 4, Up 17 sed. rate panel). Radiocesium activity is constant for the top 22 cm ($1.2\text{-}8.2 \text{ Bq/kg}$) and rises to a distinct peak at 28-29 cm depth ($39.62 \text{ Bq/kg} \pm 1.09$, 1 SD), which corresponds to a ^{210}Pb -based CRS date of 1963 (± 13.7 years, 2 SD). The CRS model determined the basal date of the core to be $\sim 1897 \text{ CE}$ (± 25 years, 2 SD).

Total ^{210}Pb activity in the core from lake Up 10 decreased rapidly with depth below the surface of the core (278.81 Bq/kg) and reaches background ($55.75 \text{ Bq/kg} \pm 12.50$, 1 SD) at 12-13 cm ($46.44 \text{ Bq/kg} \pm 5.87$, 1 SD), with a marked decline (trough) between 2 and 3 cm depth (Figure 4). The sedimentation rate is lower and less variable ($0.0214\text{-}0.0507 \text{ g cm}^{-2} \text{ year}^{-1}$) at Up 10 than at Up 17, but a discernible peak in sedimentation in the uppermost 3 cm corresponds to the trough in activity observed in the ^{210}Pb profile (Figure 4). Radiocesium activity remains constant for the uppermost 6 cm before rising to peak at 9-10 cm ($31.21 \text{ Bq/kg} \pm 1.06$, 1 SD), which corresponds to the ^{210}Pb -based CRS date of 1963 (± 14.8 years, 2 SD). Linear extrapolation to the base of the core (62 cm) using the CRS model generates a basal date of ~ 955 CE (± 135 years, 2 SD).

At lake Down 1, total ^{210}Pb activity declines from 128.42 Bq/kg at the surface of the core and reaches background ($31.52 \text{ Bq/kg} \pm 3.48$, 1 SD) at 27-28 cm depth. Despite some variability at the bottom of the core, values below 27 cm remain within 1 SD of the supported values, as estimated from ^{226}Ra activities, suggesting that background levels are reached by 27-28 cm depth ($38.61 \text{ Bq/kg} \pm 6.80$, 1 SD). This variability in activity near the bottom of the core corresponds to variability in sedimentation rate in the early 1900s when the lake was more flood-influenced (Figure 4), as indicated by relatively high mineral matter content ($\sim 69\text{-}87\%$) (Figure 5). A distinct peak in sedimentation rate is observed at an estimated age of 1931 ± 36.3 years (2 SD), which likely corresponds to the 1936 Fort McMurray flood (Winhold & Bothe, 1993). Activity of ^{137}Cs is variable at the top of the core, but forms a discernible peak ($30.63 \text{ Bq/kg} \pm 0.8956$, 1 SD) at 20-21 cm depth, before declining gradually after 24 cm. Assuming this cesium peak corresponds to 1963, the year of peak above-ground nuclear bomb testing, it corresponds within the range of error of the date determined by ^{210}Pb dating and the CRS model (1973 ± 11 years, 2

SD). A basal date of ~1807 CE (± 47 years, 2 SD) was determined for the core using the CRS dating model with extrapolation.

In the core from lake Down 26, total ^{210}Pb activity declines slightly from the top of the core (157 Bq/kg) to a narrow range of values (43.6-25.5 Bq/kg) from 8 cm to the bottom of the core. In highly flood-influenced systems, re-worked sediment from the river banks dilutes the ^{210}Pb activity, masking the atmospheric ^{210}Pb signal and creating the nearly constant measured ^{210}Pb . The high sedimentation rate ($0.1666 \text{ g cm}^{-2} \text{ year}^{-1}$) determined for the core and the high mineral matter content (76-88%) throughout the core support this assertion of a strongly flood-influenced lake (Figure 5). A distinct ^{137}Cs peak (5.44 Bq/kg) was measured at 16-17 cm (Figure 4). Average ^{137}Cs values measured above and below this peak are lower, spanning a range of 0.46-4.57 Bq/kg. The ^{137}Cs activities are considerably lower at this lake than the previous lakes, which is consistent with the more rapid deposition of river-supplied sediment to this system, and makes dating by ^{210}Pb activity impossible. This peak in measured ^{137}Cs activity was used to estimate the 1963 stratigraphic horizon (± 5.9 years, 1 SD). The subsequent chronology was developed using the average calculated sedimentation rate for the lake ($0.1666 \text{ g cm}^{-2} \text{ year}^{-1}$) and cumulative dry mass at 1963 (416.60 g), and extrapolated down-core to a basal date of ~1817 (± 21.5 years, 1 SD).

Similarly, Down 58, a strongly flood-influenced lake system with very high mineral matter content (~83-91%) was not able to be dated using ^{210}Pb techniques as the ^{210}Pb is generally at or slightly above background activity (39.3-48.1 Bq/kg) signifying high sedimentation rate diluting the atmospheric ^{210}Pb fallout. Measurable ^{137}Cs activity was detected in the core to the basal depth of 45 cm (2.33 Bq/kg), with the highest value measured at 34.5 cm (4.07 Bq/kg) (Table D5, Appendix D). We can thus infer that at a depth of 34.5 cm in lake Down

58, the sediment is likely no older than 1963, but may be as young as 1952, the start of above ground nuclear testing which led to anthropogenically-induced atmospheric Cs fallout. This assumes no downward mobility in ^{137}Cs - a valid assumption, since Cs is less mobile in organic-poor sediments.

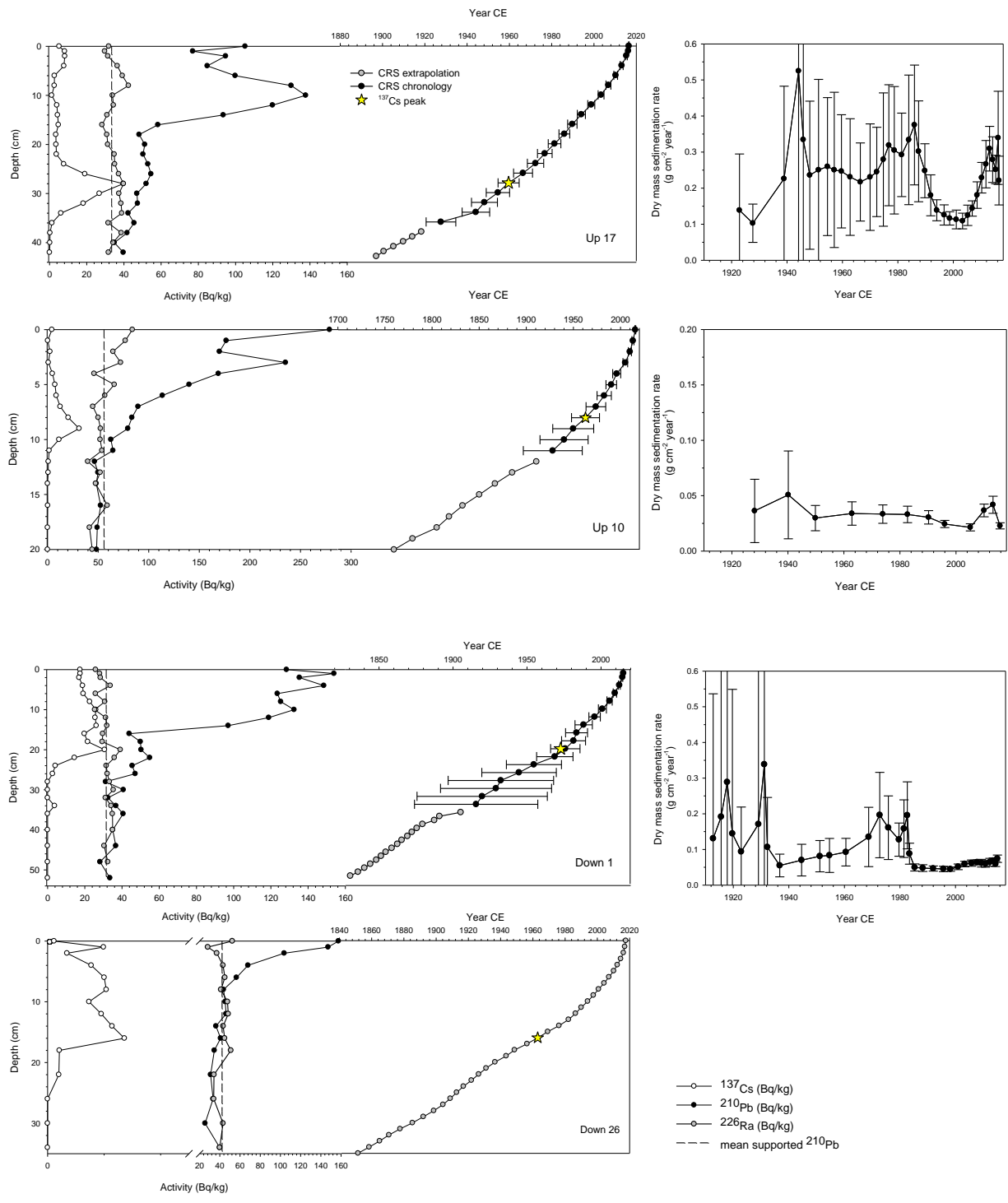


Figure 4. Activities profiles of radioisotopes ^{210}Pb (black circles), ^{137}Cs (open circles), and ^{226}Ra (dark grey circles) in Bq/kg for sediment cores from lakes Up 17, Up 10, Down 1, and Down 26. The age-depth relationship is also plotted for each graph, with extrapolation using the CRS model (light grey circles) and the ^{137}Cs peak indicated by a yellow star. Sedimentation rate is presented in the right panels. Error bars represent 1 standard deviation. Note: low ^{210}Pb values at Down 26 prevented the calculation of varying sedimentation rate ($0.1666 \text{ g cm}^{-2} \text{ year}^{-1}$).

3.2 *Temporal trends in sediment composition and inferred paleohydrology*

High sediment mineral matter content is interpreted in these floodplain lakes as indicative of strong influence of river flooding that supplies rapid influx of inorganic suspended river sediment. Conversely, intervals of relatively high organic matter content occur when river flood influence is less and in-lake productivity increases. We observed that most of the sediment cores possess high mineral matter content (> 75%) throughout their profiles, identifying that these lakes have generally been strongly flood-influenced, as was the aim of the study design. The exception is lake Down 1, where organic matter content is more variable with core depth (Figure 5). Here, an interval of relatively high organic matter content (24-42%) during ~1840-1912 is followed by an interval of lower organic matter content (9-27%) during ~1915-1983. After ~1985, organic matter content increased to 24-43%, with coincident increase in organic C and N content (18-22% and 1.3-1.9% respectively; Figure 5, see also Figure B3).

Uppermost sediments in lakes Up 17, Up 10, and Down 26 also show marked decline of mineral matter content (from > 75% to ~40-70%) after ~1990 (Up 10) and ~2014 (Up 17, Down 26; Figure 5). An interval of reduced mineral matter content was also observed in lake Up 17 between ~1995 and 2008. These declines in mineral matter content coincide with the rise of organic matter (from < 20% to ~20-47%), and organic C (7-25%) and N content (0.7-2.7%) (Figure 5, see also Figures B1, B2, and B4). The mineral matter content in the core from lake Down 58 is the most consistent, ranging from 82-91% over the length of the core (Figure 5). This suggests that this lake has consistently had the strongest flood influence among the study lakes.

Comparisons of fluctuations in organic matter, mineral matter, and organic C and N content profiles in these lake systems to chronological proxies (lake sedimentation rates and

radioisotope activity-depth relationships) were used to identify periods of stronger and weaker flood-influence. Periods of stronger flood influence generally have higher mineral matter content, depressed ^{210}Pb activity, and increases in sedimentation rate (e.g., Up 17). During periods of weaker flood influence, organic matter and organic C and N content are higher, indicating more in-lake productivity that is less frequently diluted with an influx of inorganic river sediment. Observational notes taken when sectioning the cores also offer insight into changes in mineral matter and organic matter content associated with flood-influence. Sediment deposited during intervals of higher mineral matter content (periods of higher flood influence) consisted of grey, dense, clay- and silt-rich sediment, whereas intervals of lower mineral matter content (periods of lower flood influence) had a higher content of black, organic-rich sediment, occasionally with pieces of partially-decomposed reeds and other macrophytes.

3.3 *Temporal variations in metals concentrations*

Stratigraphic profiles demonstrate that sediment metal concentrations of Al, V, and Ni in all lakes are strongly and positively correlated in all five floodplain lakes and vary in concert with temporal variations in the inferred changes in paleohydrology. In general, stratigraphic intervals of stronger flood-influence (higher mineral matter content) correspond with relatively higher sediment concentrations of Al, V, and Ni concentrations, and intervals of weaker flood-influence (lower mineral matter content) correspond with lower concentrations of these metals (Figure 6). However, a few exceptions to the trend of stronger flood-influence corresponding with higher sediment metals concentrations are observed at lakes Up 10 and Down 1. At lake Up 10, a peak is observed in V concentration just before the lake begins to become less flood-influenced in ~1973. Here, V concentration appears to increase to a larger extent than Al concentration (Figure 6). Similarly, at lake Down 1, during the less flood-influenced period that

began in ~1983, a peak in V and Ni concentrations is observed when Al concentrations decline (Figure 6).

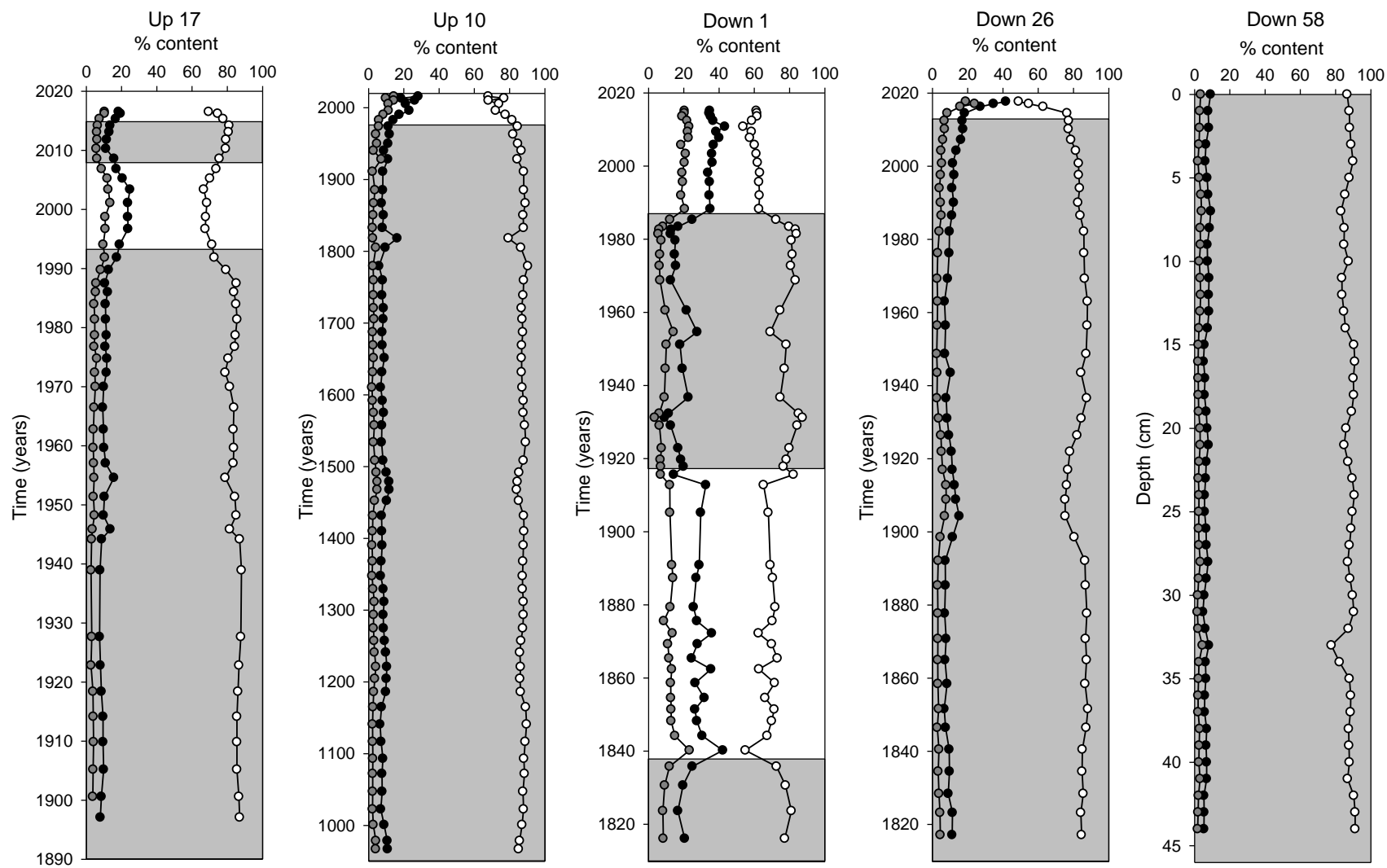


Figure 5. Stratigraphic profiles of organic matter (black circles), mineral matter (white circles), and organic carbon (dark grey circles) content in sediment cores from lakes Up 17, Up 10, Down 1, Down 26, and Down 58. Lakes are arranged in sequence from upstream to downstream. Shaded areas represent strongly flood-influenced sediment intervals.

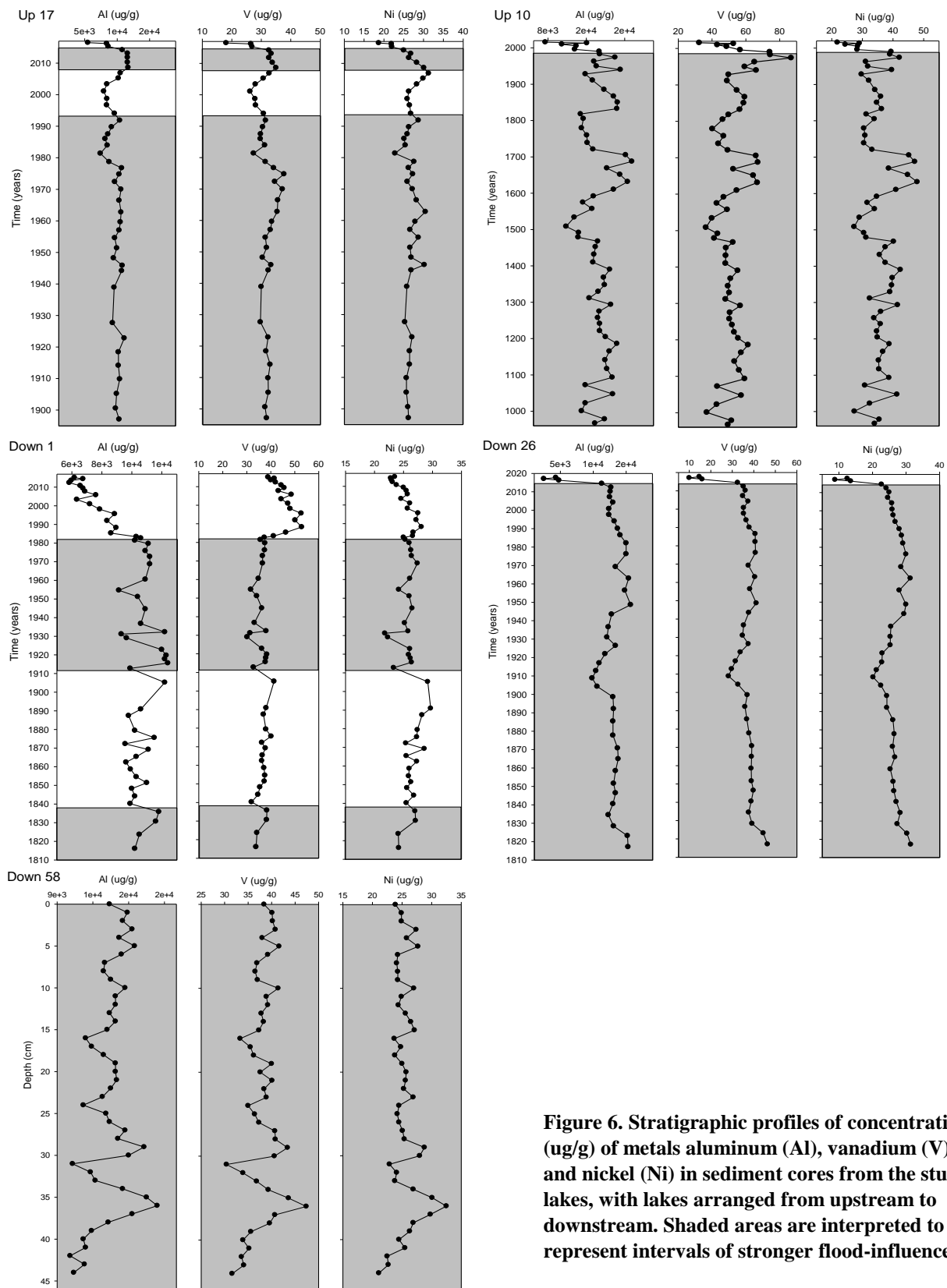


Figure 6. Stratigraphic profiles of concentrations (ug/g) of metals aluminum (Al), vanadium (V), and nickel (Ni) in sediment cores from the study lakes, with lakes arranged from upstream to downstream. Shaded areas are interpreted to represent intervals of stronger flood-influence.

3.4 *Developing a regional pre-industrial baseline*

For the floodplain lakes where sediment core chronologies could be established (Up 17, Up 10, Down 1, and Down 26), pre-industrial (pre-1967) linear relations and 95% prediction intervals were determined for concentrations of the two metals of concern (V, Ni) with respect to the normalizing agent Al. As expected, concentrations of both V and Ni follow a distinct positive linear relation with Al in these samples because the ratios of V and Ni to the normalizing agent Al is relatively constant prior to 1967 (Figure 7, A & B). Due to observations of deviations in the pre-1967 data above and below the V/Al and Ni/Al baselines that appeared slightly biased, and potentially underestimating Al in the mi-range, and V and Ni at the extreme ends (Figure 7), AICc model selection tested the hypothesis that a log-linear model would be a better fit for the data. The linear model had the highest support (Tables E1 and E2, Appendix E).

Lakes Up 17, Up 10, and Down 26 are all strongly flood-influenced prior to 1967 (Figure 5). Lake Down 1 is the only lake where a pre-1967 period of weaker flood-influence is observed, and these samples are not readily distinguished from the other strongly flood-influenced sediments in Up 17, Up 10, and Down 26 (Figure 5; Figure 7, A & B). The strong linear relationships observed for all the sediment core samples, regardless of the status of flooding, shows that pre-industrial V/Al and Ni/Al relations do not differ between periods of strong and weak flood influence. This is likely because the geological source is the same whether it is flood-supplied sediment or remobilized former flood-supplied sediment from the local lake catchment. Weakly flood-influenced samples also likely still contain sediment related to flood events and so still have some use in assessing river sediment metals concentrations. Therefore, all of the pre-industrial sediment data were utilized in baseline construction, regardless of whether the sediment is strongly flood-influenced or not.

The floodplain lakes we sampled adjacent to the Athabasca River provide a good pre-industrial baseline for sediments with Al concentrations ranging from 10,000-25,000 $\mu\text{g/g}$. Up 17 and Down 1 sediments plot near the lower end of the range (10,000-13,000 $\mu\text{g/g}$) in a cluster, whereas sediments from Up 10 and Down 26 capture the mid- to higher-end (10,000-25,000 $\mu\text{g/g}$) (Figure 7, A & B). The sediment samples from the study lakes, however, do not include values at the low end of the range of sediment Al concentration ($< 10,000 \mu\text{g/g}$). Notably, Athabasca River river-bottom and suspended sediment samples collected by the RAMP and JOSM monitoring programs have much lower concentrations of Al ($< 10,000 \mu\text{g/g}$), V, and Ni compared to sediments of the floodplain lakes, likely because the sediment is coarser grained than what is deposited in the floodplain lakes. Thus, the gap of floodplain lake sediment values at the low end of the plot requires that the linear regression is extrapolated outside the range of measured values to assess the low Al content RAMP and JOSM samples for evidence of pollution. This increases the uncertainty for evaluation of the RAMP/ JOSM data, as well as other potential test samples with Al concentrations $< 10,000 \mu\text{g/g}$.

To expand the range of concentrations of Al and the metals of concern (V, Ni) to include Al concentrations $< 10,000 \mu\text{g/g}$, the use of pre-1967 sediment core data from three small, shallow (mean depth 2.1 m) lakes (NE13, NE20, and RAMP 418/Kearle) located 10-35 km from AR6 were explored (published in Cooke *et al.*, 2017) (Figure 3). Sediments of these headwater lakes, located in the AOSR and within the Athabasca River watershed, possess lower concentrations of Al ($< 10,000 \mu\text{g/g}$) and, correspondingly, lower concentrations of V and Ni with metal-Al ratios similar to the floodplain lake sediments; thus, they capture lower portions of the linear relations (Figure 7, C & D). Sediments from lakes NE13 and NE20 have Al concentrations $< 1,000 \mu\text{g/g}$ and plot near the origin of the V/Al and Ni/Al scatterplots. At lake

RAMP 418/Kearle Al concentrations are between 2,000-4,000 $\mu\text{g/g}$. Although a gap (~5,000-10,000 $\mu\text{g/g}$) remains between the floodplain study lakes and the AOSR headwater lakes, the linear relations are now well-anchored at the lower end of the concentrations and both the floodplain and AOSR data are readily captured by the same linear relations (Figure 7, C & D).

The pre-industrial baselines characterizing V/Al (Eqn. 3) and Ni/Al (Eqn. 4) relations, established using pre-1967 sediment metal concentrations from floodplain lakes Up 17, Up 10, Down 1, and Down 26 and AOSR headwater lakes NE13, NE20, and RAMP 418/Kearle (V/Al: $R^2 = 0.9632$; Ni/Al: $R^2 = 0.9332$) (Figure 7, C & D) can be expressed as follows:

$$[\text{V}] \mu\text{g/g} = 0.0026 * ([\text{Al}] \mu\text{g/g}) + 4.8712 \quad (\text{Equation 4})$$

$$[\text{Ni}] \mu\text{g/g} = 0.0016 * ([\text{Al}] \mu\text{g/g}) + 6.8138 \quad (\text{Equation 5})$$

Sediment from both floodplain and headwater lakes follow close along the same linear relations and pass close to the origin (V/Al and Ni/Al), indicating that both datasets have similar V/Al and Ni/Al ratios, which suggests that similar parent geological materials for both floodplain and headwater lakes are the source of these pre-industrial metals in the surrounding AOSR. The crossplots in Figure 7 (C & D) show that samples from each of the headwater lakes vary over quite a narrow range of values, whereas the floodplain lake samples vary over a much wider range of values. This illustrates how natural inputs of metals to non-flooded lakes are quite consistent in the headwater lakes, in comparison to the periodic flooding and non-flooding intervals at the floodplain lakes, which results in a wider range of metal concentrations from the variation in energy conditions of river floodwaters and consequently particle sizes.

The 95% prediction intervals about the regression line, developed as per methods in Wiklund *et al.* (2014), define the natural range of variation of V and Ni concentrations relative to Al concentration for individual lake sediment samples in the AOSR prior to possible pollution from oil sands development (Figure 7, C & D). If unpolluted, 95% of individual sediment samples would be expected to fall within the 95% P.I.s. If > 2.5% of the test samples fall above the upper 95% P.I., this could identify a new enriched source of materials possibly due to pollution from industrial activities.

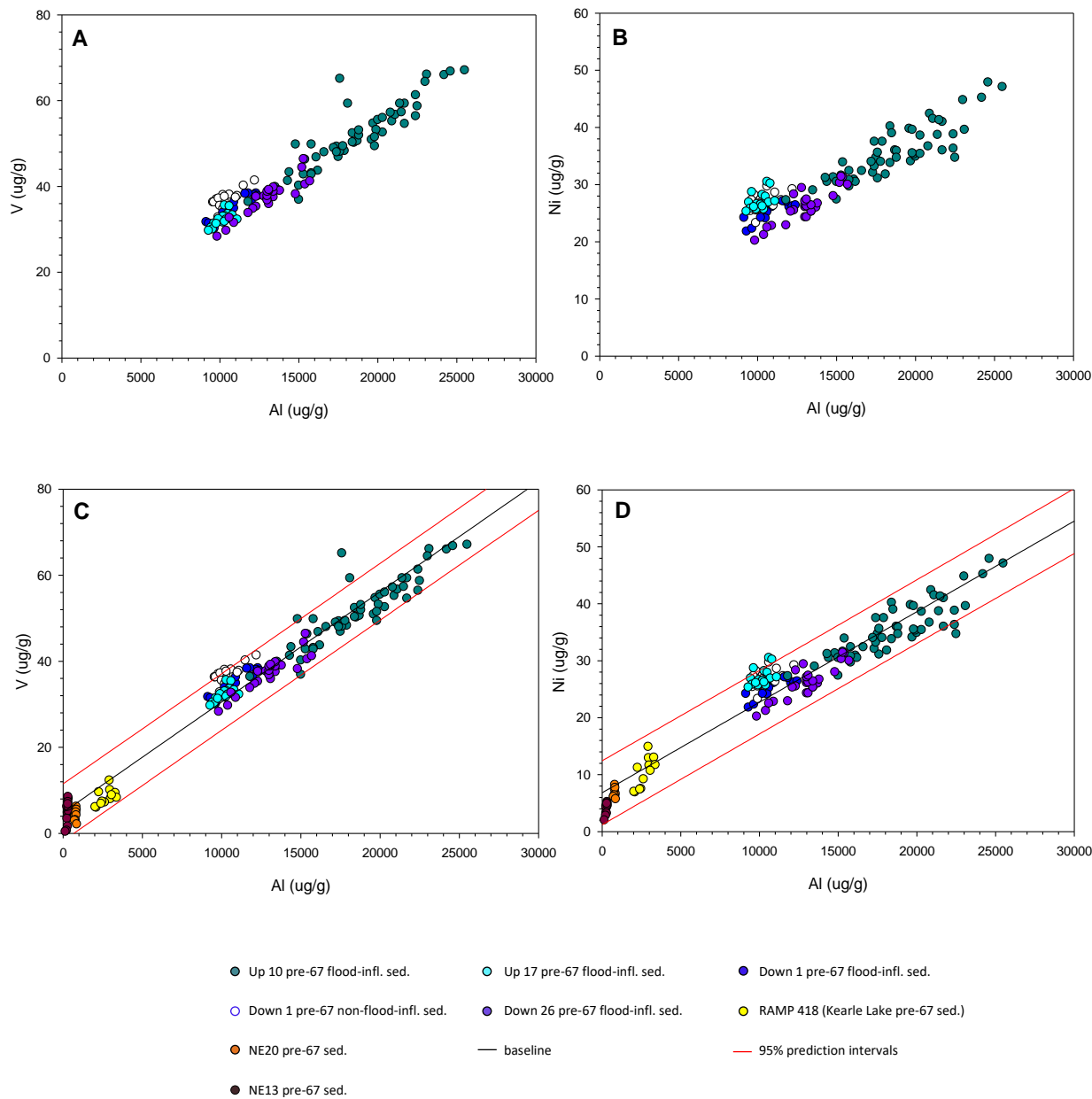


Figure 7. Crossplots showing the relations between sedimentary concentrations of Al and V (left column, A & C) and Al and Ni (right column, B & D) in pre-1967 floodplain lake sediment from lakes Up 17 (light blue), Up 10 (green), Down 1 (dark blue), Down 26 (purple), with the open circles denoting less-flood-influenced sediment from Down 1. Pre-1967 headwater lake sediment from lakes NE13 (dark red), NE20 (orange), and RAMP418/ Kearle (yellow) were added to the floodplain lake data (C: V/Al, D: Ni/Al). The linear regression line (black line) and the 95% prediction intervals (red) are based on pre-1967 sediments from all the lakes listed.

3.5 Assessment for V and Ni pollution

Sediments deposited in the study lakes after onset of oil sands development in 1967 were plotted on the established pre-1967 regional baseline to evaluate for evidence of V and Ni enrichment. For V, post-1967 sediment samples at lakes Up 17, Down 26, and Down 58 all plot within the 95% P.I.s, indicating no evidence of enrichment (Figure 8). This includes during both the strongly and weakly flood-influenced periods at lakes Up 17, which overlap substantially, and at Down 26, where the values for strongly and weakly flood-influenced sediment samples follow the same linear relation but are distinctly lower for the weakly flood-influenced sediments, likely due to dilution of organic matter. For lakes Up 10 and Down 1, however, there is clear indication of V enrichment above baseline in the less flood-influenced sediments, indicating an additional source of the metal to these lakes, which lie within a 10 km distance from AR6 (Figure 8). As seen in Figure 9, both Up 10 and Down 1 are located in an area of high airborne V net loading ($572-715 \mu\text{g}/\text{m}^2$) as measured in snowpack samples from February-March 2011 and 2012 across the AOSR (Kirk *et al.*, 2014). For lake Down 1, this is evident in the data from 1983-2015 (30% of post-1967 sediment samples), which cluster distinctly above the upper 95% P.I. At lake Up 10, there is evidence of enrichment above baseline from 1974-2016 (88% of post-1967 sediment samples), but the data here are more dispersed. V concentrations of post-1967 sediment samples that plot above the baseline for Down 1 and Up 10 do not exceed the CCME guideline of 120 ug V/g, however, some samples do exceed the chronic hazardous HC5 concentration of 50 ug V/g. Schiffer & Liber (2017) suggest that this new benchmark should act as an interim guideline for protection of aquatic life in the AOSR until appropriate, region-specific water quality guidelines are developed.

On the Ni/Al baseline, no enrichment is observed in post-1967 flood-influenced or less-flood-influenced sediment from lakes Up 10, Down 26, and Down 58, as all data plot within the 95% P.I.s (Figure 10). Enrichment of Ni, clustering just above the upper 95% P.I., is observed for Up 17, and Down 1 (14% and 26% of each lake's post-1967 data points, respectively). This enrichment is observed in recent, less flood-influenced sediments at Down 1, likely reflecting a different source of Ni to the lake, as observed for V at this lake (Figure 8). For lake Up 17, marginal enrichment in some flood-influenced sediments is observed, but since they are upstream of major industry this is likely attributed to airborne oil sands pollution, or inputs to the river from the upstream, urban center of Fort McMurray or other upstream industries. Overlap between strongly and weakly flood-influenced sediments is evident at Up 17. The CCME does not have a guideline for freshwater sediment concentrations of Ni for the protection of aquatic life and has determined that this value needs to be assessed on a site-specific basis, since background values of Canadian freshwater sediments can range from 2 to 50 mg/kg dry weight (Moore and Ramamoorthy, 1984; CCME, 2015). Since there currently are no Canadian oil sands-specific guidelines for the toxicology of Ni in AOSR freshwater sediment, the worst-case scenario chronic HC5-50 threshold value of 94 mg Ni/kg determined in Vangheluwe *et al.* (2013) was used to evaluate the sediment taken in these lakes, but all values including those enriched above the Ni/Al baseline fall well below that concentration.

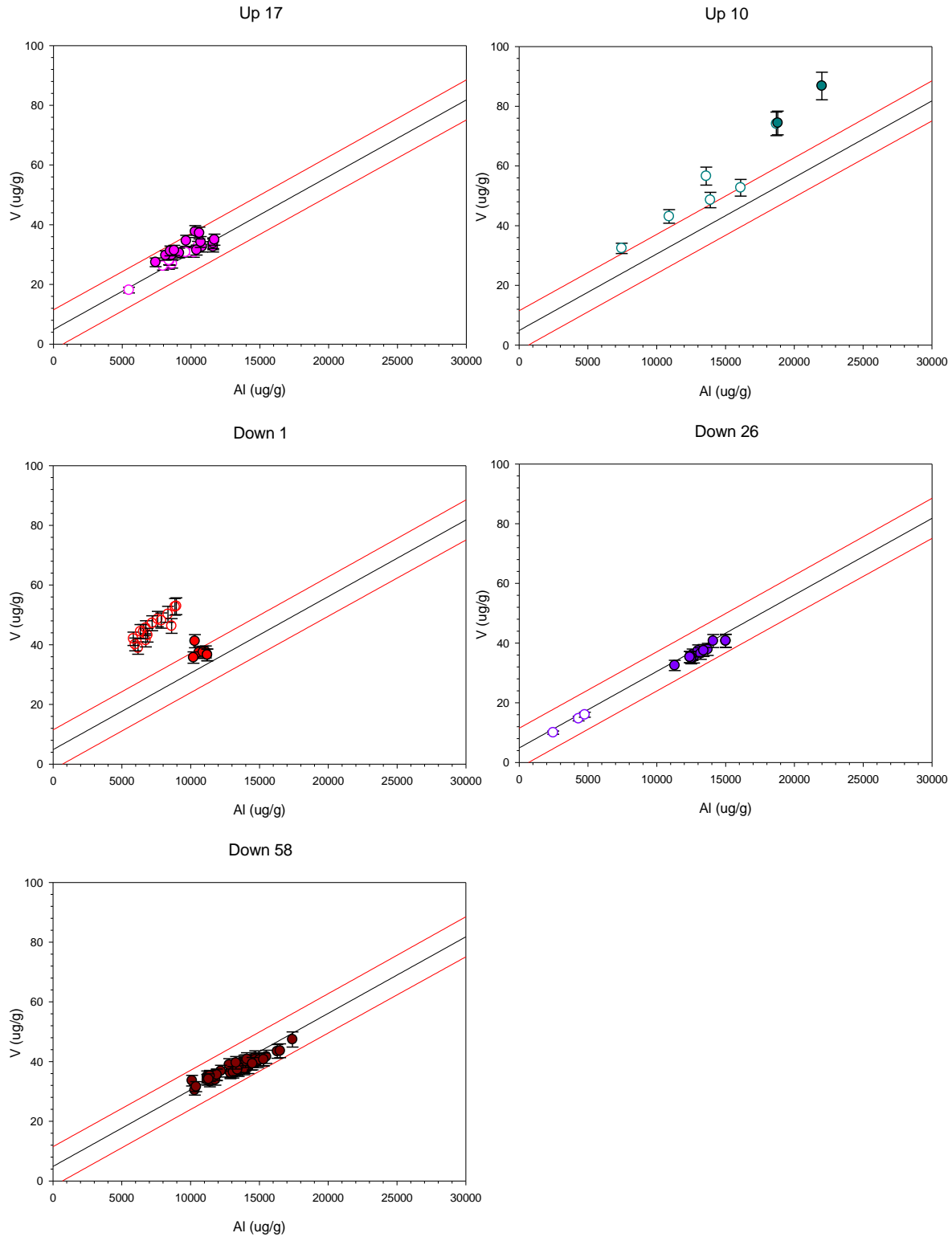


Figure 8. Crossplots assessing Al-normalized V concentrations in sediments deposited in the study lakes since 1967-onset of oil sands development (circles) relative to the pre-industrial baseline (black line) and 95% prediction intervals (red lines). Closed circles: flood-influenced sediment intervals; Open circles: less-flood-influenced sediment intervals. Error bars are from the mean % precision of V calculated from ALS-analyzed duplicate lake sediment samples 200 km downstream (Wiklund *et al.*, 2014).

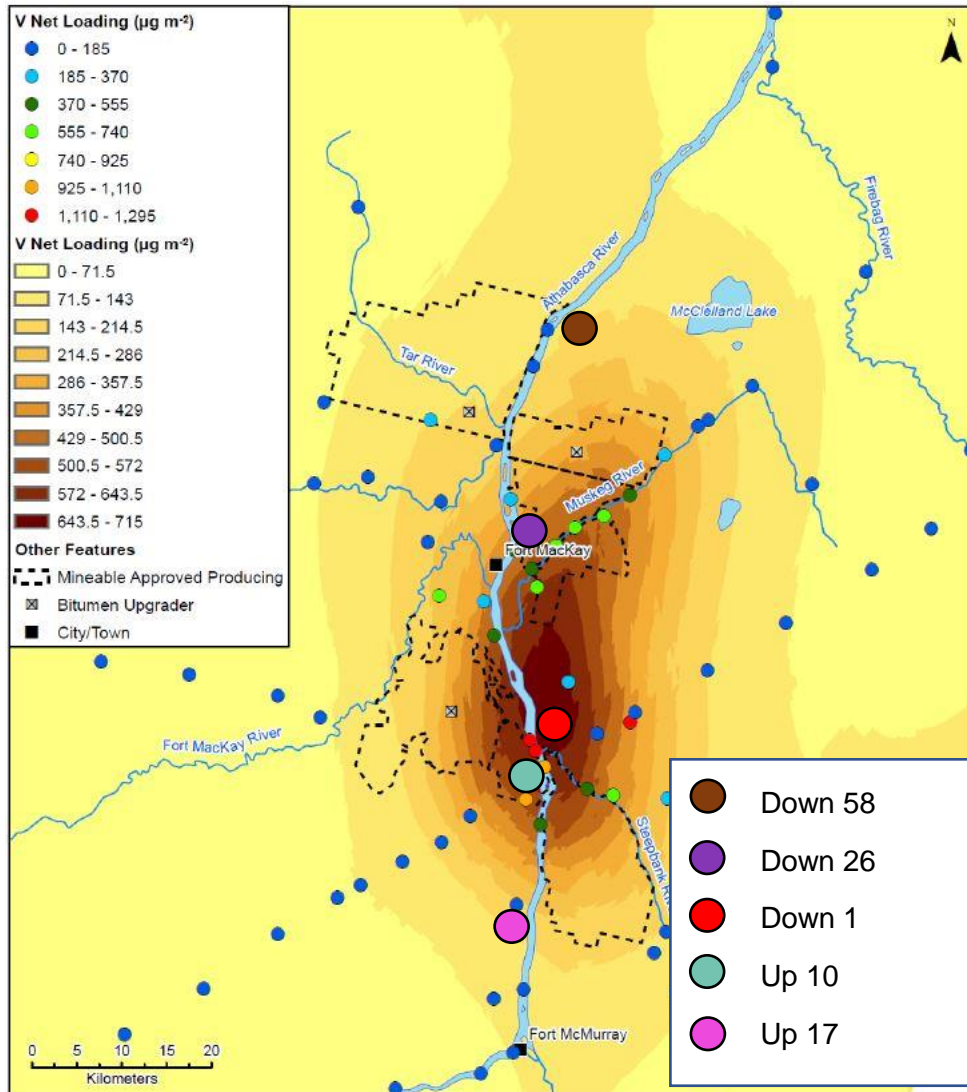


Figure 9. Map of the AOSR mining region showing locations of the study floodplain lakes Up 17, Up 10, Down 1, Down 26, and Down 58, superimposed on a vanadium net loading map to the snowpack in winter of 2012 (adapted from Figure S6: Kirk *et al.*, 2014).

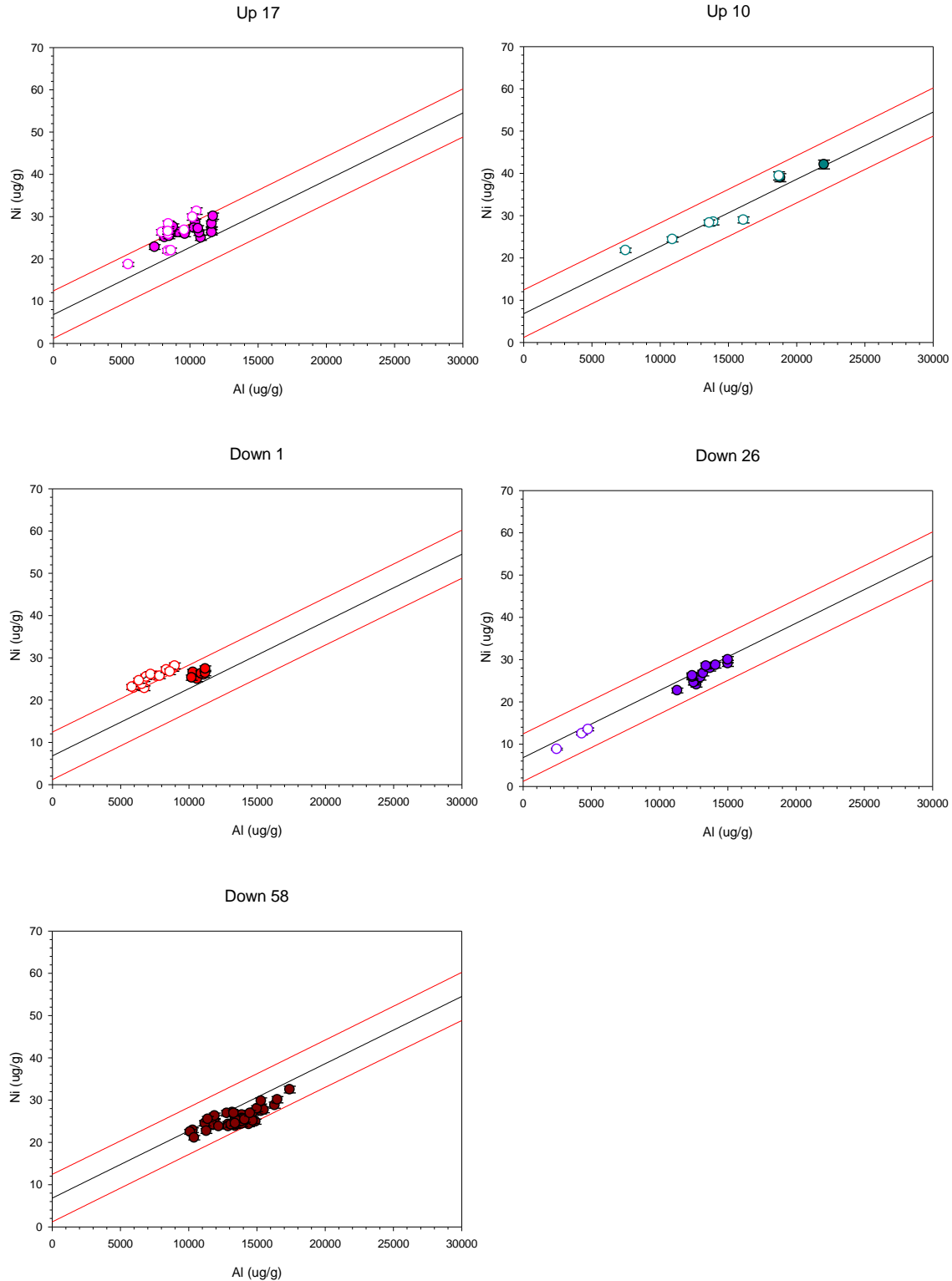


Figure 10. Crossplots assessing Al-normalized Ni concentrations in sediments deposited in the study lakes since 1967-onset of oil sands development (circles) relative to the pre-industrial baseline (black line) and 95% prediction intervals (red lines). Closed circles: flood-influenced sediment intervals; Open circles: less-flood-influenced sediment intervals. Error bars are from the mean % precision of Ni calculated from ALS-analyzed duplicate lake sediment samples 200 km downstream (Wiklund *et al.*, 2014).

3.6 *Evaluating regional river sediment monitoring data for evidence of pollution*

Athabasca River-bottom V and Ni data collected by RAMP and JOSM, as well as suspended-sediment data from JOSM, were evaluated using the pre-1967 V/Al and Ni/Al baselines (Figure 11). Nearly all the river-bottom sediment and the suspended-sediment samples follow the V/Al linear relation, plotting within the 95% P.I.s. Two RAMP samples out of the 75 RAMP/JOSM combined Athabasca River-bottom samples (2.7%) have values that fall above the baseline (site IDs: ATR-SR-W (Oct. 2000), ATR-MR-E (Oct. 2000)) (Figure 11A). This is very close to the 2.5% threshold, which indicates that the V present in the post-1967 Athabasca River sediment samples are only slightly above the expected range of natural (pre-industrial) variability.

The majority of the river-bottom sediment and suspended-sediment Ni data plot within the 95% P.I.s for the Ni/Al baseline. The normalized concentrations of Ni in the Athabasca River sediment samples (suspended and bottom sediments) follow a slightly steeper Ni/Al relation than the pre-industrial baseline, which is particularly apparent for the JOSM river-bottom samples. Five of the 75 river-bottom sediment samples (6.7%) collected by RAMP (site IDs: ATR-DC-E (Oct. 2000), ATR-SR-E (Sept. 2002), ATR-SR-W (Sept. 2002)) and JOSM (site ID: M7C (Sept. 2012, 2014)) plot above the 95% P.I.s (Figure 11B). Suspended sediment samples collected along the lower Athabasca River cluster near the upper 95% P.I., with 8 out of the 25 samples (32%) above the upper 95% P.I. (site IDs: M0 (Sept. 2012; and Feb., June & Sept. 2014), M2 (Sept. 2012, 2013), M3 (Sept. 2012, 2013)) (Figure 11B). This is higher than the 2.5% threshold, indicating that there is evidence of enrichment of Ni in post-1967 Athabasca River sediment. Exposed river-bottom sediment collected in 2016 and 2017 during coring excursions, and the

flood deposit sample collected after the spring flood in 2017, follow closely along the baseline linear regression for the V/Al and Ni/Al relationships.

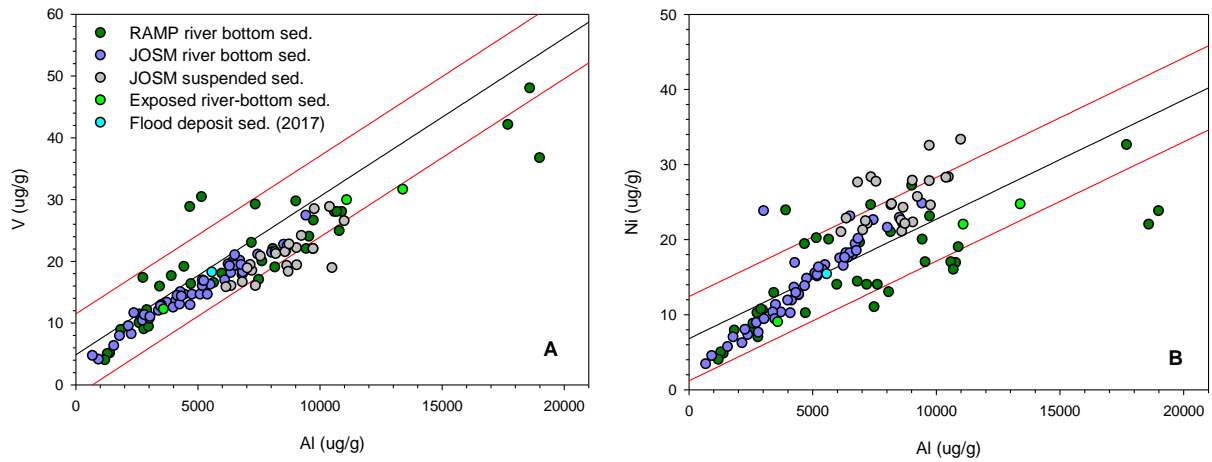


Figure 11. Scatterplot of post-1967 Athabasca River sediment vanadium (A) and nickel (B) concentrations versus aluminum concentrations in the Athabasca River sediment samples collected by the Regional Aquatics Monitoring Program (RAMP) and the Joint Oil Sands Monitoring Program (JOSM). Exposed river-bottom sediment and a flood deposit sample collected during this study (2016, 2017) are also shown. Samples are plotted relative to the V/Al and Ni/Al linear regressions (black line) and 95% prediction intervals (red lines) from Figure 7.

3.7 *Enrichment factor and excess flux analyses*

To quantify temporal trends in sedimentary V and Ni concentrations, enrichment factors (EF) were calculated for floodplain lakes where a chronology was developed: Up 17, Up 10, Down 1, and Down 26. Enrichment factors were also calculated for RAMP/JOSM samples to quantify enrichment of samples that plot outside the upper 95% P.I. on the baselines. In Figure 12 below, a line is drawn at an EF of 1, which indicates no enrichment, and the upper 95% P.I. corresponding to the upper 95% P.I. of the baseline metal-Al linear regression is shown. This 95% P.I. for the EFs represents the same relationship between the linear regression and the 95% P.I. calculated for the baseline, indicating the natural range of variation.

A significant trend of increasing V EFs from the 1960s to 2016 was observed at both Up 10 and Down 1 (Mann-Kendall trend test, $p < 0.05$, Figure 12, Table 2). At Up 10, EFs of V increased to 1.4x above the baseline beginning in the 1970s and remained elevated until ~1995 when the EF began to decline. At Down 1, V increased rapidly to a doubling above the baseline beginning in the early 1980s (breakpoint at 1982, $p < 0.05$, Figure E3 (Appendix E)), after which values levelled out but remained high (breakpoint at 1986, $p < 0.05$, Figure E3 (Appendix E)). Of the EFs calculated for V in the RAMP and JOSM Athabasca River sediment samples, only four RAMP river-bottom sediment samples plotted outside the 95% P.I. (~1.2-1.7x baseline, Figure 12). These river-bottom samples were collected in October 2000 (ATR-MR-E and ATR-SR-W) and September 2002 (ATR-DC-E and ATR-SR-W), at depositional environments located near the Muskeg River (MR), Steepbank River (SR), and Donald Creek (DC) tributary mouths (Figure 12).

A significant trend of increasing Ni EFs above baseline was detected at Down 1 (Mann-Kendall trend test, $p < 0.05$, Figure 12, Table 3). EFs of Ni increased to 1.45x above baseline

beginning during the same 1980s period identified for V at this lake and then levelled out in recent years (breakpoints at 1982 and 1986, $p < 0.05$, Figure E4 (Appendix E)). While no significant temporal trend was detected at Up 17 (Mann-Kendall trend test, $p > 0.05$, Figure 12, Table 3), EFs of Ni increased to 1.4x baseline beginning in the late 1970s, before declining back toward baseline starting in the early 2000s. In RAMP river-bottom samples, Ni EFs plotted above the 95% P.I. (~1.3-1.8x baseline, Figure 12) for similar sites where V enrichment was also detected in October 2000 (ATR-MR-E, ATR-SR-W, and ATR-DC-E) and September 2002 (ATR-SR-W, ATR-SR-E). Enrichment was also detected in a depositional area near the Firebag River in September 2002 (ATR-FR-W). Ni EFs calculated for JOSM river-bottom samples displayed enrichment above the 95% P.I.s in September 2012 (M4 and M7C, 1.2 and 2.0x baseline) and 2014 (M7C, 1.3x baseline) (Figure 12). Site M7C is a new JOSM sampling site, established to estimate Athabasca River water and sediment quality downstream of the Ells River and the total mining area, but upstream of the Tar River (Figure 3). Site M4 was also a RAMP sampling location (formerly ATR-MR) on the Athabasca River mainstem, which was designed to capture Athabasca River water and sediment quality downstream of the Steepbank River and Suncor and Syncrude mining operations, and upstream of Fort McKay and the MacKay River (Figure 3). The Ni EFs calculated for several JOSM suspended sediment samples plotted above the 95% P.I. (1.2-1.5x baseline, Figure 12) from samples collected at M0 (Sept. 2012, 2014; Feb. 2014, Jun. 2014), M2 (Sept. 2012, 2013), M3 (Sept. 2012, 2013), and M9 (Oct. 2012). Interestingly, M0, M2, and M3 are all sites located upstream of oil sands operations. Sites M0 and M2 are both upstream of Fort McMurray and considered ‘baseline/reference sites’ for the new JOSM monitoring program. Site M0 is intended to represent the status of the Athabasca River water and sediment quality prior to reaching the oil sands area, and M2 is located

immediately upstream of Fort McMurray (former RAMP site ATR-UFM). Site M3 (formerly RAMP site ATR-DC) is located directly downstream of Fort McMurray and the Clearwater River. Site M9, a new JOSM site located downstream of the Firebag River and upstream of the Embarras River, is the only downstream site that exhibited Ni enrichment.

Table 2. Results of Mann-Kendall trend tests on the vanadium EF values from sediment cores from lakes Up 17, Up 10, Down 1, and Down 26. The symbols (*) = denotes stat. significance, $p < 0.05$; (+) = upwards trend; (-) = downwards trend.

Lake	Up 17	Up 10	Down 1	Down 26
Kendall's tau	- 0.152	+ 0.410	+ 0.420	- 0.485
Two-sided p-value	0.158	2.62×10^{-6} *	9.42×10^{-6} *	1.25×10^{-5} *
Kendall Score (S)	- 140	774	594	- 401
Denominator (D); tau=S/D	919.63	1887.50	1413.39	826.30
Variance of Kendall Score	9687	27097	17922	8385
Timescale	~1897-2016	~966-2015	~1816-2015	~1817-2017

Table 3. Results of Mann-Kendall trend tests on the nickel EF values from sediment cores from lakes Up 17, Up 10, Down 1, and Down 26. The symbols (*) = denotes stat. significance, $p < 0.05$; (+) = upwards trend; (-) = downwards trend.

Lake	Up 17	Up 10	Down 1	Down 26
Kendall's tau	+ 0.137	+ 0.014	+ 0.39	- 0.138
Two-sided p-value	0.198	0.874	3.99×10^{-5} *	0.211
Kendall Score (S)	128	27	551	- 116
Denominator (D); tau=S/D	934.93	1885.99	1413.90	838.20
Variance of Kendall Score	9750	27093	17926	8448
Timescale	~1897-2016	~966-2015	~1816-2015	~1817-2017

To quantify the increase in deposition rate above the V/Al and Ni/Al pre-industrial baselines, adjusted excess flux (ΔF_{adj}) was calculated. Excess flux was calculated for lakes that showed > 2.5% enrichment (or “excess”) above the baselines’ upper 95% P.I. (Figures 9 and 10). Since enrichment of V above the baseline was observed at lakes Up 10 and Down 1 (Figure 8), and enrichment of Ni above the baseline was observed at Up 17 and Down 1 (Figure 10), excess flux was calculated for these three lakes. The V ΔF_{adj} at lake Up 10 peaked at ~16x the baseline in 1973, before declining to an excess of ~4x baseline in ~2015 (Figure 13A). The V ΔF_{adj} at Down 1, however, steadily increased during the 1980s, peaking at ~17x the baseline in ~2005 when it levelled out (Figure 13A). At both Up 10 and Down 1, ΔF_{adj} was highest when the lakes were weakly flood-influenced.

The Ni ΔF_{adj} at lake Up 17 peaked at ~11x the baseline in ~1979 when the lake was strongly flood-influenced, likely associated with the 1977 Fort McMurray flood, and declined after ~1981 when the lake became weakly flood-influenced (Figure 13B). After a decline starting in the 1990s, the Ni ΔF_{adj} levelled out to a doubling of baseline values. The Ni ΔF_{adj} at lake Down 1 did not peak as high as the V ΔF_{adj} observed, reaching an adjusted excess flux of ~6x the baseline in the 2000s, after which values levelled out with no indication of subsequent decline (Figure 13B).

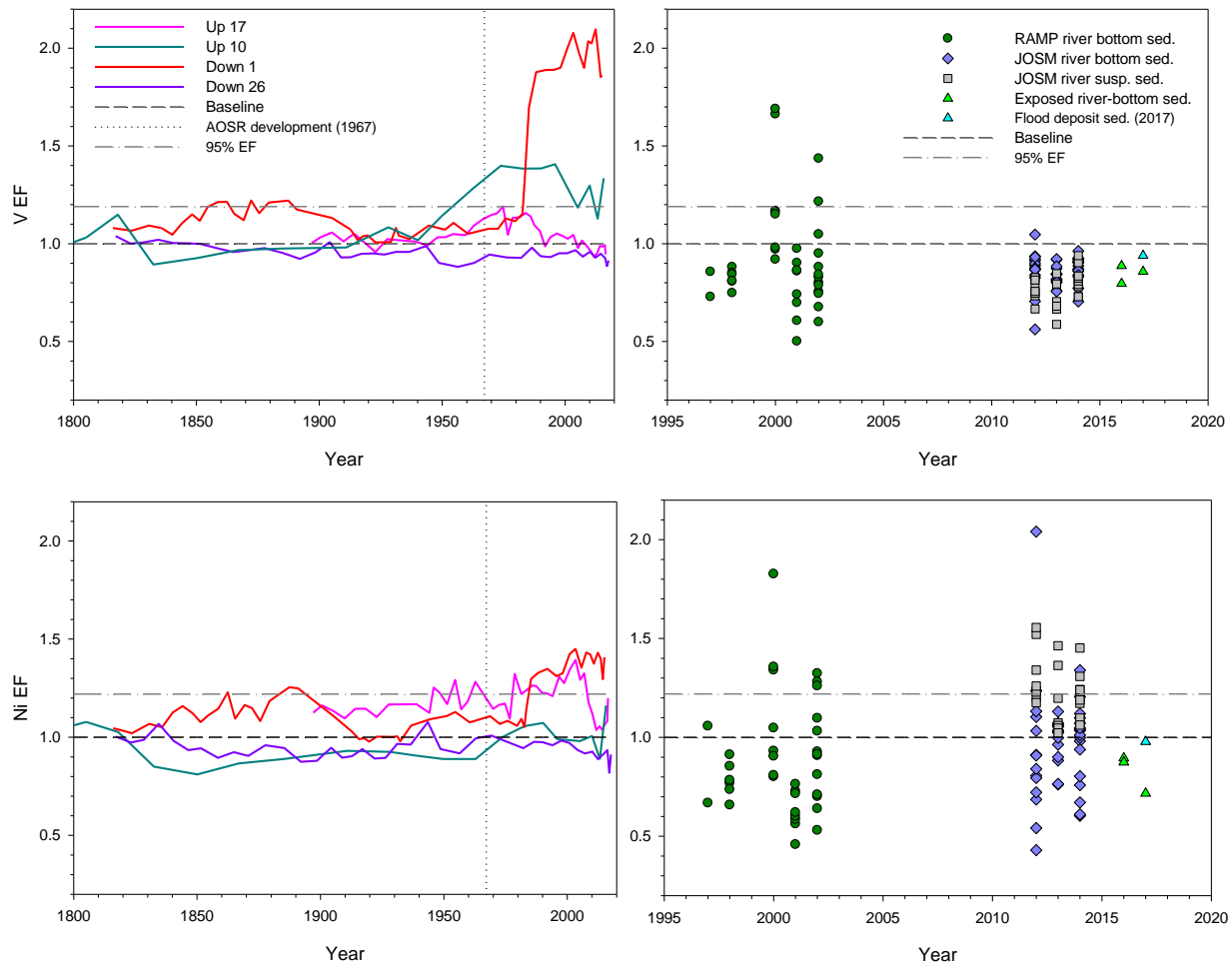


Figure 12. Enrichment factors for V and Ni at lakes Up 17 (pink), Up 10 (green), Down 1 (red), and Down 26 (purple) in the two left-hand panels. In the right-hand panels, enrichment factors for Athabasca River-bottom sediment monitoring data from RAMP (dark green circles) and JOSM (purple triangles) are plotted beside JOSM suspended sediment data (grey squares), exposed river-bottom samples collected during this study (light green triangles), and a flood deposit sample (light blue triangle). The dashed line at an EF = 1 represents the baseline, and the grey dashed-and-dotted line above it represents the upper 95% prediction interval EF. A dotted line at 1967 represents the start of AOSR development.

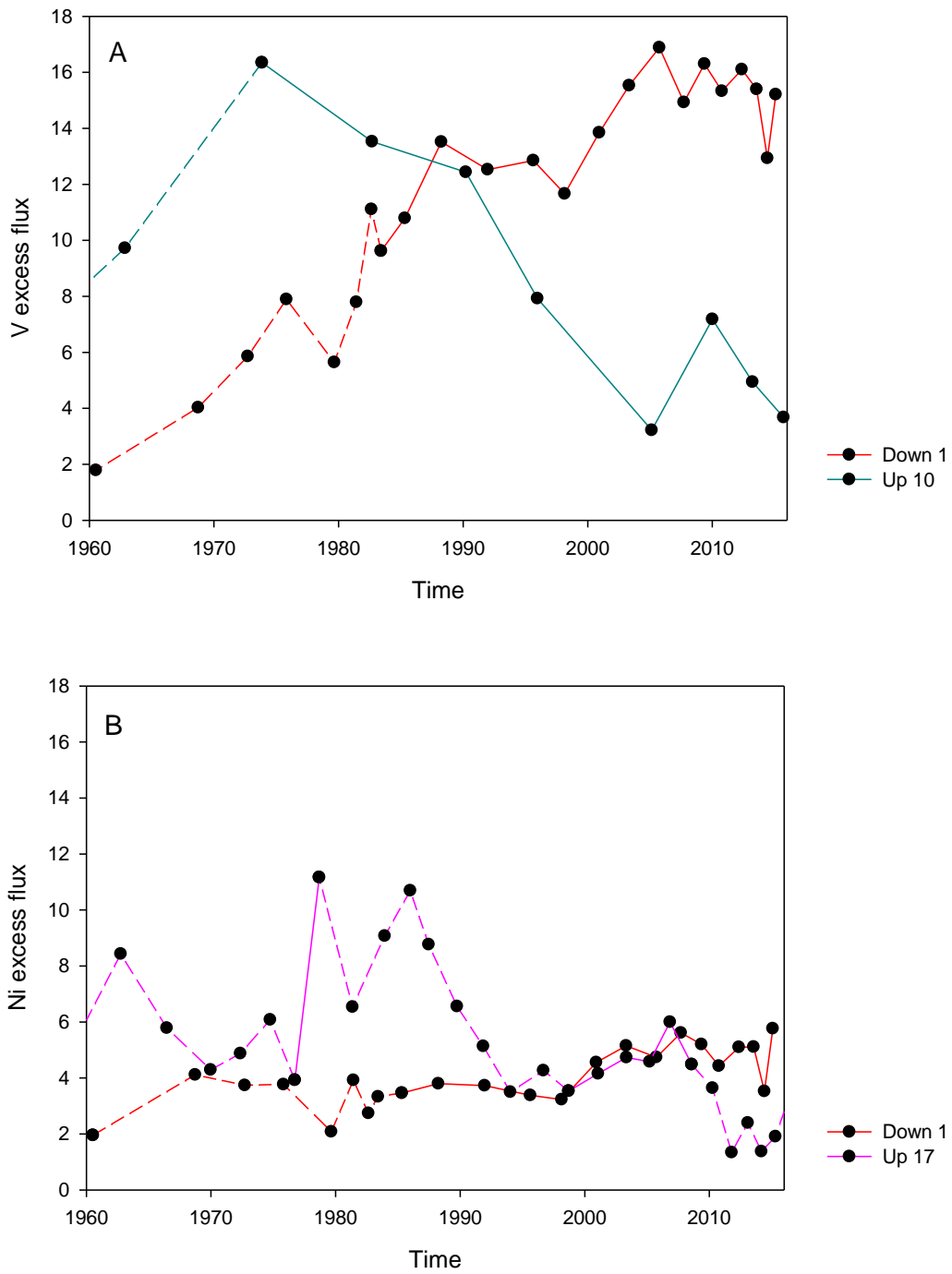


Figure 13. Adjusted excess flux (ΔF_{adj}) of V (plot A) for lakes Up 10 (green) and Down 1 (red) and Ni (plot B) for lakes Up 17 (pink) and Down 1 (red), from 1960-2017. The solid line connects intervals that are enriched above the upper 95% P.I. on the V/Al baseline. The dashed line represents points that do not display enrichment above the baseline.

Chapter 4 – Discussion

The absence of knowledge about the natural range of variation for concentrations of contaminants in Athabasca River water and sediment in the AOSR region before industrial development has made it difficult to determine the extent of river pollution by oil sands mining and processing activities. Such knowledge, however, is essential to disentangle “natural” from industrial sources of contaminants and to detect evidence of pollution. Erosion of natural bitumen exposures continues to contribute loadings of contaminants of concern to the Athabasca River, but industrial pollution cannot be evaluated when these contributions have never been characterized. Development of pre-industrial baselines has been a key recommendation ever since the 2010 Federal Expert Panel report, which proposed that “The natural, pre-development state of the [Athabasca River] waters could be further investigated by analysis of information preserved in sediment profiles that can be obtained from lakes and ponds that are situated in locations prone to river flooding (e.g., along the lower Athabasca River and its tributaries...).” (Dowdeswell *et al.*, 2010, p. 32). Here, we demonstrate the use of floodplain lakes as an archive of natural river-sourced metal concentrations to characterize baseline conditions and natural variation, and evaluate their uppermost sediment and Athabasca River sediment monitoring data for evidence of pollution.

4.1 *Use of floodplain lake sediment cores to develop baseline metal concentrations*

Floodplain lakes provide a useful archive of past river sediment composition because they store and preserve river sediments conveyed by floodwaters in their stratigraphic profiles. The flood-supplied sediments that get deposited in floodplain lakes along the Athabasca River are generally fine-grained, mineral-rich suspended sediments to which metals preferentially adhere. In this study, we show that sediment cores extracted from floodplain lakes provide

dateable, decipherable, stratigraphic profiles of hydrological changes and river-sediment metals concentrations. Despite some challenges (e.g., dating) associated with paleolimnological investigations in floodplain lakes presented by fluctuating sedimentary environments, evidence presented here demonstrates that generating accurate and informative data is possible. Analyses of LOI and elemental organic C and N concentration allowed identification of periods of varying river flood influence. Periods of stronger flood influence in the sediment cores were identified as intervals with clay-rich sediment (small grain size) possessing relatively high mineral matter content and minimal organic matter and C and N content. In comparison, periods of weaker flood influence were identified as sediment intervals with relatively high organic matter and C and N content, and low mineral matter content. These distinguishable sedimentary features allowed for the determination of stratigraphic intervals when each lake was receiving strong influence of Athabasca River floodwaters, from which pre-industrial river sediment could be evaluated.

Despite concerns over the ability to date floodplain lake sediments, developing reliable sediment core chronologies is possible, as demonstrated by the combined application of ^{210}Pb and ^{137}Cs dating techniques. Where the ^{210}Pb signal, primarily used for determining lake sediment ages, was diluted by rapid river sediment deposition during flood regimes, a chronology could be developed or estimated based on peak ^{137}Cs activity in 1963, the height of above-ground nuclear bomb testing. One lake core could not be dated due to very strong flood influence, which depressed ^{210}Pb activities to near background throughout the core and prevented detection of the ^{137}Cs peak. Evidence of ^{137}Cs found throughout the core, however, suggests the stratigraphic record obtained was likely deposited since the onset of oil sands development, which allowed the core from this lake to be used to test for evidence of industrial pollution. The

close match between peaks in estimated sedimentation rates and known flood events for the Athabasca River at Fort McMurray also increases confidence in the accuracy of the estimated core ages. This comparison is similar to other studies where hydrometric river data was used to identify past flood events in the paleolimnological record (Brock *et al.*, 2010; Lintern *et al.*, 2016a). The effective dating techniques employed in this study allowed for the determination of the pre- and post-industrial periods in floodplain lake sediment cores, in order to evaluate the natural range of variation of metals.

In evaluating the stratigraphic profiles of metals concentrations in the floodplain lake cores used in this study it was found that sedimentary concentrations of metals associated with bitumen (V, Ni) were strongly and positively associated with Al concentrations. This identified a need to normalize sedimentary V and Ni concentrations to the lithogenic element prior to evaluating the extent of pollution. Since increases in Al supply to the environment by oil sands operations occurs in addition to increases in V and Ni, it has been suggested that this normalization procedure could mask the full impact of oil sands effects on lakes (Blais & Donahue, 2015). Therefore, accumulation rates (excess flux) and enrichment calculations were used to elucidate changes in these metals compared to average pre-industrial accumulation of V and Ni ratios to Al, following Cooke *et al.* (2017). Excess flux calculations evaluate the increased rate of anthropogenic deposition above the pre-industrial baseline using the product of sedimentation rate to V and Ni concentrations, and enrichment factors present the magnitude of increase in concentrations above the pre-industrial baseline. This allowed for the assessment of the extent of pollution to be evaluated using other lines of evidence, to help avoid potential errors of omission due to post-industrial increase in Al.

Pre-industrial baselines (V/Al, Ni/Al) were established following the procedure in Wiklund *et al.* (2014), which used 95% P.I.s to allow detection of samples enriched in V and Ni above the baseline. Pre-1967 metals concentration data were used from floodplain lakes (higher V, Ni, Al concentrations) and headwater lakes (lower V, Ni, Al concentrations). Headwater lakes were incorporated into the baseline in an effort to extend the range of the V/Al and Ni/Al relations, since they follow the same linear relation (V:Al and Ni:Al ratio) as the floodplain lakes, and even weakly flood-influenced pre-1967 intervals from Down 1 show the same relation of V and Ni with Al. The use of headwater lakes on a river-specific baseline is unlike previous studies, where only strongly flood-influenced intervals were used to establish baselines to approximate river conditions (e.g., Wiklund *et al.*, 2014; MacDonald *et al.*, 2016). However, we suggest that a common geologic source for V, Ni, and Al across the AOSR explains the strong V/Al and Ni/Al linear relations and similar V/Al and Ni/Al ratios among all the lakes, including those outside of the floodplain. Indeed, NE13, NE20, and RAMP 418/Kearle are all located on the bitumen-rich McMurray Formation (Conly *et al.*, 2002; Hein & Cotterill, 2006). From analyzing Google Earth and aerial images of the AOSR, it appears as though NE13 and NE20 were also likely part of the river floodplain in the past and, therefore, may contain similar fluvial-derived materials. Prior to industrialization of the region, sediment deposited in these headwater lakes was likely allochthonous, from erosion and runoff of the local McMF catchment. This offers evidence that the regional geology is comparable between the two lake types located in the McMF.

Although the use of headwater lakes on a baseline targeting river floodplain sediment was not originally what was planned in the study design for this project, incorporation of data from these lakes helped to extend the range of metals concentrations so that the values included

in the pre-industrial baselines could overlap with a broad set of river monitoring samples obtained after development of the oil sands. The atmospheric pollution signals detected above the baseline in select floodplain lakes follows temporal trends shown in other research (Kurek *et al.*, 2013; Cooke *et al.*, 2017), providing evidence in support of this approach. With the addition of pre-1967 data from more geologically-similar lakes in the McMF region of the AOSR, the linear relationship could be further extended to fill in gaps in ranges not covered by the floodplain lakes used in this study (4,000-9,000 $\mu\text{g Al/g}$). As well, the original study design of this project was based on the upstream-downstream model of river monitoring, to assess river sediment loadings upstream and then downstream of industry. While this model is useful when the primary mechanism of contaminant delivery is river transport, here we saw that this was not the case, and rather aerial transport of contaminants showed a stronger signal in the floodplain lakes. Considering this now, an “inside-outside” monitoring setup, where lakes located inside and outside the 50 km zone of aerial deposition would be better suited for comparison in future studies. Future research could also attempt to target high-energy floodplain lakes (that receive a coarser grain size) along the Athabasca River to fill in the lower end of the linear relationship although they are likely going to be challenging to date using radiometric methods.

This study generated pre-industrial data that can, for the first time, be used to evaluate Athabasca River sediment samples deposited within the AOSR since the onset of development for evidence of pollution. The method for evaluating river sediment in floodplain lakes that was used in this study is comparable to other studies which have conducted paleolimnological work in other flood-influenced aquatic basins, including the analysis of a floodplain lake in the Slave River Delta (NWT, Canada; Brock *et al.*, 2010) and oxbow lakes along the Yarra River (Australia; Lintern *et al.*, 2016a,b). These studies examined lakes that receive periodic

floodwaters and defined periods of flooding using a multi-proxy approach. Both the Brock *et al.* (2010) and Lintern *et al.* (2016a,b) studies treated flood periods in lake sediment as a binary variable (i.e., flooded vs. not flooded). A similar method to differentiate flooding periods was used in this study, however sections of the core were indicated as either “strongly” or “weakly” flood-influenced, to acknowledge that there is some portion of the sediment that is not entirely either river- or lake-derived. Treating flooding as a binary variable can prevent fully capturing the variability in the mixing of autochthonous and allochthonous sediment when a system floods. In other instances, flooding should be treated as a continuous variable assessing the various proportions of sediment from each source especially for lakes highly susceptible to flood events. One way to address this challenge in the future is through the development of a sediment mixing model. Mixing models have been used to estimate source proportions in aquatic environments, usually involving tools like isotope tracers to track lake food web dynamics and sediment source fingerprinting (e.g., Bird *et al.*, 2010; Zigah *et al.*, 2012; Stock *et al.*, 2018). The development of a mixing model to evaluate river sediment proportions was not possible in this study, as the attempted use of river sediment (coarse-grained, metal-poor, organic-matter poor) as an end member was not representative of the floodplain river flood sediment (fine-grained, metal-rich, organic-matter poor). Hydrologic gradients exert a large amount of control on the composition of sediment at depositional areas along rivers, such as floodplain lakes. River flood events influence the relative contributions of allochthonous and autochthonous sediment present in a floodplain lake at a given time, dictating variations in sediment grain size and metal concentrations. When Al values for the lakes and RAMP/JOSM river sediment samples were plotted relative to organic C values, some of the strongly flood-influenced, metal-rich lakes (e.g., Down 58) were more depleted in organic matter than the river samples, making the river end-member not applicable to

these lakes (Figure B6, Appendix B). If end members can be better determined, this could be a highly effective future tool to tease apart allochthonous and autochthonous contributions to lakes in the Athabasca River floodplain.

4.2 *Evaluating the extent of pollution to the Athabasca River*

The Athabasca River is vulnerable to multiple sources of exposure to anthropogenic contaminants from oil sands industrial operations, mainly in the forms of direct aerial deposition within a 50 km radius of AR6, contaminants supplied via snowmelt runoff and river ice processes during breakup, and surface runoff to the river from intense rain events. The potential inputs of contaminants to the Athabasca River, particularly from contaminated snowmelt, have elevated concerns for human and ecosystem health in downstream, depositional reaches of the river. Historically flood-influenced lakes that capture episodic floodwaters from the Athabasca River were used to assess if metal enrichment above natural, baseline conditions, can be detected in stratigraphic sequences of the sediment when the lakes were strongly flood-influenced. At the downstream Athabasca River floodplain lakes (Down 26 and Down 58) that remained strongly river-influenced throughout most of the time captured by their respective sediment cores (high mineral matter content, low organic content, low/variable ^{210}Pb), there was no evidence of post-industrial enrichment of V or Ni above the pre-industrial baseline in Athabasca River supplied sediment. Down 58 has remained strongly and consistently flood-influenced over the length of the sediment core, likely due in part to its proximity to the river and low elevation in comparison to the other lakes. Analyses of the core from this lake, which likely captured entirely post-industrial sediment based on ^{137}Cs radiometric activity measured at the base of the core, did not detect any enrichment of V or Ni. Until 2014, Down 26, another small lake system proximal to the river, had remained consistently river-influenced, and no post-industrial enrichment of V or

Ni was detected. Post-1967 sediment at these floodplain lakes falls very closely along the pre-industrial Al-normalized baseline for V and Ni, suggesting no evidence of pollution of Athabasca River sediment at these downstream locations.

The Athabasca River sediment V and Ni baselines developed in this study provide a unique ability to assess river sediment samples obtained by monitoring programs in the region for evidence of pollution. Monitoring in the region has been criticized for its inability to detect pollution or evaluate trends, but with the method of baseline development shown here this is now possible. The post-1997 RAMP/JOSM river sediments evaluated in this study represent depositional areas of the river from upstream of Fort McMurray to the Embarras River. The V and Ni concentrations in the RAMP/JOSM samples plot at the lower end of both the V/Al and Ni/Al baselines, overlapping with the pre-1967 headwater lake concentration data. Most of the river sediment samples plot along the linear relationship observed with the V/Al and Ni/Al baselines, showing that the river samples have similar metal ratios. It is expected that the river samples, which are coarser than the fine-grained, silty sediments primarily received by the floodplain lakes, would naturally have lower concentrations of metals.

Results from this study demonstrate how sampling of both river bottom sediment and suspended sediment are valuable indicators of river sediment enrichment. Of the downstream sites that show enrichment outside the range of natural variation, most are located near tributary mouths (Steepbank, Ells, Muskeg), where they are in direct and frequent contact with exposures of bitumen (Conly *et al.*, 2002; Conly *et al.*, 2007) and pass directly through a heavily altered landscape, and therefore may be more representative of the tributary itself than of the Athabasca River as a whole. The detection of > 2.5% of samples above the 95% P.I.s could either identify that these sites have been polluted in recent years, or the pre-industrial baselines developed from

4 floodplain lakes adjacent to the Athabasca River mainstem and 3 headwater lakes within the AOSR are unable to provide adequate baselines for sediments conveyed by the smaller tributaries where these samples were collected. As well, due to differences in energy between the Athabasca River and its tributaries, it is likely that the grain size of sediment brought from these tributaries is smaller, less coarse, and therefore more metal-rich, as they are slower moving river systems. Spatial patterns observed for Σ PAHs in the Athabasca River and its tributaries (including the Steepbank and Muskeg Rivers) have been reported previously for RAMP samples, where the highest concentrations were observed to be near exposed bitumen beds (Evans *et al.*, 2016). Depositional areas, like those sampled as a part of RAMP, are generally in slow-moving portions of the river where benthic invertebrates live and fish spawn. In fact, weathered bitumen sediments, typical of natural exposures downstream of the Athabasca, Ells, and Steepbank rivers, were found to be toxic to fish native to northern Alberta that were in early development stages (Colavecchia *et al.*, 2004, 2006). Canadian interim sediment quality guidelines for V toxicity ($120 \mu\text{g V/L}$) and the chronic HC5-50 threshold value of 94 mg Ni/L determined in Vangheluwe *et al.* (2013) are currently not exceeded at any of these monitoring sites, however there may be other exceedances of metals (or PAHs) that were not examined in this study. This study was able to take modern river sampling data and place it in a long-term context to evaluate post-industrial signals. Our results show that these depositional areas of the river, that are downstream of oil sands activities and that exhibit enrichment, may require further consideration and analysis of source contributions.

The clear enrichment of Ni in suspended sediment samples at upstream JOSM sites (M0, M2, and M3) indicates that there may be a different geological footprint or river pollution source upstream compared to what is observed farther downstream, as these samples appear to be more

enriched compared to locations downstream of oil sands development. As noted earlier, when plotted on the Ni/Al baseline, the suspended sediment samples follow a steeper trend than that of the baseline linear relationship established using pre-industrial lake data. This additional input at sites M2 and M3 could be from upstream tributaries exposed to natural bitumen exposures, such as the Clearwater River, which contributes more than 60% of the total tributary suspended sediment load to the Athabasca River and passes through the McMF (Conly *et al.*, 2002). Kelly *et al.* (2010) found that occasionally there were some particulate and dissolved fractions of water samples from the Athabasca River that had metal concentrations higher than background levels, at distant sites > 50 km away from oil sands activities, similar to observations here. Due to their distant location, they were determined to be “local sources un-related to oil sands mining and processing,” and given a background designation. This is evidence that the observed Ni enrichment in the suspended sediment samples from the most distant upstream site M0 (chosen to reflect upstream boundary conditions in the Athabasca River outside the region of oil sands development) is precedented.

Interpretation of Athabasca River sediment monitoring data using these baselines does have its limitations. For example, the time period captured by the river-bottom surface-sediment samples is unknown. The sample may contain sediments deposited over several years, not just the season when it was collected. Some sediment is re-deposited from depositional locations upstream. So, there is uncertainty as to what the surface sediment samples represent, which makes it challenging to draw conclusions about the extent to which oils sands operations have caused pollution of the river. As well, RAMP only has sediment data available from fall sampling, and JOSM has fall river-bottom data, and some fall, winter, and summer suspended sediment data. As is well known, the spring freshet brings an influx of contaminants into the

river from contaminated snowmelt, which is missed if sediment monitoring is not year-round. By adapting the river sediment sampling frequency to capture seasonal differences and major hydrological events (i.e., significant floods), a temporal perspective for river sediment could be better defined and anticipated.

4.3 *Atmospheric signals of pollution at floodplain lakes*

Declining river discharge and climate warming in northern Alberta have led to changes in the flood regime of the river (Schindler & Donahue, 2006; Wolfe *et al.*, 2008a), which has resulted in reduction of flood frequency in recent decades at most of the floodplain lakes used in this study. The transition from strong to weak flood-influence at many of these lakes resulted in a shift from dominantly allochthonous sediment inputs to more autochthonous-generated organic matter. This transition to greater isolation of the basins from the Athabasca River floodwaters occurred at Up 17 after ~1994, Up 10 after ~1990, Down 1 after ~1988, and Down 26 after ~2014. The decline in flood frequency makes these sites unhelpful in assessing recent river pollution, but provided opportunity to evaluate these sites for deposition of aerially-transported pollution at the study sites closest to mining activities.

Results of this study display evidence of V and Ni enrichment above the Al-normalized baseline in weakly flood-influenced sediments at lakes very close to AR6 (within 20 km), suggesting detection of localized atmospheric pollution where flooding became less frequent due to reduction of river discharge. For V, excess flux calculations show a dramatic rise to ~16x baseline in 1973 and ~14x baseline in 1988 for Up 10 and Down 1, respectively (Figure 13A). These results are consistent with the timings of PAH increases recorded at nearby lakes in the AOSR by Kurek *et al.* (2013), which indicated that since ~1970-1980, Σ PAH concentrations have risen sharply. The alignment of these findings with established patterns of increasing air

pollution at lakes that receive no flood influence, suggests the study lakes capture an accurate record of airborne metal pollution for the AOSR.

As oil sands surface mining and bitumen processing activities have improved over time, it is likely that sources of atmospheric pollutants to the landscape have changed as well, as suggested by studies of Jautzy *et al.* (2013), Kurek *et al.* (2013), and Cooke *et al.* (2017). In the early days of oil sands activity (~1978-1993), conveyer belt dust and stack emissions were two predominant sources of metal-associated fugitive dust released to the landscape (Landis *et al.*, 2012; Atkinson, 2017). At Up 10, the V excess flux reaches a peak ~16x the baseline ΔF_{adj} in the early 1970s, and then begins to decline around 1980 to an excess flux of only ~4x baseline ΔF_{adj} in recent years (Figure 13). The pattern of decreasing V flux at Up 10 is similar to temporal metal patterns detected by Cooke *et al.* (2017). At near-field lakes NE13 and NE20 (< 20 km away from AR6), Cooke *et al.* (2017) observed that V flux ratios rose to 24x the baseline at NE13 in the 1970s and 15x the baseline at NE20 in the 1980s, coincident with increased dust emissions during this time. In recent decades, however, the flux in metals has declined substantially to ~8 at both headwater lakes, which has been attributed to modern improvements in mining technologies such as the addition of electrostatic precipitators on emissions stacks (late 1970s) and decommissioning of the conveyer belts (early 1990s).

Despite these improvements to mining technologies since the 1990s, aerial deposition continues in the AOSR, as demonstrated by the black snow filters presented in Kelly *et al.* (2009) as well as subsequent snowpack studies (e.g., Kirk *et al.*, 2014; Manzano *et al.*, 2016). Here, it is evident primarily in the V excess flux calculated for post-1983 sediments in the Down 1 sediment record, which continue to be high and above background levels (ΔF_{adj} peaks ~17x the baseline in 2005 and remains at ~15x baseline in 2015), unlike the recent decline

observed at lake Up 10 (Figure 13) and headwater lakes NE13 and NE20 (Cooke *et al.*, 2017). Possible sources of the continuation of airborne deposition to lake Down 1 include wind-blown particulate matter from open pit mining, wind-blown petcoke dust from stockpiling, stack emissions from the process of upgrading bitumen, fine tailings from reclamation sites, land disturbance from mining activities, emissions from vehicles, or dust from activity on haul roads. Zhang *et al.* (2016) suggest that the primary source of modern aerial deposition in the AOSR is petcoke dust, which is heavily enriched in V and Ni. Using a chemical mass-balance model to quantify the contribution of prospective PAH and metal sources to moss and peat contamination in the AOSR, Zhang *et al.* (2016) estimated that mean V and Ni contributions to moss from delayed petcoke as a source were 30% and 21%, respectively. Down 1 is located on the east side of the river, across from stockpiled petcoke dust, and so this may be the origin of the excess V and Ni observed in the lake sediment record.

4.4 *EF development for establishing a foundation for ongoing monitoring*

The expression of metals concentration data as an enrichment factor allows concentration data to be presented as the magnitude above the pre-industrial baseline, and to present the data in a chronological sequence to identify the timing of changes. This is a distinct advantage over simply expressing the data as a crossplot of the metal of interest normalized to Al. The use of enrichment factors in evaluating river sediments can be a useful tool to add value to using monitoring data in the future. EFs express the data as the number of doublings of the metal concentration above the pre-industrial baseline ($EF = 2 =$ two times higher than baseline), allowing for simple quantification of the extent of pollution. As we show in Figure 12, EFs also allow for the interpretation of sediment samples collected from the Athabasca River for evidence of pollution, including the samples collected by RAMP and JOSM. Since the data can be plotted

by year, trends can be more easily evaluated, providing an ongoing application to interpret monitoring data in the Athabasca River which was not possible before.

Chapter 5 – Conclusions, Implications, and Recommendations

5.1 *Summary of findings*

This study examined sediment cores from floodplain lakes located upstream and downstream of major oil sands activities along the Athabasca River in the Alberta Oil Sands Region. Using a paleolimnological approach, pre-industrial levels of bitumen-associated metals V and Ni were evaluated and assessed for post-industrial river and atmospheric pollution. This study is the first paleolimnological investigation into lakes located on the floodplain of the lower Athabasca River within the AOSR, responding to recommendations in the Expert Panel Report (2010) and the JOSM monitoring implementation plan (2011), to specifically target and investigate pre-industrial river-supplied sediment to establish baseline, reference conditions.

Pre-industrial baselines for Athabasca River sediment V and Ni concentrations were developed to detect pollution (i.e., when > 2.5% of samples above the upper 95% P.I.) and to quantify the magnitude of pollution (as EF and ΔF_{adj} values) since the onset of development. Sediments analyzed from floodplain lakes along the Athabasca River do not show evidence of V or Ni enrichment in post-industrial river-supplied sediment at these sites (Down 26 and Down 58). Flood influence has declined at several of the lakes due to declining river flows in recent decades. Enrichment above the natural range of variation of V in lakes within 10 km of AR6 (Up 10 and Down 1), and enrichment of Ni at lakes Up 17 and Down 1 was present in modern, weakly flood-influenced sediment, indicating local atmospheric deposition. In fact, some upper sediment samples at Down 1 exceed the chronic hazardous HC5 concentration of 50 $\mu\text{g V/g}$ (Schiffer & Liber, 2017). The evidence of continuing V and Ni pollution at Down 1 may indicate localised pollution from nearby petcoke stockpiles at the Mildred Lake Mine, as petcoke is

highly enriched in both V and Ni (up to 1000 mg/kg, or higher), and stores are located nearby, across the river from Down 1.

Enrichment was detected in samples collected by the former monitoring program RAMP, which was criticized for its inability to detect pollution or evaluate trends in the Athabasca River. Elevated levels of V and Ni in RAMP (2000, 2002) river-bottom sediments, and Ni in JOSM (2012, 2014) river-bottom sediments, was detected at key depositional locations along the river, usually near, or downstream of, tributary mouths such as the Steepbank, MacKay, and Ells rivers. Enrichment of Ni in JOSM (2012-2014) suspended sediment is observed mainly at upstream sampling locations, and therefore attributed to natural loadings from the river and its upstream tributaries (e.g., Clearwater River) that contribute a smaller sediment grain size. V and Ni sediment quality guidelines for the protection of aquatic life were not exceeded at any of the river sampling locations. Archived RAMP samples and current JOSM samples can now be evaluated for contaminant enrichment relative to a pre-industrial baseline.

5.2 *Research significance and implications*

Where pre-industrial measurements of river sediment are unavailable, and the monitoring time frame is too short to detect any trends, inference of baseline conditions using paleolimnological approaches is a valuable tool (Forstner & Müller, 1981; Smol, 1992). Due to the impact of multiple stressors in the AOSR, the determination of baseline or reference conditions for the Athabasca River has proved to be difficult. This study responded to recommendations in the Expert Panel Report on the state of oil sands monitoring, which highlighted the need to better establish pre-industrial baseline conditions in the AOSR and recommended the use of floodplain lakes along the Athabasca River as a means to evaluate future river trends (Dowdeswell *et al.*, 2010). The research questions and methodologies used to

outline the research objectives of this study also align with the baseline monitoring goals of the new JOSM program, which was developed in response to the 2010 report. JOSM highlights the need for lake sediment coring and additional paleolimnological analyses to help establish regional and localized baseline conditions, which they acknowledge are a key requirement to evaluate environmental change in the AOSR (Wrona & di Cenzo, 2011). This study is a valuable contribution to knowledge of baseline conditions in the lower Athabasca River floodplain, as it shows that the sediment records from floodplain lakes can be used to assess regional, pre-industrial concentrations of metals in sediment conveyed by the Athabasca River and evaluate the magnitude of post-industrial metals enrichment.

Predictions of future warming in northern Alberta are rising coincident with industrial development (Gosselin *et al.*, 2010; Timoney & Lee, 2011). Coupled with expanding industrial activity in the lower Athabasca are threats of reduced snow-pack in the headwaters and other upstream stressors (e.g., agriculture, pulp and paper mills, population growth, etc.), making the lower Athabasca River increasingly vulnerable to ecological degradation (Schindler & Donahue, 2006). The evidence of declining Athabasca River influence was seen in 4 of the 5 floodplain lakes analyzed in this study, which have become increasingly isolated from the river after having been strongly flood-influenced for several decades. This prevents the ability to use recent sediments at these lakes to evaluate for river pollution. Instead, these lakes have become recorders of pollution by aerial pathways, particularly those within 20 km of AR6. Water levels are expected to continue declining in these lakes and this provides incentive to keep monitoring them as an atmospheric archive, upon which to examine the legacy of bitumen mining activities in the AOSR.

This study showed that long term, baseline data from river-influenced lakes can be informative to the interpretation of current river monitoring data. Sample collection by RAMP was done in such a way that trends could not be evaluated (e.g. inconsistent sampling times, locations, methodologies, etc.) (Dowdeswell *et al.*, 2010; Gosselin *et al.*, 2010). Using the method this study employed, the RAMP/JOSM monitoring database can be utilized to interpret post-industrial metal concentrations against pre-industrial values. This has important implications for JOSM as they work towards developing a more strategic monitoring framework in the AOSR that encompasses an understanding of natural and industrial sources of contaminants and their pathways of release to the environment, and that situates that information in an understanding of decadal from multi-decadal variability.

5.3 *Future recommendations*

The new JOSM monitoring plan aims to establish long-term monitoring sites to more effectively evaluate trends in anthropogenic influence across the region. It is recommended that the focus of future sediment sampling should be on suspended sediment at key locations along the Athabasca River, given that such data can be compared to the pre-industrial floodplain baselines to detect and quantify contaminant enrichment and evaluate trends. This is the finer-grained sediment that will end up being deposited in the floodplain lakes and other slow-moving depositional areas and will bind more of the metals that enter the river, and is therefore more representative than the coarser-grained river-bottom sediment. In addition to focusing on suspended sediment along the Athabasca mainstem, it is recommended that spring be chosen as a key sampling time as well. Currently, suspended sediment data are only available from the winter, fall, and summer. This is not as useful in assessing river contaminant loadings, as expected river loadings are lower. Spring sampling of river sediment could be a way to

potentially detect influxes of contaminated snowpack to the Athabasca River, and assess the concentrations of contaminants in river sediment. The spring and early summer is also the peak time of exposure risk for aquatic organisms during sensitive life stages, and therefore a key period to assess potential risks to vulnerable river species (Colavecchia *et al.*, 2007). Due to hazardous conditions along the river when it is ice jamming, which would make sampling the river dangerous to people and equipment, flood sediment deposited on levees and the adjacent floodplain of the river shortly after floodwaters recede might be the best course of action. The flood deposit sample analyzed in this study, from the 2017 spring flood, demonstrated this application. In this sample, collected at an upstream site ~30 km from AR6, the ratios of the metals of interest were consistent with the baseline linear regression. Analysis of flood deposit samples more proximal to, and downstream of, industrial activity would be a key next step.

The normalized V and Ni baselines established in this study provide a starting point to evaluate river monitoring data collected in the past, present, and future, for evidence of pollution. Expanding on this method, baselines could be developed for other metals of interest, as well as PAHs. Paleolimnology studies at additional floodplain lakes in the AOSR are also recommended, to provide additional pre-industrial river information to the baseline. In this study, a binary approach to generally defining sediment flooding intervals was applied, using simple methods of loss-on-ignition and organic carbon and nitrogen elemental analyses. Future studies could employ Bayesian mixing models (e.g., MixSIAR, an open-source R package for mixing systems) to more accurately determine the relative source proportion contributions of autochthonous and allochthonous sediment at a finer scale (for example, Stock *et al.*, 2018). The use of suspended sediment as a river end member, as opposed to river-bottom sediment, should be explored as this is likely more representative of the type of sediment that ultimately ends up in

the floodplain lakes. Paleolimnological investigations could also continue in the floodplains along some of the major tributaries of the Athabasca River, including the Steepbank, Muskeg, Mackay, Ells, and Firebag rivers. Sites downstream of tributaries remain valuable in assessing contaminant concentrations delivered by the tributaries, but as this study determined, they may not be comparable to the floodplain lakes pre-industrial baselines which reflect the Athabasca River mainstem. From examination of the tributaries on Google Earth, there appear to be a few options for floodplain lakes to core, particularly several kilometers upstream, and away from the AOSR, which could provide an adequate control. Sediment monitoring along the tributaries could then be applied to baselines that better reflect the natural geology of the tributaries.

The missing knowledge of pre-industrial Athabasca River contaminant concentrations has been a key area of concern surrounding the interpretation of river monitoring data in the AOSR for decades. Today, the combined influences of multiple environmental stressors (e.g., climate change, declining river discharge) with industrial expansion, provide more incentive than ever to understand natural variation in this river system. According to Reuther (2009), effective monitoring involves choosing meaningful and achievable objectives, and designing a proper strategy and method. As the JOSM program continues to grow its monitoring scope, evolve with modern monitoring practices, and adapt to new scientific findings from monitoring activities, the governments of Alberta and Canada should continue to evaluate and interpret monitoring data in a long-term context whenever possible. Surface sediments from the floodplain lakes used in this study can continue to be collected and assessed for trends in aerial deposition and as markers of changing river dynamics. As well, following any efforts to better store and control petcoke in the AOSR, it would be interesting to monitor potential changes in sediment and water chemistry in proximal aquatic ecosystems (e.g., Down 1). If we continue to monitor the same locations

consistently, seasonal and yearly trends in contaminants can be evaluated, especially if the oil sands industry implements beneficial changes and wants to know if these changes are having a positive impact.

River systems are complex and dynamic, and no one monitoring site or event is going to be representative of the whole river, with all its seasonal changes. Monitoring of the Athabasca River in the AOSR must be strategic in its efforts to establish representative monitoring sites and frame modern monitoring data in a long-term perspective. Oil sands industrial activities are projected to keep expanding (CAPP, 2018c), and knowledge of natural, baseline conditions in AOSR aquatic ecosystems is of utmost importance for the evaluation of pollution. In demonstrating the application of regional-specific Athabasca River sediment-metal baselines, the state of knowledge of pre-industrial conditions for the Athabasca River has been advanced, setting a new model for the future of river monitoring in the AOSR.

References

- Alberta Energy Regulator. (2014). ST98–2014: Alberta’s Energy Reserves 2013 and Supply/Demand Outlook 2014–2023. Retrieved from <https://www.aer.ca/documents/sts/ST98/ST98-2014.pdf>
- Alberta Environment & Parks. (2017). Flood Hazard Mapping. Retrieved from <http://aep.alberta.ca/water/programs-and-services/flood-hazard-identification-program/flood-hazard-mapping.aspx>
- Appleby, P. G. (2001). Chronostratigraphic techniques in recent sediments. In: Last WM, Smol JP, editors. Tracking environmental change using lake sediments: Basin analysis, coring, and chronological techniques. Dordrecht: Kluwer Academic Publishers, pp. 171–203.
- Atkinson, N. (2017). Landscapes of the Alberta Oil Sands. In *Landscapes and Landforms of Western Canada* (pp. 395-410). Springer, Cham.
- Audry, S., Schäfer, J., Blanc, G., & Jouanneau, J. M. (2004). Fifty-year sedimentary record of heavy metal pollution (Cd, Zn, Cu, Pb) in the Lot River reservoirs (France). *Environmental Pollution*, 132(3), 413-426.
- Balogh, S. J., Engstrom, D. R., Almendinger, J. E., Meyer, M. L., & Johnson, D. K. (1999). History of mercury loading in the Upper Mississippi River reconstructed from the sediments of Lake Pepin. *Environmental Science & Technology*, 33(19), 3297-3302.
- Balogh, S. J., Engstrom, D. R., Almendinger, J. E., McDermott, C., Hu, J., Nollet, Y. H., ... & Johnson, D. K. (2009). A sediment record of trace metal loadings in the Upper Mississippi River. *Journal of Paleolimnology*, 41(4), 623-639.
- Barton, D. R., & Wallace, R. R. (1979). Effects of eroding oil sand and periodic flooding on benthic macroinvertebrate communities in a brown-water stream in northeastern Alberta, Canada. *Canadian Journal of Zoology*, 57(3), 533-541.
- Binford, M. W. (1990). Calculation and uncertainty analysis of ^{210}Pb dates for PIRLA project lake sediment cores. *Journal of Paleolimnology*, 3: 253–267.
- Bird, G., Brewer, P. A., Macklin, M. G., Nikolova, M., Kotsev, T., Mollov, M., & Swain, C. (2010). Quantifying sediment-associated metal dispersal using Pb isotopes: Application of binary and multivariate mixing models at the catchment-scale. *Environmental pollution*, 158(6), 2158-2169.
- Blais, J. M., & Donahue, W. F. (2015). Comment on “Sphagnum mosses from 21 ombrotrophic bogs in the Athabasca bituminous sands region show no significant atmospheric contamination of ‘heavy metals’”. *Environmental Science & Technology*, 49(10), 6352-6353.

- Boës, X., Rydberg, J., Martinez-Cortizas, A., Bindler, R., & Renberg, I. (2011). Evaluation of conservative lithogenic elements (Ti, Zr, Al, and Rb) to study anthropogenic element enrichments in lake sediments. *Journal of Paleolimnology*, 46(1), 75-87.
- Brock, B. E., Martin, M. E., Mongeon, C. L., Sokal, M. A., Wesche, S. D., Armitage, D., ... & Edwards, T. W. D. (2010). Flood frequency variability during the past 80 years in the Slave River Delta, NWT, as determined from multi-proxy paleolimnological analysis. *Canadian Water Resources Journal*, 35(3), 281-300.
- Canadian Association of Petroleum Producers (CAPP). (2018a). Canada's oil sands fact book. Publication no. 2018-0010, p.31. Retrieved from <https://www.capp.ca/publications-and-statistics/publications/316441>
- Canadian Association of Petroleum Producers (CAPP). (2018b). Oil sands history and milestones. Retrieved from <https://www.canadasoilsands.ca/en/what-are-the-oil-sands/oil-sands-history-and-milestones>
- Canadian Association of Petroleum Producers (CAPP). (2018c). 2018 Crude oil forecast, markets and transportation. Retrieved from <https://www.capp.ca/publications-and-statistics/crude-oil-forecast>
- Canadian Council of Ministers of the Environment (CCME). (2015). Canadian soil quality guidelines for the protection of environmental and human health: nickel. In: Canadian environmental quality guidelines, 1999, Canadian Council of Ministers of the Environment, Winnipeg.
- Canadian Council of Ministers of the Environment (CCME). (2001). Canadian Sediment Quality Guidelines for the Protection of Aquatic Life (Winnipeg: Canadian Council of Ministers of the Environment).
- Chapman, D. V. (Ed.). (1996). Water quality assessments: a guide to the use of biota, sediments and water in environmental monitoring. Published on behalf of the United Nations Educational, Scientific and Cultural Organization, the World Health Organization, & UN Environment Programme. University Press, Cambridge. Retrieved from http://www.who.int/water_sanitation_health/resourcesquality/watqualassess.pdf
- Cohen, A. S. (2003). Paleolimnology: the history and evolution of lake systems. Oxford University Press.
- Colavecchia, M. V., Backus, S. M., Hodson, P. V., & Parrott, J. L. (2004). Toxicity of oil sands to early life stages of fathead minnows (*Pimephales promelas*). *Environmental Toxicology and Chemistry*, 23(7), 1709-1718.

- Colavecchia, M. V., Hodson, P. V., & Parrott, J. L. (2006). CYP1A induction and blue sac disease in early life stages of white suckers (*Catostomus commersoni*) exposed to oil sands. *Journal of Toxicology and Environmental Health, Part A*, 69(10), 967-994.
- Colavecchia, M. V., Hodson, P. V., & Parrott, J. L. (2007). The relationships among CYP1A induction, toxicity, and eye pathology in early life stages of fish exposed to oil sands. *Journal of Toxicology and Environmental Health, Part A*, 70(18), 1542-1555.
- Conly, F. M., Crosley, R. W., & Headley, J. V. (2002). Characterizing sediment sources and natural hydrocarbon inputs in the lower Athabasca River, Canada. *Journal of Environmental Engineering and Science*, 1(3), 187-199.
- Conly, F. M., Crosley, R. W., Headley, J. V., & Quagraine, E. K. (2007). Assessment of metals in bed and suspended sediments in tributaries of the Lower Athabasca River. *Journal of Environmental Science and Health*, 42(8), 1021-1028.
- Cooke, C. A., Kirk, J. L., Muir, D. C., Wiklund, J. A., Wang, X., Gleason, A., & Evans, M. S. (2017). Spatial and temporal patterns in trace element deposition to lakes in the Athabasca oil sands region (Alberta, Canada). *Environmental Research Letters*, 12(12), 124001.
- Curtis, C. J., Flower, R., Neil, R. O. S. E., Shilland, J., Simpson, G. L., Turner, S., ... & Sergi, P. L. A. (2010). Palaeolimnological assessment of lake acidification and environmental change in the Athabasca Oil Sands Region, Alberta. *Journal of Limnology*, 69(1s), 92-104.
- Cronmiller, J. G., & Noble, B. F. (2018). The discontinuity of environmental effects monitoring in the Lower Athabasca region of Alberta, Canada: institutional challenges to long-term monitoring and cumulative effects management. *Environmental Reviews*, 26(2), 169-180.
- Davis, R. B., Norton, S. A., Hess, C. T., & Brakke, D. F. (1983). Paleolimnological reconstruction of the effects of atmospheric deposition of acids and heavy metals on the chemistry and biology of lakes in New England and Norway. *Hydrobiologia*, 103(1), 113-123.
- Dowdeswell, L., Dillon, P., Ghoshal, S., Miall, A., Rasmussen, J., & Smol, J. P. (2010). A foundation for the future: building an environmental monitoring system for the oil sands. Retrieved from the Government of Canada Publications website: http://publications.gc.ca/collections/collection_2011/ec/En4-148-2010-eng.pdf
- Environment and Climate Change Canada (ECCC). (2016). Federal Environmental Quality Guidelines Vanadium. Retrieved from <http://www.ec.gc.ca/ese-ees/default.asp?lang=En&n=48D3A655-1>
- Ek, A. S., & Renberg, I. (2001). Heavy metal pollution and lake acidity changes caused by one thousand years of copper mining at Falun, central Sweden. *Journal of Paleolimnology*, 26(1), 89-107.

- Evans, M., Davies, M., Janzen, K., Muir, D., Hazewinkel, R., Kirk, J., & de Boer, D. (2016). PAH distributions in sediments in the oil sands monitoring area and western Lake Athabasca: concentration, composition and diagnostic ratios. *Environmental Pollution*, 213, 671-687.
- Förstner, U., & Müller, G. (1981). Concentrations of heavy metals and polycyclic aromatic hydrocarbons in river sediments: geochemical background, man's influence and environmental impact. *GeoJournal*, 5(5), 417.
- Giovannetti, J. (2016, 2 August). Fort McMurray hit with 'biblical' flood amid wildfire recovery efforts. The Globe and Mail. Retrieved from <https://www.theglobeandmail.com/news/national/fort-mcmurray-hit-with-biblical-flood-amid-wildfire-recovery-efforts/article31250698/>
- Glew, J. R. (1988). A portable extruding device for close interval sectioning of unconsolidated core samples. *Journal of Paleolimnology*, 1(3), 235-239.
- Glew, J. R., Smol, J. P., & Last, W. M. (2002). Sediment core collection and extrusion. In: Tracking environmental change using lake sediments (pp. 73-105). Springer, Dordrecht.
- Gosselin, P., Hruday, S. E., Naeth, M. A., Plourde, A., Therrien, R., Van Der Kraak, G., & Xu, Z. (2010). Environmental and health impacts of Canada's oil sands industry. Royal Society of Canada Ottawa, Ontario, Canada.
- Hatfield Consultants. (2009). RAMP: Technical Design and Rationale. Retrieved from http://www.ramp-alberta.org/UserFiles/File/RAMP_Design_&_Rationale.pdf
- Hatfield Consultants. (2016). Regional aquatics monitoring in support of the Joint Oil Sands Monitoring Plan final 2015 program report. Retrieved from http://www.ramp-alberta.org/UserFiles/File/AnnualReports/2015/1_Regional%20Aquatics%20Monitoring%20in%20support%20of%20the%20JOSMP_Final%20Program%20Report.pdf
- Hazewinkel, R. R., Wolfe, A. P., Pla, S., Curtis, C., & Hadley, K. (2008). Have atmospheric emissions from the Athabasca Oil Sands impacted lakes in northeastern Alberta, Canada?. *Canadian Journal of Fisheries and Aquatic Sciences*, 65(8), 1554-1567.
- Headley, J. V., & McMartin, D. W. (2004). A review of the occurrence and fate of naphthenic acids in aquatic environments. *Journal of Environmental Science and Health, Part A*, 39(8), 1989-2010.

- Hein, F. J., & Cotterill, D. K. (2006). The Athabasca oil sands—a regional geological perspective, Fort McMurray area, Alberta, Canada. *Natural Resources Research*, 15(2), 85-102.
- Heiri, O., Lotter, A. F., & Lemcke, G. (2001). Loss on ignition as a method for estimating organic and carbonate content in sediments: reproducibility and comparability of results. *Journal of Paleolimnology*, 25(1), 101-110.
- Hodgson, G. W. (1954). Vanadium, nickel, and iron trace metals in crude oils of western Canada. *AAPG Bulletin*, 38(12), 2537-2554.
- Jack, T. R., Sullivan, E. A., & Zajic, J. E. (1979). Leaching of vanadium and other metals from Athabasca Oil Sands coke and coke ash. *Fuel*, 58(8), 589-594.
- Jacobs, F. S., & Filby, R. H. (1983). Solvent extraction of oil-sand components for determination of trace elements by neutron activation analysis. *Analytical Chemistry*, 55(1), 74-77.
- Jautzy, J., Ahad, J. M., Gobeil, C., & Savard, M. M. (2013). Century-long source apportionment of PAHs in Athabasca oil sands region lakes using diagnostic ratios and compound-specific carbon isotope signatures. *Environmental Science & Technology*, 47(12), 6155-6163.
- Jernström, J., Lehto, J., Dauvalter, V. A., Hatakka, A., Leskinen, A., & Paatero, J. (2010). Heavy metals in bottom sediments of Lake Umbozero in Murmansk Region, Russia. *Environmental Monitoring and Assessment*, 161(1-4), 93-105.
- Joint Canada/ Alberta Implementation Plan for Oil Sands Monitoring. (2012). Governments of Canada and Alberta. Retrieved from <https://www.canada.ca/en/environment-climate-change/services/oil-sands-monitoring/documents-reports.html>
- Kelly, E. N., Short, J. W., Schindler, D. W., Hodson, P. V., Ma, M., Kwan, A. K., & Fortin, B. L. (2009). Oil sands development contributes polycyclic aromatic compounds to the Athabasca River and its tributaries. *Proceedings of the National Academy of Sciences*, pnas-0912050106.
- Kelly, E. N., Schindler, D. W., Hodson, P. V., Short, J. W., Radmanovich, R., & Nielsen, C. C. (2010). Oil sands development contributes elements toxic at low concentrations to the Athabasca River and its tributaries. *Proceedings of the National Academy of Sciences*, 107(37), 16178-16183.
- Kersten, M., & Smedes, F. (2002). Normalization procedures for sediment contaminants in spatial and temporal trend monitoring. *Journal of Environmental Monitoring*, 4(1), 109-115.
- Kirk, J. L., Muir, D. C., Gleason, A., Wang, X., Lawson, G., Frank, R. A., ... & Wrona, F. (2014). Atmospheric deposition of mercury and methylmercury to landscapes and

- waterbodies of the Athabasca oil sands region. *Environmental Science & Technology*, 48(13), 7374-7383.
- Kurek, J., Kirk, J. L., Muir, D. C., Wang, X., Evans, M. S., & Smol, J. P. (2013). Legacy of a half century of Athabasca oil sands development recorded by lake ecosystems. *Proceedings of the National Academy of Sciences*, 110(5), 1761-1766.
- Landis, M. S., Pancras, J. P., Graney, J. R., Stevens, R. K., Percy, K. E., & Krupa, S. (2012). Receptor modeling of epiphytic lichens to elucidate the sources and spatial distribution of inorganic air pollution in the Athabasca Oil Sands Region. *Alberta Oil Sands: Energy, Industry and the Environment* ed K E Percy (Oxford: Elsevier Press), Volume 11: pp. 427-467.
- Lima, A. C., & Wrona, F. J. (2018). Multiple threats and stressors to the Athabasca River Basin: What do we know so far?. *Science of The Total Environment*, 690, 640–651.
- Lintern, A., Leahy, P. J., Zawadzki, A., Gadd, P., Heijnis, H., Jacobsen, G., ... & McCarthy, D. T. (2016a). Sediment cores as archives of historical changes in floodplain lake hydrology. *Science of the Total Environment*, 544, 1008-1019.
- Lintern, A., Leahy, P. J., Heijnis, H., Zawadzki, A., Gadd, P., Jacobsen, G., ... & McCarthy, D. T. (2016b). Identifying heavy metal levels in historical flood water deposits using sediment cores. *Water Research*, 105, 34-46.
- Loring, D. H. (1991). Normalization of heavy-metal data from estuarine and coastal sediments. *ICES Journal of Marine Science*, 48(1), 101-115.
- MacDonald, L. A., Wiklund, J. A., Elmes, M. C., Wolfe, B. B., & Hall, R. I. (2016). Paleolimnological assessment of riverine and atmospheric pathways and sources of metal deposition at a floodplain lake (Slave River Delta, Northwest Territories, Canada). *Science of the Total Environment*, 544, 811-823.
- Manzano, C. A., Muir, D., Kirk, J., Teixeira, C., Siu, M., Wang, X., ... & Kelly, E. (2016). Temporal variation in the deposition of polycyclic aromatic compounds in snow in the Athabasca Oil Sands area of Alberta. *Environmental Monitoring and Assessment*, 188(9), 542.
- Mazerolle, M. J. (2017). AICcmodavg: Model Selection and Multimodel Inference Based on (Q)AIC(c). R Package Version 2.1-1. Available at <https://cran.r-project.org/web/packages/AICcmodavg/AICcmodavg.pdf>
- McLachlan, S., 2014. “Water is a living thing”. Environmental and Human Health Implications of the Athabasca Oil Sands for the Mikisew Cree First Nation and Athabasca Chipewyan First Nation in Northern Alberta. Phase Two Report: July 7, 2014

- McLeod, A. I. (2011). kendall: Kendall rank correlation and Mann-Kendall trend test. R Package Version 2.2. Available at <https://cran.r-project.org/web/packages/Kendall/Kendall.pdf>
- Meyers, P. A., & Teranes, J. L. (2002). Sediment organic matter. In Tracking environmental change using lake sediments (pp. 239-269). Springer, Dordrecht.
- Moore, J. W., & Ramamoorthy, S. (1984). Nickel. In *Heavy Metals in Natural Waters* (pp. 161-181). Springer, New York, NY.
- Muir, D. C. G., Wang, X., Yang, F., Nguyen, N., Jackson, T. A., Evans, M. S., ... & Smol, J. P. (2009). Spatial trends and historical deposition of mercury in eastern and northern Canada inferred from lake sediment cores. *Environmental Science & Technology*, 43(13), 4802-4809.
- Müller, G. (1969). Index of geoaccumulation in sediments of the Rhine River. *Geojournal*, 2, 108-118.
- Muggeo, V. M. (2017). segmented: Regression Models with Break-Points / Change-Points Estimation. R Package Version 0.5-3.0. Available at <https://cran.r-project.org/web/packages/segmented/segmented.pdf>
- Ota, Y., Kawahata, H., Sato, T., & Seto, K. (2017). Flooding history of Lake Nakaumi, western Japan, inferred from sediment records spanning the past 700 years. *Journal of Quaternary Science*, 32(8), 1063-1074.
- Parsons, B. G., Watmough, S. A., Dillon, P. J., & Somers, K. M. (2010). Relationships between lake water chemistry and benthic macroinvertebrates in the Athabasca Oil Sands Region, Alberta. *Journal of Limnology*, 69(1s), 118-125.
- Peeters, E. T., Gylstra, R., & Vos, J. H. (2004). Benthic macroinvertebrate community structure in relation to food and environmental variables. *Hydrobiologia*, 519(1-3), 103-115.
- Renberg, I. (1987). Concentration and annual accumulation values of heavy metals in lake sediments: their significance in studies of the history of heavy metal pollution. In *Paleolimnology IV* (pp. 379-385). Springer, Dordrecht.
- Reuther, R. (2009). Lake and river sediment monitoring. *Environmental monitoring Encyclopedia of Life Support Systems (EOLSS) vol, 2*, 120-47.
- Robbins, J. A. (1978) Geochemical and geophysical applications of radioactive lead. In: Nriagu JO, editor. *The biogeochemistry of lead in the environment*. Amsterdam: Elsevier. 285–393.
- Rooney, R. C., Bayley, S. E., & Schindler, D. W. (2012). Oil sands mining and reclamation cause massive loss of peatland and stored carbon. *Proceedings of the National Academy of Sciences*, 109(13), 4933-4937.

- Salonen, V. P., Tuovinen, N., & Valpola, S. (2006). History of mine drainage impact on Lake Orijärvi algal communities, SW Finland. *Journal of Paleolimnology*, 35(2), 289-303.
- Schelske, C. L., Peplow, A., Brenner, M., & Spencer, C. N. (1994). Low-background gamma counting: applications for 210 Pb dating of sediments. *Journal of Paleolimnology*, 10(2), 115-128.
- Schiffer, S., & Liber, K. (2017). Estimation of vanadium water quality benchmarks for the protection of aquatic life with relevance to the Athabasca Oil Sands region using species sensitivity distributions. *Environmental Toxicology and Chemistry*, 36(11), 3034-3044.
- Schindler, D. W., & Donahue, W. F. (2006). An impending water crisis in Canada's western prairie provinces. *Proceedings of the National Academy of Sciences*, 103(19), 7210-7216.
- Schindler, D. W. (2010). Tar sands need solid science. *Nature*, 468(7323), 499.
- Sediment quality. (2015). Regional Aquatics Monitoring Program monitoring database. Retrieved from <http://www.ramp-alberta.org/data/Sediment/default.aspx>
- Sediment quality mainstem and tributaries, oil sands region. (2016). Environment and Climate Change Canada Data. Retrieved from <http://donnees.ec.gc.ca/data/substances/monitor/sediment-oil-sands-region/sediment-quality-mainstem-and-tributaries-oil-sands-region/>
- Shotyk, W., Belland, R., Duke, J., Kempster, H., Krachler, M., Noernberg, T., ... & Zhang, S. (2014). Sphagnum mosses from 21 ombrotrophic bogs in the Athabasca Bituminous Sands region show no significant atmospheric contamination of “heavy metals”. *Environmental Science & Technology*, 48(21), 12603-12611.
- Shotyk, W., Appleby, P. G., Bicalho, B., Davies, L., Froese, D., Grant-Weaver, I., ... & Pelletier, R. (2016a). Peat bogs in northern Alberta, Canada reveal decades of declining atmospheric Pb contamination. *Geophysical Research Letters*, 43(18), 9964-9974.
- Shotyk, W., Bicalho, B., Cuss, C. W., Duke, M. J. M., Noernberg, T., Pelletier, R., ... & Zaccone, C. (2016b). Dust is the dominant source of “heavy metals” to peat moss (*Sphagnum fuscum*) in the bogs of the Athabasca Bituminous Sands region of northern Alberta. *Environment International*, 92, 494-506.
- Smol, J. P. (1992). Paleolimnology: an important tool for effective ecosystem management. *Journal of Aquatic Ecosystem Health*, 1(1), 49-58.
- Smol, J. P. (2009). *Pollution of lakes and rivers: a paleoenvironmental perspective*. John Wiley & Sons.

- Stock, B. C., Jackson, A. L., Ward, E. J., Parnell, A. C., Phillips, D. L., Semmens, B. X. (2018). Analyzing mixing systems using a new generation of Bayesian tracer mixing models. *PeerJ*, 6:e5096.
- Sturgess, P. K. (2014). Athabasca River historical review: provided at the request of the Alberta Flood Recovery Task Force. Alberta Water Smart, Water Management Solutions. Retrieved from <https://albertawater.com/docs-work/projects-and-research/>
- Summers, J. C., Kurek, J., Kirk, J. L., Muir, D. C., Wang, X., Wiklund, J. A., ... & Smol, J. P. (2016). Recent warming, rather than industrial emissions of bioavailable nutrients, is the dominant driver of lake primary production shifts across the Athabasca Oil Sands Region. *PLoS One*, 11(5), e0153987.
- Summers, J. C., Kurek, J., Rühland, K. M., Neville, E. E., & Smol, J. P. (2017). Assessment of multi-trophic changes in a shallow boreal lake simultaneously exposed to climate change and aerial deposition of contaminants from the Athabasca Oil Sands Region, Canada. *Science of the Total Environment*, 592, 573-583.
- Tchounwou, P. B., Yedjou, C. G., Patlolla, A. K., & Sutton, D. J. (2012). Heavy metal toxicity and the environment. In *Molecular, clinical and environmental toxicology* (pp. 133-164). Springer, Basel.
- Teffera, Y., Kusmierz, J. J., & Abramson, F. P. (1996). Continuous-flow isotope ratio mass spectrometry using the chemical reaction interface with either gas or liquid chromatographic introduction. *Analytical Chemistry*, 68(11), 1888-1894.
- Timoney, K. P., & Lee, P. (2009). Does the Alberta tar sands industry pollute? The scientific evidence. *The Open Conservation Biology Journal*, 3(2009), 65-81.
- Timoney, K. P., & Lee, P. (2011). Polycyclic aromatic hydrocarbons increase in Athabasca River Delta sediment: Temporal trends and environmental correlates. *Environmental Science & Technology*, 45(10), 4278-4284.
- United States Environmental Protection Agency (US EPA). (1998). Method 6020A: Inductively coupled plasma – mass spectrometry. Retrieved from <https://www.epa.gov/sites/production/files/2015-07/documents/epa-6020a.pdf>
- United States Environmental Protection Agency (US EPA). (2014). Toxic and priority pollutants under the Clean Water Act. Retrieved from <https://www.epa.gov/eg/toxic-and-priority-pollutants-under-clean-water-act#priority>
- Vangheluwe, M. L., Verdonck, F. A., Besser, J. M., Brumbaugh, W. G., Ingersoll, C. G., Schlekat, C. E., & Garman, E. R. (2013). Improving sediment-quality guidelines for nickel: Development and application of predictive bioavailability models to assess chronic toxicity

- of nickel in freshwater sediments. *Environmental Toxicology and Chemistry*, 32(11), 2507-2519.
- Ripley, B. (2002). MASS: Support Functions and Datasets for Venables and Ripley's MASS. R Package Version 7.3-51.1. Available at <https://cran.r-project.org/web/packages/MASS/MASS.pdf>
- Wang, J., Liu, G., Lu, L., Zhang, J., & Liu, H. (2015). Geochemical normalization and assessment of heavy metals (Cu, Pb, Zn, and Ni) in sediments from the Huaihe River, Anhui, China. *Catena*, 129, 30-38.
- Wiklund, J. A., Hall, R. I., Wolfe, B. B., Edwards, T. W., Farwell, A. J., & Dixon, D. G. (2014). Use of pre-industrial floodplain lake sediments to establish baseline river metal concentrations downstream of Alberta oil sands: a new approach for detecting pollution of rivers. *Environmental Research Letters*, 9(12), 124019.
- Wiklund, J. A., Hall, R. I., Wolfe, B. B., Edwards, T. W., Farwell, A. J., & Dixon, D. G. (2012). Has Alberta oil sands development increased far-field delivery of airborne contaminants to the Peace–Athabasca Delta?. *Science of the Total Environment*, 433, 379-382.
- Wiklund, J. A., Kirk, J. L., Muir, D. C., Carrier, J., Gleason, A., Yang, F., ... & Keating, J. (2018). Widespread atmospheric tellurium contamination in industrial and remote regions of Canada. *Environmental Science & Technology*, 52(11), 6137-6145.
- Winhold, T. & Bothe, R. (1993). Review of flood stage frequency estimates for the City of Fort McMurray: Final Report. Technical Services & Monitoring Division, Alberta Env & Parks.
- Wolfe, B. B., Hall, R. I., Edwards, T. W. D., Jarvis, S. R., Sinnatamby, R. N., Yi, Y., & Johnston, J. W. (2008a). Climate-driven shifts in quantity and seasonality of river discharge over the past 1000 years from the hydrographic apex of North America. *Geophysical Research Letters*, 35(24).
- Wolfe, B. B., Hall, R. I., Edwards, T. W. D., Vardy, S. R., Falcone, M. D., Sjunneskog, C., ... & van Driel, P. (2008b). Hydroecological responses of the Athabasca Delta, Canada, to changes in river flow and climate during the 20th century. *Ecohydrology*, 1(2), 131-148.
- Wrona, F. J., & di Cenzo, P. (Eds.). (2011). Lower Athabasca Water Quality Monitoring Program, Phase 1: Athabasca River Mainstem and Major Tributaries. Environment Canada, pp. 97.
- Zeileis, A., Grothendieck, G., Ryan, J. A., Ulrich, J. M., Andrews, F. (2018). zoo: S3 Infrastructure for Regular and Irregular Time Series (Z's Ordered Observations). R Package Version 1.8-4. Available at <https://cran.r-project.org/web/packages/zoo/zoo.pdf>

- Zhang, Y., Shotyk, W., Zaccone, C., Noernberg, T., Pelletier, R., Bicalho, B., ... & Martin, J. W. (2016). Airborne petcoke dust is a major source of polycyclic aromatic hydrocarbons in the Athabasca Oil Sands Region. *Environmental Science & Technology*, 50(4), 1711-1720.
- Zigah, P. K., Minor, E. C., Werne, J. P., & Leigh McCallister, S. (2012). An isotopic ($\delta^{14}\text{C}$, $\delta^{13}\text{C}$, and $\delta^{15}\text{N}$) investigation of the composition of particulate organic matter and zooplankton food sources in Lake Superior and across a size-gradient of aquatic systems. *Biogeosciences*, 9(9), 3663-3678.

Appendix A – Study site information

Table A1. Lake coring coordinates (latitude and longitude) for floodplain lakes Up 17, Up 10, Down 1, Down 26, and Down 58, and headwater lakes cored with the JOSM program NE13, NE20, and RAMP 418/Kearle.

Site ID	Latitude	Longitude
Up 17	56.85278	-111.4333
Up 10	56.96111	-111.4372
Down 1	57.02500	-111.4847
Down 26	57.21806	-111.6044
Down 58	57.52417	-111.5231
NE13 (JOSM)	57.07117	-111.4752
NE20 (JOSM)	57.12517	-111.5575
RAMP 418/ Kearle (JOSM)	57.29180	-111.2383

Table A2. RAMP & JOSM river sediment sampling locations (latitude and longitude) for river-bottom and suspended sediment.

Site ID	Monitoring Agency	Sediment type	Latitude	Longitude
ATR-DD-W	RAMP	River-bottom	57.45273	-111.616
ATR-MR-W	RAMP	River-bottom	57.13019	-111.608
ATR-DD-E	RAMP	River-bottom	57.4516	-111.605
ATR-MR-E	RAMP	River-bottom	57.1319	-111.603
ATR-ER	RAMP	River-bottom	58.35332	-111.542
ATR-SR-W	RAMP	River-bottom	57.01536	-111.481
ATR-SR-E	RAMP	River-bottom	57.01927	-111.479
ATR-DC-W	RAMP	River-bottom	56.82655	-111.408
ATR-DC-E	RAMP	River-bottom	56.82644	-111.408
ATR-UFM	RAMP	River-bottom	56.71833	-111.403
ATR-FR-W	RAMP	River-bottom	57.74684	-111.369
ATR-FC-E	RAMP	River-bottom	57.40829	-111.641
ATR-DC-CC	RAMP	River-bottom	56.82656	-111.409
ATR-FC-CC-D	RAMP	River-bottom	57.40902	-111.645
ATR-FC-E-D	RAMP	River-bottom	57.40959	-111.64
ATR-MR-W-D	RAMP	River-bottom	57.1323	-111.609
ATR-MR-E-D	RAMP	River-bottom	57.13303	-111.605
M0	JOSM	Suspended sediment	54.72363	-113.29
M2	JOSM	Suspended sediment	56.7186	-111.409
M3	JOSM	Suspended sediment	56.83859	-111.415
M4	JOSM	Suspended sediment	57.12697	-111.602
M9	JOSM	Suspended sediment	58.17258	-111.366
M0	JOSM	River-bottom	54.72691	-113.302
M1	JOSM	River-bottom	56.68025	-111.508
M2	JOSM	River-bottom	56.75048	-111.397
M3	JOSM	River-bottom	56.83536	-111.417
M4	JOSM	River-bottom	57.09341	-111.565
M6	JOSM	River-bottom	57.19812	-111.618
M7C	JOSM	River-bottom	57.50351	-111.546
M8	JOSM	River-bottom	57.67897	-111.406
M9	JOSM	River-bottom	58.05738	-111.371

Table A3. RAMP/JOSM sample site name location descriptors (sources: Hatfield Consultants, 2009; Wrona & diCenzo, 2011).

Site ID	Location description	Monitoring Agency
ATR-DD-W	Downstream of development (DD), West bank (W)	RAMP
ATR-MR-W	Upstream of Muskeg River (MR), West bank (W)	RAMP
ATR-DD-E	Downstream of development (DD), East bank (E)	RAMP
ATR-MR-E	Upstream of Muskeg River (MR), East bank (E)	RAMP
ATR-ER	Upstream of Embarras River (ER)	RAMP
ATR-SR-W	Upstream of Steepbank River (SR), West bank (W)	RAMP
ATR-SR-E	Upstream of Steepbank River (SR), East bank (E)	RAMP
ATR-DC-W	Upstream of Donald Creek (DC), West bank (W)	RAMP
ATR-DC-E	Upstream of Donald Creek (DC), East bank (E)	RAMP
ATR-UFM	Upstream of Fort McMurray (UFM)	RAMP
ATR-FR-W	Upstream of Firebag River (FR), West bank (W)	RAMP
ATR-FC-E	Upstream of Fort Creek (FC), East bank (E)	RAMP
ATR-DC-CC	Upstream of Donald Creek (DC), composite sample (CC)	RAMP
ATR-FC-CC-D	Downstream of Fort Creek (FC), composite sample (CC)	RAMP
ATR-FC-E-D	Downstream of Fort Creek (FC), East bank (E)	RAMP
ATR-MR-W-D	Downstream of Muskeg River (MR), West bank (W)	RAMP
ATR-MR-E-D	Downstream of Muskeg River (MR), East bank (E)	RAMP
M0	U/S of Ft. McMurray: Athabasca River at Athabasca	JOSM
M1	U/S of Ft. McMurray: Athabasca River at Mountain Rapids	JOSM
M2	U/S of Ft. McMurray (formerly: ATR-UFM)	JOSM
M3	D/S Ft. McMurray, U/S oil sands (formerly: ATR-DC)	JOSM
M4	D/S of Steepbank R, U/S of Muskeg R (formerly: ATR-MR)	JOSM
M5	D/S of Muskeg R, U/S of MacKay R	JOSM
M6	D/S of MacKay R, U/S of Ells R	JOSM
M7C	D/S of Ells R, U/S of Tar R	JOSM
M8	D/S of Calumet R, U/S of Firebag R (formerly: ATR-FR)	JOSM
M9	D/S of Firebag and near Embarras Airport	JOSM

Table A4. YSI probe (YSI ProDSS) data for limnological measurements taken at floodplain lakes at the time of coring for Up 17, Down 1, Down 26, Down 58 (October 2016) and Up 10 (July 2017 – denoted by a *). N/A = indicates measurement was below detection limit of the probe.

Lake ID	Depth (m)	Temperature (°C)	pH	Dissolved oxygen (%)	Turbidity (FNU)	Specific conductivity (µS/cm)
Up 17	1.4	8.3	7.87	66.5	1.0	762.0
Up 10*	4.7	25.2	8.43	121.7	N/A	740.0
Down 1	0.6	6.9	7.93	77.9	4.3	757.2
Down 26	N/A	7.0	8.21	63.7	16.3	864.0
Down 58	1.3	6.4	8.20	68.1	4.0	403.5

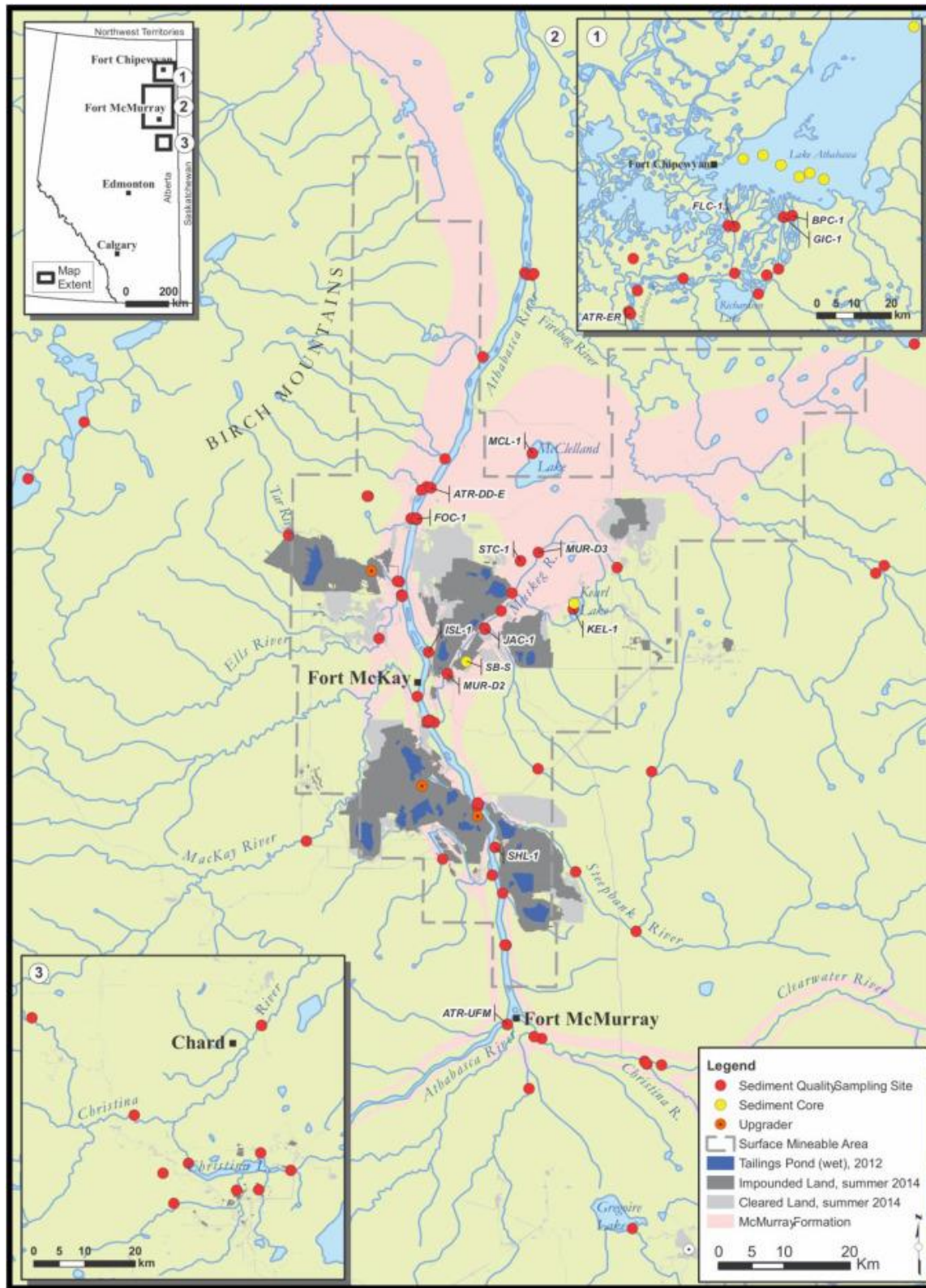


Figure A1. Map of the RAMP monitoring area (1997-2014) with sediment sampling locations indicated (red dots) (Hatfield Consultants, 2015).

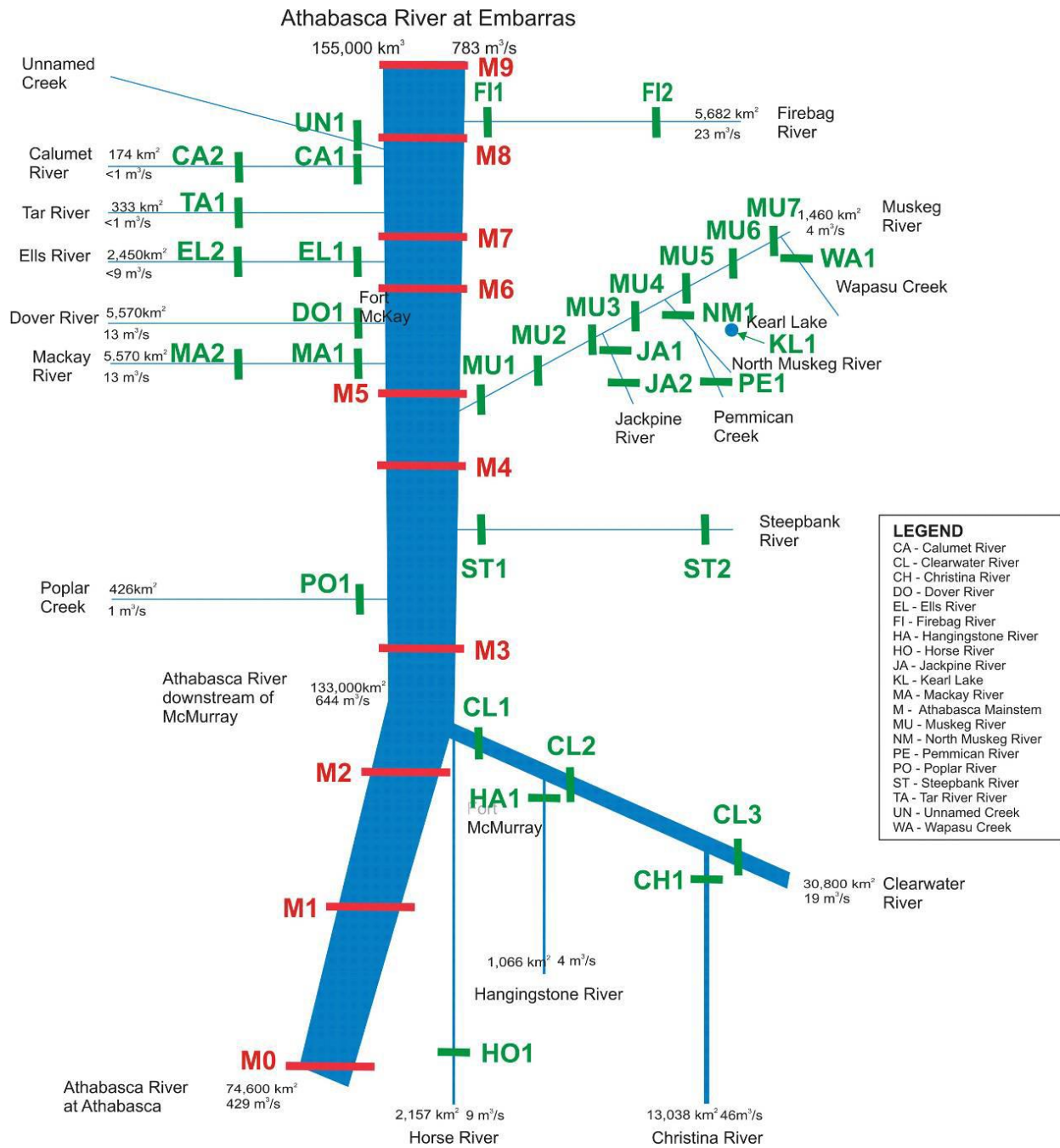


Figure A2. Schematic of the sampling site locations along the Athabasca River and key tributaries proposed for JOSM in the Phase 1 Water Quality Monitoring Plan for the Lower Athabasca (Wrona & DiCenzo, 2011).

Appendix B – Compiled loss-on-ignition & organic carbon and nitrogen elemental and isotope composition data and graphs

Table B1. Up 17: LOI data (water content (% H₂O), organic matter (% OM), mineral matter (%MM), and calcium carbonate (%CaCO₃)) and carbon & nitrogen data (%C, %N, C/N, δ¹³C, and δ¹⁵N) by CRS year (constant rate of supply).

Depth (cm)	CRS year	% H ₂ O	% OM	% MM	% CaCO ₃	% C	% N	C/N	δ ¹³ C	δ ¹⁵ N
1	2016	94.1211	18.2724	69.4352	27.9372	10.3323	1.0127	10.2023	-28.303	-0.4429
2	2016	89.3226	19.3548	74.552	13.8482	10.3323	1.0127	10.2023	-28.303	-0.4429
3	2015	80.036	16.6499	77.6329	12.9935	7.4578	0.7048	10.5808	-28.4305	-0.155
4	2014	73.8406	13.4799	81.0256	12.4875	6.4024	0.5719	11.1948	-28.3448	0.3645
5	2013	71.5757	12.987	80.7245	14.2919	5.9972	0.5606	10.6971	-28.6529	0.1821
6	2012	71.5962	11.5385	79.2735	20.8819	6.2068	0.6138	10.1126	-28.7638	-0.0896
7	2010	73.0339	11.1508	79.0565	22.2562	5.654	0.5574	10.144	-29.0282	0.3711
8	2009	74.7919	15.745	75.4992	19.8995	6.1135	0.5955	10.2655	-29.167	0.2557
9	2007	79.0495	17.037	73.7037	21.0438	8.6135	0.7984	10.7879	-29.6995	0.2738
10	2005	80.7494	20.4943	70.1339	21.2995	11.8618	1.0756	11.0283	-29.9332	0.0539
11	2003	81.064	24.7578	66.6308	19.5714	12.3973	1.1091	11.178	-29.8941	-0.00221
12	2001	79.5308	23.5912	68.3859	18.2339	13.4727	1.1759	11.4578	-29.2432	-0.21
13	1999	78.1375	23.5832	67.8245	19.528	10.7329	1.0122	10.6035	-28.5558	-0.3018
14	1997	77.3805	23.6234	67.4956	20.1841	10.7779	1.0149	10.6193	-28.3998	-0.2002
15	1994	71.9807	18.8937	71.3362	22.2048	9.5854	0.9061	10.5782	-28.555	0.1072
16	1992	69.068	17.263	72.6303	22.9698	10.4618	0.9632	10.8619	-28.1446	-0.1867
17	1990	61.8094	12.6834	79.2453	18.3438	8.1259	0.7519	10.8072	-29.3539	0.0105
18	1987	53.5656	10.4871	85.0812	10.0722	5.5654	0.5166	10.7733	-28.5005	0.0169
19	1986	54.3229	12.1435	83.7943	9.2323	5.3102	0.4082	13.0076	-27.7294	0.7783
20	1984	54.4896	10.8885	84.9303	9.5027	4.3541	0.3384	12.8677	-27.5071	0.6457
21	1981	49.9032	11.0166	85.5431	7.8188	4.8464	0.3634	13.3354	-27.5348	1.0958
22	1979	51.659	11.4525	84.6369	8.8878	4.8341	0.376	12.8568	-27.5898	0.7788
23	1977	53.2727	10.7067	84.1727	11.6377	4.4505	0.3611	12.3245	-27.6967	0.8224
24	1975	59.1027	11.7532	80.5583	17.474	5.9766	0.5053	11.828	-28.074	0.2331
25	1972	56.8244	11.4504	78.8505	22.0435	4.8565	0.4196	11.5745	-28.0792	0.3445
26	1970	53.5832	9.8211	81.3983	19.9561	5.1565	0.4243	12.152	-27.9433	0.1498
27	1966	50.3479	9.3032	83.7291	15.8357	4.4799	0.3749	11.9483	-27.8767	0.6778
28	1963	49.8118	9.7908	83.4189	15.4327	4.033	0.3259	12.3768	-28.0199	1.2858
29	1960	50.1777	10.0238	83.7163	14.2271	3.9968	0.3305	12.0916	-28.0063	0.4961
30	1957	52.6584	10.9725	83.4337	12.7132	4.231	0.3322	12.7358	-28.0209	1.4351
31	1955	58.5022	15.6744	78.8372	12.4736	4.4704	0.3401	13.1432	-27.9903	0.9647
32	1951	49.6467	10.2646	84.2823	12.3934	4.0702	0.3237	12.5756	-27.9171	1.6205
33	1948	50.0193	9.726	85.0251	11.9294	4.6564	0.349	13.3421	-28.2443	1.6437
34	1946	49.8275	13.5652	81.3527	11.5504	3.4341	0.2608	13.1659	-27.6419	1.4785
35	1944	41.933	8.7392	86.9913	9.7034	2.9862	0.212	14.0858	-27.5366	1.8329
36	1939	37.5662	7.8206	88.057	9.3692	2.678	0.1921	13.9388	-27.1329	2.6147
37	1928	39.1279	7.5472	87.7199	10.7568	3.1175	0.2362	13.2002	-27.4509	2.2597
38	1923	40.7443	8.0703	86.6254	12.0551	2.6929	0.2114	12.7355	-27.1775	1.7803
39	1918	42.0929	8.5637	86.0755	12.1835	3.8345	0.2857	13.4211	-27.5768	1.3569
40	1914	41.6266	9.5058	85.4839	11.387	3.9581	0.3084	12.835	-27.3873	1.5103
41	1910	40.8774	9.5447	85.43	11.4211	4.1728	0.324	12.8777	-27.3875	1.3806
42	1905	40.2008	9.8805	85.5021	10.494	3.8419	0.2972	12.9276	-27.4478	1.3341
43	1901	37.7161	8.575	86.5606	11.0554	3.7196	0.2787	13.3445	-27.5638	1.4817

Table B2. Up 10: LOI data (water content (% H₂O), organic matter (% OM), mineral matter (%MM), and calcium carbonate (%CaCO₃)) and carbon & nitrogen data (%C, %N, C/N, δ¹³C, and δ¹⁵N) by CRS year (constant rate of supply).

Depth (cm)	CRS year	% H ₂ O	% OM	% MM	% CaCO ₃	% C	% N	C/N	δ ¹³ C	δ ¹⁵ N
1	2016	93.5286	28.1346	67.8899	9.0353	14.3238	1.3552	10.5698	-33.1413	-1.1686
2	2013	86.7061	18.3976	76.8546	10.7904	9.7216	0.8592	11.3147	-32.6601	-0.9595
3	2010	91.0667	26.226	68.0171	13.0839	14.2418	1.3267	10.7346	-32.6879	-0.8129
4	2005	90.4149	21.0421	73.9479	11.3864	11.1827	1.0863	10.2943	-31.1288	-1.0873
5	1996	89.7886	23.0469	72.0703	11.0973	11.2754	1.0664	10.5734	-31.384	-0.5744
6	1990	85.0219	17.4434	77.6298	11.1972	8.3979	0.7503	11.1927	-31.1063	-0.2934
7	1983	81.0407	13.9853	81.4932	10.2763	5.8471	0.5266	11.1036	-30.0392	-0.4886
8	1974	77.2208	11.215	84.537	9.6547	5.792	0.443	13.073	-30.1662	-0.1703
9	1963	74.3907	11.9335	81.9486	13.9041	4.1373	0.3721	11.1201	-29.2748	0.2755
10	1950	70.9029	11.0731	84.689	9.6315	4.7011	0.3988	11.788	-28.4878	0.6204
11	1940	64.5059	8.6275	86.6667	10.6952	2.753	0.2405	11.4478	-29.2016	0.3033
12	1928	69.2369	10.9819	84.3669	10.5708	7.225	0.5785	12.4894	-29.1765	0.2694
13	1911	53.8837	8.1253	88.0237	8.7524	2.2971	0.1788	12.8473	-29.0642	-0.0957
14	1885	49.7631	8.055	88.055	8.8409	3.6602	0.1848	19.8073	-28.2842	0.8843
15	1867	59.7225	7.3819	88.9272	8.3885	2.9332	0.1519	19.3039	-27.6987	0.9401
16	1850	64.4849	8.5189	87.6949	8.605	2.6219	0.1838	14.2642	-27.8348	0.4998
17	1832	62.0608	7.8493	87.9644	9.5143	2.2991	0.1833	12.5457	-27.9862	0.6693
18	1818	73.9629	16.2261	79.2952	10.1789	2.4673	0.1799	13.7166	-30.0461	0.8022
19	1805	66.1478	9.4878	86.3795	9.3925	4.1418	0.3045	13.6	-31.787	0.3877
20	1779	53.2829	5.9625	90.4174	8.2275	2.5019	0.1479	16.9159	-27.7153	0.8527
21	1760	61.3018	8.002	88.0224	9.0353	2.8234	0.2102	13.4305	-28.3146	0.4252
22	1739	59.1697	7.6026	87.6866	10.7064	2.7445	0.2194	12.507	-28.0447	0.3849
23	1721	65.6536	8.4442	86.7553	10.9101	2.8925	0.2371	12.2013	-28.1503	0.1318
24	1705	66.9826	8.433	87.1411	10.0587	3.0868	0.2647	11.6606	-29.8803	0.4086
25	1687	62.1732	7.7317	87.5064	10.8225	2.329	0.1939	12.0114	-27.4873	0.6836
26	1669	61.7405	7.8381	86.8852	11.9924	2.5803	0.212	12.174	-27.1749	0.4135
27	1651	63.2111	8.9978	86.7996	9.5513	2.8406	0.237	11.9834	-27.1505	0.637
28	1632	60.1614	7.6181	86.837	12.6019	2.3985	0.1907	12.5786	-26.863	1.0141
29	1610	54.5847	6.8742	87.1595	13.5597	1.9546	0.1478	13.2244	-29.2688	1.4358
30	1592	59.6065	7.9274	87.8701	9.5511	2.2697	0.176	12.8927	-27.1436	0.7173
31	1575	63.8744	8.5288	87.7932	8.3592	2.8548	0.2339	12.203	-27.519	0.8431
32	1557	60.7828	7.5099	88.6364	8.7585	3.2579	0.2469	13.1928	-27.5141	0.8138
33	1534	53.7111	7.3372	89.1179	8.0567	2.7299	0.1742	15.6688	-27.3257	0.8041
34	1508	51.8746	8.2028	87.8401	8.9935	3.6134	0.253	14.2831	-28.2025	0.1868
35	1492	63.8983	10.1266	85.3605	10.2567	4.3997	0.3246	13.5556	-28.653	0.4216
36	1479	71.6864	11.6518	84.4414	8.8791	4.9741	0.4414	11.268	-29.337	-0.0252
37	1468	73.8219	11.7468	83.9817	9.7081	4.8785	0.4251	11.4761	-28.5162	0.2915
38	1452	70.1737	10.2581	85.2416	10.228	3.4441	0.2954	11.6606	-27.9261	0.4454
39	1432	58.5568	7.3739	88.059	10.3797	2.4651	0.1936	12.7308	-27.2154	0.9448
40	1410	57.9434	7.5269	88.172	9.7752	2.2785	0.1832	12.4371	-26.8741	1.7251
41	1390	59.4046	7.6736	87.8096	10.2654	1.9642	0.1592	12.337	-26.4038	2.0099
42	1368	55.571	7.1652	87.5952	11.9082	2.2346	0.1652	13.5248	-26.8466	1.3926
43	1348	51.0993	6.8647	87.3143	13.2294	2.0085	0.1485	13.5256	-26.507	1.4316
44	1329	59.0402	8.4103	87.3116	9.7229	2.5102	0.1906	13.173	-29.172	0.8973
45	1311	61.7924	8.832	87.8378	7.5684	3.2827	0.2668	12.3038	-28.0423	0.5583
46	1294	59.9009	8.3045	87.8893	8.6505	2.8888	0.2293	12.5992	-27.9372	0.7961
47	1275	60.462	8.5249	87.5	9.0343	2.7599	0.2094	13.1817	-27.4641	0.7063
48	1257	61.6332	9.0864	86.4691	10.101	3.085	0.2519	12.2479	-27.8385	0.1414

49	1241	61.8157	9.7959	85.8163	9.9722	3.3576	0.266	12.6235	-27.7828	0.659
50	1221	65.1949	10.4	86.2286	7.6623	4.1296	0.3087	13.3758	-28.2386	0.6884
51	1204	64.9551	10.1307	85.8932	9.0364	3.5188	0.2768	12.7115	-28.3241	0.4334
52	1186	61.2672	9.7549	86.1931	9.2092	2.9721	0.2349	12.6538	-30.0885	0.5887
53	1165	53.9722	7.3675	89.1142	7.9959	2.5059	0.1734	14.4531	-27.2789	1.0843
54	1141	52.0191	6.5417	89.6689	8.6122	2.2589	0.1542	14.6511	-28.5449	0.7425
55	1117	53.4169	7.1459	88.9029	8.9801	2.3608	0.1565	15.0806	-27.0472	0.9786
56	1093	53.7251	8.136	88.1188	8.5117	2.4239	0.1561	15.5297	-28.1993	1.1148
57	1072	54.2184	7.6187	88.4324	8.9749	2.3193	0.1523	15.2278	-27.0107	0.6787
58	1047	52.3151	7.7357	87.5907	10.6219	2.3026	0.1736	13.2625	-26.7606	1.8609
59	1022	47.796	6.9322	87.9056	11.7324	2.2675	0.1677	13.5203	-26.8744	1.4088
60	1001	53.6135	8.8061	87.0449	9.4296	2.6874	0.176	15.2663	-27.2915	1.2547
61	978	59.241	10.6208	85.742	8.2665	4.1619	0.2803	14.8485	-28.6151	-0.5483
62	967	60.8945	10.7794	85.1215	9.3163	4.0766	0.3109	13.1122	-28.9925	0.1252

Table B3. Down 1: LOI data (water content (% H₂O), organic matter (% OM), mineral matter (%MM), and calcium carbonate (%CaCO₃)) and carbon & nitrogen data (%C, %N, C/N, δ¹³C, and δ¹⁵N) by CRS year (constant rate of supply).

Depth (cm)	CRS year	% H ₂ O	% OM	% MM	% CaCO ₃	% C	% N	C/N	δ ¹³ C	δ ¹⁵ N
1	2015	93.7166	34.7003	61.1987	9.3203	20.4205	1.6387	12.4617	-28.4995	-0.9126
2	2014	92.4586	34.4388	61.4796	9.2764	20.3297	1.6084	12.6397	-28.6843	-1.0473
3	2014	89.7639	35.2713	61.6279	7.0472	19.0754	1.4703	12.9738	-28.5475	-1.3132
4	2012	90.1232	36.6337	58.6139	10.8011	21.8254	1.6312	13.3804	-28.557	-0.7776
5	2011	92.2685	43.2911	53.6709	6.9045	22.995	1.8661	12.3228	-28.3471	-0.8644
6	2009	90.4157	38.3534	58.4337	7.3019	22.1861	1.6569	13.3904	-28.4227	-1.0074
7	2008	88.2826	40.0335	57.4539	5.7104	22.6356	1.7242	13.128	-28.3764	-0.8234
8	2006	88.2159	36.9028	60.1318	6.7396	18.4385	1.2936	14.2537	-28.6013	-1.0416
9	2003	90.1656	35.9343	61.191	6.5335	21.0479	1.533	13.7302	-28.4331	-0.9458
10	2001	88.1135	36.1526	61.8574	4.5228	20.4404	1.4644	13.9584	-28.4579	-0.7688
11	1998	87.1161	33.7461	63.1579	7.0363	19.065	1.3896	13.7198	-28.3279	-0.8779
12	1996	87.3824	34.6273	62.5776	6.3523	19.4267	1.4207	13.6744	-28.4887	-0.9617
13	1992	85.387	34.5191	62.9776	5.6893	18.4963	1.3675	13.5254	-28.2871	-1.056
14	1988	85.3483	34.9669	62.649	5.4184	20.5382	1.6526	12.428	-28.5929	-0.8423
15	1985	80.0672	24.8016	72.3214	6.5386	12.1767	0.8753	13.9122	-28.4131	-0.7985
16	1983	70.7444	16.831	79.6844	7.9194	8.1982	0.5774	14.1996	-28.2621	-0.2563
17	1983	61.9648	12.9406	83.4298	8.2492	6.0259	0.4145	14.5382	-28.0645	-0.1164
18	1981	62.4597	12.4933	83.9142	8.1648	5.4798	0.3766	14.5521	-27.8177	-0.1365
19	1980	66.8802	15.1817	81.0668	8.5261	7.1767	0.4839	14.8303	-28.0479	-0.2556
20	1976	64.1352	14.8004	81.6519	8.0629	6.402	0.4377	14.628	-28.1162	-0.4714
21	1973	63.7495	15.5043	80.6867	8.6568	6.2151	0.4296	14.468	-28.2163	0.0752
22	1969	58.9115	12.6152	83.3091	9.2629	6.547	0.4446	14.7246	-27.8025	0.0808
23	1961	70.8509	21.5648	74.622	8.6665	9.468	0.6518	14.527	-28.0788	-0.3409
24	1955	74.1942	27.5991	69.1099	7.4794	14.1159	0.9722	14.5197	-28.4424	-0.0911
25	1951	64.7047	17.8866	78.1508	9.0059	10.1384	0.6967	14.5529	-28.519	-0.535
26	1945	66.1465	19.208	77.1277	8.328	9.5736	0.679	14.1001	-28.6946	-0.5686
27	1937	69.5306	22.5196	74.7389	6.2307	9.0072	0.6435	13.9963	-28.5592	-0.5044
28	1932	48.8641	11.3705	85.128	7.958	6.0885	0.4167	14.6103	-28.6074	0.0577
29	1931	45.6206	9.1008	87.3601	8.0436	3.4256	0.2205	15.5327	-28.0062	0.374
30	1929	52.0366	12.5965	84.356	6.9262	6.1861	0.4054	15.2587	-27.7486	-0.2159
31	1923	59.481	16.7488	79.803	7.837	7.3948	0.491	15.0597	-27.7884	0.2747

32	1920	57.7598	18.3473	78.1979	7.8516	6.6881	0.4698	14.2374	-27.6633	-0.0484
33	1918	63.8528	19.8118	76.5357	8.3011	6.9081	0.456	15.1493	-27.7143	0.1388
34	1916	57.3694	14.2468	82.2595	7.9401	6.8615	0.4529	15.1489	-27.3867	-0.1937
35	1913	81.7054	32.5212	65.2542	5.0559	12.0491	0.8176	14.7368	-26.6586	-1.4894
36	1905	71.2657	29.617	67.9891	5.4409	12.1232	0.7836	15.472	-27.5946	-0.247
37	1891	70.2857	28.7798	69.0981	4.8228	13.2171	0.8189	16.1409	-27.6675	-0.3392
38	1887	68.9595	27.0287	70.4744	5.6747	13.8263	0.8395	16.4697	-28.7506	-0.3237
39	1879	69.8368	25.5277	71.8338	5.9966	12.3519	0.7819	15.798	-28.4841	-0.224
40	1876	69.0593	27.3704	70.2276	5.4591	8.6389	0.4857	17.785	-27.8892	-0.3036
41	1872	71.5798	35.8835	62.3561	4.0007	13.5965	0.7819	17.3888	-27.5346	-0.502
42	1869	68.2343	27.7601	69.8787	5.3664	10.9936	0.6929	15.8658	-28.2773	-0.3808
43	1865	65.8613	24.4534	73.13	5.4922	11.6592	0.736	15.8417	-27.9533	-0.2151
44	1862	71.829	35.427	62.597	4.4909	13.1538	0.7467	17.6155	-27.9426	-0.0847
45	1859	70.6846	26.4468	71.5343	4.5883	12.5895	0.6784	18.5576	-28.8508	-0.0928
46	1855	70.8743	31.6766	66.1365	4.9702	12.64	0.7288	17.3447	-28.4425	0.3797
47	1851	64.0703	26.2924	71.3174	9.03	12.7971	0.7392	17.3127	-28.9897	0.1072
48	1848	66.8381	27.3866	69.8687	6.2378	12.8499	0.7388	17.3923	-28.8149	-0.2269
49	1844	71.1055	30.5017	67.291	5.0167	14.9883	0.9801	15.2931	-28.3172	-0.4071
50	1840	82.1907	42.146	54.9779	6.5366	23.1909	1.7388	13.3372	-28.3307	-0.8461
51	1836	69.2783	24.854	72.5503	5.8994	11.9012	0.8519	13.9707	-27.7903	-0.2914
52	1831	63.5366	19.5699	77.6882	6.2317	9.1884	0.6079	15.1157	-27.9963	-0.2053
53	1824	53.049	16.6384	81.0272	5.3056	8.162	0.4866	16.7727	-27.664	0.171
54	1816	59.6293	20.509	77.2455	5.1034	8.3672	0.4997	16.7459	-27.5036	-0.1892

Table B4: Down 26: LOI data (water content (% H₂O), organic matter (% OM), mineral matter (%MM), and calcium carbonate (%CaCO₃)) and carbon & nitrogen data (%C, %N, C/N, δ¹³C, and δ¹⁵N) by CRS year (constant rate of supply).

Depth (cm)	CRS year	% H ₂ O	% OM	% MM	% CaCO ₃	% C	% N	C/N	δ ¹³ C	δ ¹⁵ N
1	2018	96.4441	41.6667	48.8889	21.4646	18.8608	2.2379	8.4278	-29.3692	0.3681
2	2017	93.3307	34.6269	54.6269	24.4233	23.9066	2.7237	8.7772	-30.1919	0.0666
3	2016	91.1597	27.1715	62.8062	22.7779	15.7192	1.672	9.4011	-30.8543	0.1055
4	2014	79.4795	18.2962	76.3795	12.1007	8.405	0.7333	11.4625	-29.6922	0.3792
5	2012	74.6893	16.9135	77.2408	13.2856	6.7584	0.5845	11.5633	-29.5443	0.4211
6	2010	70.9722	17.3616	77.1018	12.5831	6.9404	0.5665	12.2508	-29.1008	0.2444
7	2007	70.8523	16.1465	78.5617	12.0266	5.9815	0.4936	12.1187	-28.7882	0.5294
8	2004	61.3721	13.5369	81.2723	11.7974	4.8947	0.3926	12.4679	-28.3461	0.5397
9	2001	56.4545	11.5665	82.9235	12.5228	5.2986	0.4099	12.9275	-28.1995	0.707
10	1998	63.8774	12.3437	82.9799	10.6283	4.61	0.3628	12.7079	-28.0836	0.7018
11	1994	55.8865	11.101	83.4617	12.3574	4.0061	0.3061	13.0873	-28.0109	0.6854
12	1990	60.404	12.0852	82.5656	12.1572	4.6666	0.3659	12.7537	-28.3464	0.5525
13	1986	54.3042	11.0108	83.828	11.7302	5.0603	0.3884	13.0277	-28.6378	0.4804
14	1982	44.1602	9.6591	85.902	10.0885	3.9132	0.2779	14.0798	-28.1538	0.6738
15	1976	43.2782	9.4803	85.9902	10.2943	3.0114	0.2046	14.7171	-27.7021	1.0276
16	1969	46.128	8.6909	86.2853	11.4178	2.727	0.1968	13.8569	-27.6799	1.1301
17	1963	37.6057	6.8368	87.9647	11.8147	2.9701	0.2167	13.7041	-27.7718	1.2325
18	1956	38.6462	7.4407	87.7806	10.8607	2.791	0.2005	13.9195	-27.7325	0.8952
19	1949	35.7213	7.0116	87.1402	13.2912	2.4511	0.1714	14.3037	-27.369	1.4056
20	1943	42.9481	10.251	84.3096	12.3621	2.739	0.1793	15.2735	-27.6372	0.2022
21	1937	38.7895	7.7689	87.4799	10.7982	2.6265	0.1693	15.5117	-27.7065	1.0331
22	1931	43.2347	8.2696	84.4336	16.5835	3.4964	0.2512	13.9168	-28.5997	0.7675
23	1926	45.4979	9.4457	82.0204	19.3953	4.8227	0.3926	12.2851	-29.2296	0.1607
24	1922	49.1894	10.7782	77.9767	25.5571	5.1355	0.4253	12.0745	-29.5239	0.1294
25	1917	50.2367	11.2961	76.8133	27.0241	5.7333	0.4836	11.8553	-29.582	-0.1009
26	1913	51.3234	12.4693	76.1774	25.8028	7.6777	0.6382	12.0299	-29.931	-0.3813
27	1909	52.5464	13.2576	75.2525	26.1134	7.7604	0.6728	11.5339	-30.1746	-0.4725
28	1904	52.1163	15.2416	75.3408	21.4036	6.9082	0.5583	12.374	-29.6903	0.1551
29	1899	46.1342	11.4754	80.4372	18.3805	4.4978	0.3305	13.6085	-29.1192	0.6051
30	1892	38.2232	7.2698	86.5079	14.1414	3.3145	0.229	14.4725	-28.1354	0.8876
31	1885	37.3527	7.3981	86.8652	13.0379	2.9562	0.1968	15.0234	-27.56	1.2752
32	1878	35.6857	6.9319	87.5971	12.4339	3.0897	0.2044	15.1155	-27.4987	0.9964
33	1871	37.1863	7.7697	86.7883	12.3681	3.0952	0.2114	14.6395	-27.6764	0.8452
34	1865	38.24	7.1406	87.3914	12.4273	3.0201	0.2087	14.4729	-27.8201	0.8585
35	1858	36.3438	8.2763	86.5588	11.7384	3.0878	0.2143	14.4095	-27.7764	0.6572
36	1852	37.2958	6.7169	88.1984	11.5562	3.5212	0.2409	14.6197	-28.0391	0.7339
37	1846	38.9554	7.43	87.1985	12.208	2.8078	0.1896	14.8129	-27.7234	0.7257
38	1841	41.2714	9.5351	85.0696	12.2621	3.7097	0.2532	14.6491	-28.039	0.5345
39	1834	42.466	9.6542	84.9024	12.3712	3.3017	0.2274	14.5187	-27.9871	0.8741
40	1828	41.3056	8.9653	85.5747	12.4092	3.7456	0.2541	14.7405	-28.0939	0.8596
41	1823	42.8203	11.4117	84.2178	9.9328	4.3414	0.2909	14.9222	-27.8362	0.622
42	1817	41.6387	11.2314	84.6414	9.38	4.4703	0.3019	14.8082	-27.9017	0.9557

Table B5. Down 58: LOI data (water content (% H₂O), organic matter (% OM), mineral matter (%MM), and calcium carbonate (%CaCO₃)) and carbon & nitrogen data (%C, %N, C/N, δ¹³C, and δ¹⁵N) by depth.

Depth (cm)	% H ₂ O	% OM	% MM	% CaCO ₃	% C	% N	C/N	δ ¹³ C	δ ¹⁵ N
1	83.2254	9.0806	86.6061	9.8029	3.4918	0.2834	12.3227	-28.2786	1.0426
2	64.0286	7.7461	87.7891	10.1472	2.9126	0.2134	13.6503	-28.2589	1.8576
3	57.864	8.0481	88.0204	8.9353	2.8636	0.2083	13.7497	-28.041	1.5656
4	57.5055	6.444	88.8053	10.7971	2.4989	0.19	13.1532	-27.9074	2.0695
5	47.7355	5.9816	89.8773	9.4116	1.9248	0.1461	13.1784	-27.4499	1.7201
6	59.4504	7.1	87.7363	11.7356	2.6256	0.2052	12.7957	-28.0086	1.5256
7	61.6549	7.6884	85.3409	15.8427	3.5885	0.3312	10.8348	-28.9738	0.6883
8	65.5669	9.1754	83.043	17.6856	3.9752	0.3642	10.9152	-29.0106	0.2946
9	63.9029	8.4992	84.9919	14.7929	3.2091	0.2905	11.0474	-28.0954	0.7807
10	61.1232	7.2228	84.7915	18.1494	3.3465	0.2965	11.288	-28.35	1.0603
11	53.6131	7.341	87.3666	12.0281	2.6443	0.2077	12.7292	-27.6897	1.5642
12	61.0156	8.2665	83.5671	18.5598	3.2149	0.2843	11.3088	-28.4232	0.8673
13	60.5386	7.9624	83.6795	18.9956	3.4408	0.3069	11.2119	-28.6664	1.1123
14	58.7022	8.1743	84.6794	16.2417	3.112	0.2773	11.2242	-28.4845	1.1347
15	57.8474	7.3899	85.5992	15.9339	2.4934	0.195	12.7875	-28.0919	1.3514
16	42.4727	5.5283	90.3827	9.2931	2.1627	0.1572	13.7605	-27.472	1.9831
17	36.1601	5.1114	90.9064	9.0504	2.0071	0.1174	17.0891	-27.2321	2.2951
18	44.2052	5.8947	90.1053	9.0909	2.0946	0.1385	15.1185	-27.0279	2.4422
19	40.2977	5.5609	90.3484	9.2972	2.166	0.1487	14.5708	-26.9548	2.4166
20	46.1312	6.5818	89.1273	9.7521	2.3411	0.1763	13.2789	-27.3523	1.8315
21	52.4239	7.0957	85.9736	15.7516	3.0831	0.2666	11.5655	-28.2434	1.1884
22	55.5682	7.8723	84.8936	16.441	3.1697	0.248	12.7806	-27.9739	1.1318
23	49.9117	6.6223	87.069	14.3381	2.5635	0.1798	14.2572	-27.5393	1.6218
24	40.2336	6.248	89.4905	9.6851	2.1761	0.144	15.1113	-26.805	1.6795
25	37.0198	5.6559	90.6426	8.4125	2.5057	0.1541	16.2556	-26.9578	1.7321
26	43.2008	5.7053	89.5695	10.7392	2.4315	0.1768	13.7506	-27.2468	1.7068
27	44.9363	6.5101	88.794	10.6724	2.3048	0.1745	13.2068	-27.5767	1.4323
28	43.7685	6.7088	87.8469	12.3735	2.5228	0.1932	13.0587	-27.675	1.2987
29	52.8116	7.6986	86.9369	12.1919	3.2912	0.2761	11.9206	-28.2356	1.2141
30	47.6646	6.7301	88.2224	11.4717	2.3602	0.176	13.4093	-27.3785	1.3787
31	44.1523	5.4111	89.6697	11.18	1.84	0.1276	14.4229	-28.7427	1.9112
32	37.6691	4.7543	90.3318	11.1678	1.6175	0.0951	17.0135	-26.5677	1.6209
33	48.156	6.0708	87.2626	15.1515	1.9846	0.1285	15.4476	-26.6954	1.8482
34	58.4315	8.039	77.6487	32.5279	4.4392	0.4323	10.2686	-27.9186	0.1985
35	51.4582	6.1694	82.2177	26.393	2.5329	0.2064	12.2706	-27.2798	1.5232
36	49.0295	6.4737	87.8903	12.809	2.2268	0.1661	13.4077	-26.9431	1.6325
37	42.5121	5.7479	88.6387	12.7578	1.9971	0.1371	14.5718	-26.3838	1.9708
38	43.4774	5.6637	88.4248	13.4352	1.99	0.1309	15.1981	-26.3853	1.8458
39	46.8732	6.8869	87.3858	13.0167	2.8649	0.1804	15.8834	-27.5267	1.0413
40	46.2339	6.547	87.5748	13.3596	2.5722	0.1731	14.8614	-27.256	1.7123
41	45.7327	6.8954	87.8736	11.8886	2.4468	0.188	13.0145	-27.2785	1.0915
42	46.3516	6.871	86.8569	14.2546	3.145	0.2854	11.0193	-27.4836	0.3294
43	36.8797	5.3533	90.3334	9.8028	2.2471	0.1548	14.5117	-27.1983	1.0982
44	35.0591	5.3747	91.1018	8.0078	1.9989	0.1266	15.7902	-26.6261	1.429
45	34.6863	5.3524	91.1091	8.0421	1.7828	0.1106	16.1128	-26.4547	1.6542

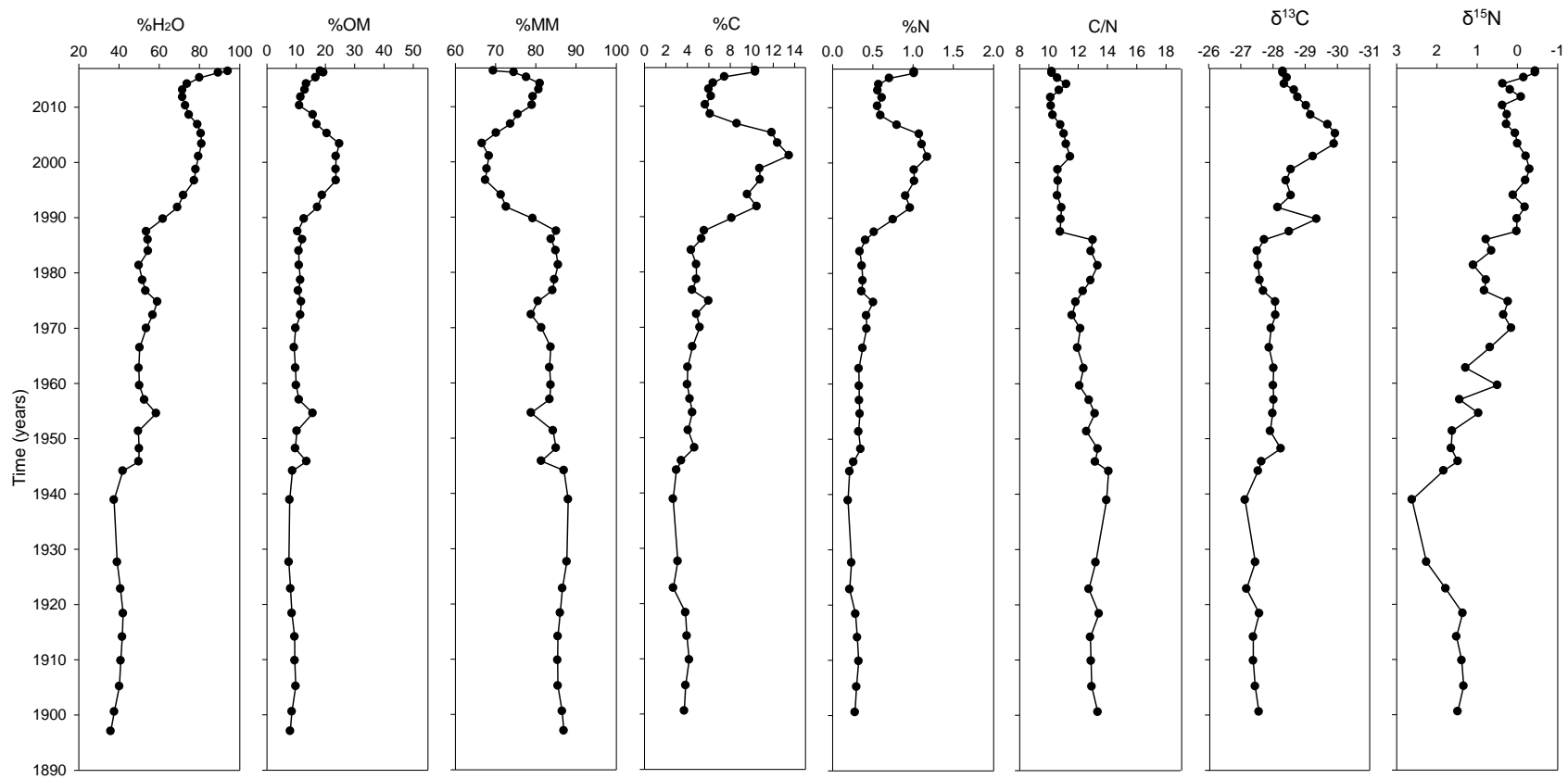


Figure B1. Stratigraphies for loss-on-ignition (% H₂O, OM & MM) and organic carbon and nitrogen elemental and isotopic composition (%C, %N, C/N, δ¹³C, and δ¹⁵N) at lake Up 17

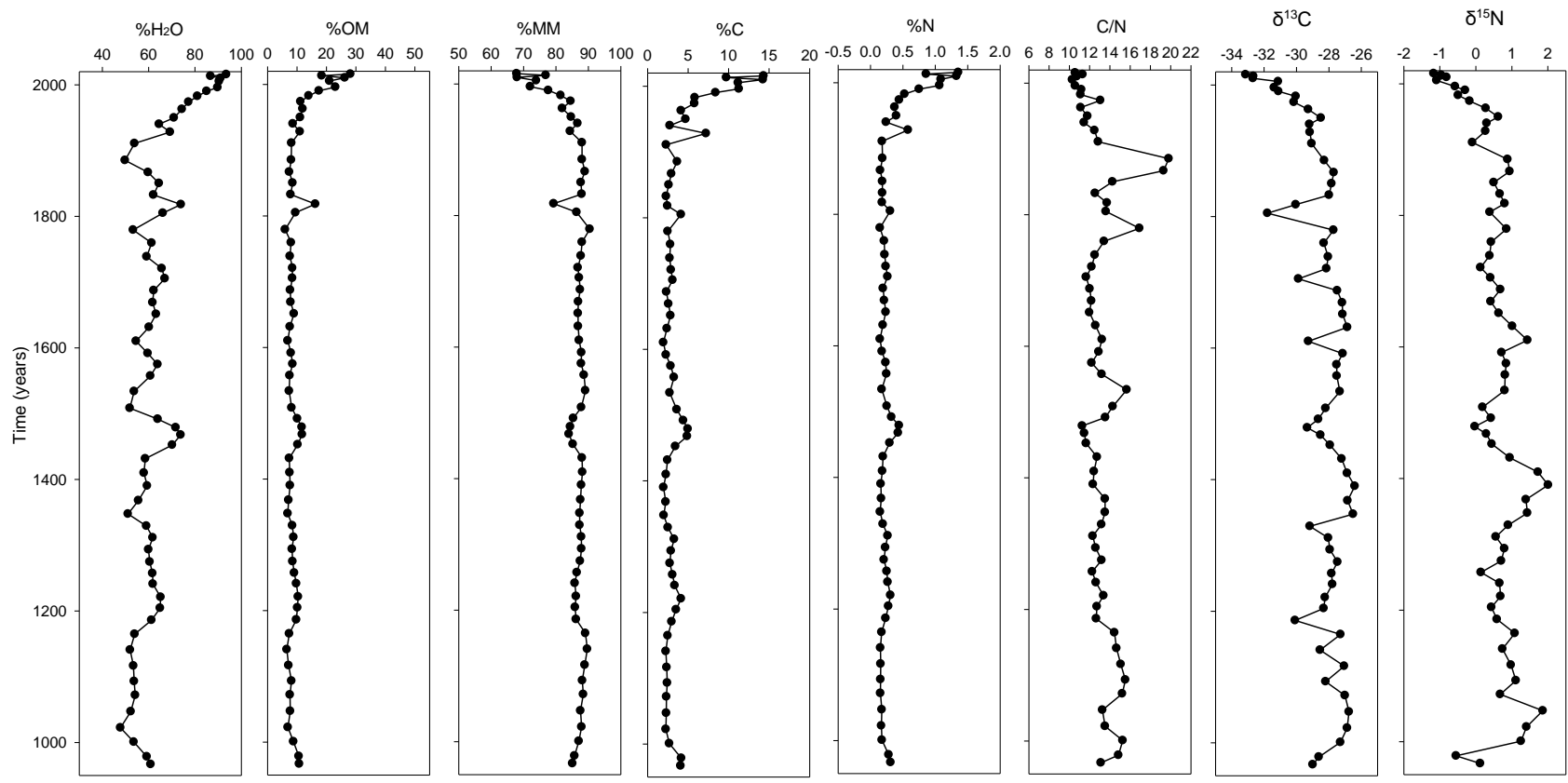


Figure B2. Stratigraphies for loss-on-ignition (% H₂O, OM & MM) and organic carbon and nitrogen elemental and isotopic composition (%C, %N, C/N, δ¹³C, and δ¹⁵N) at lake Up 10.

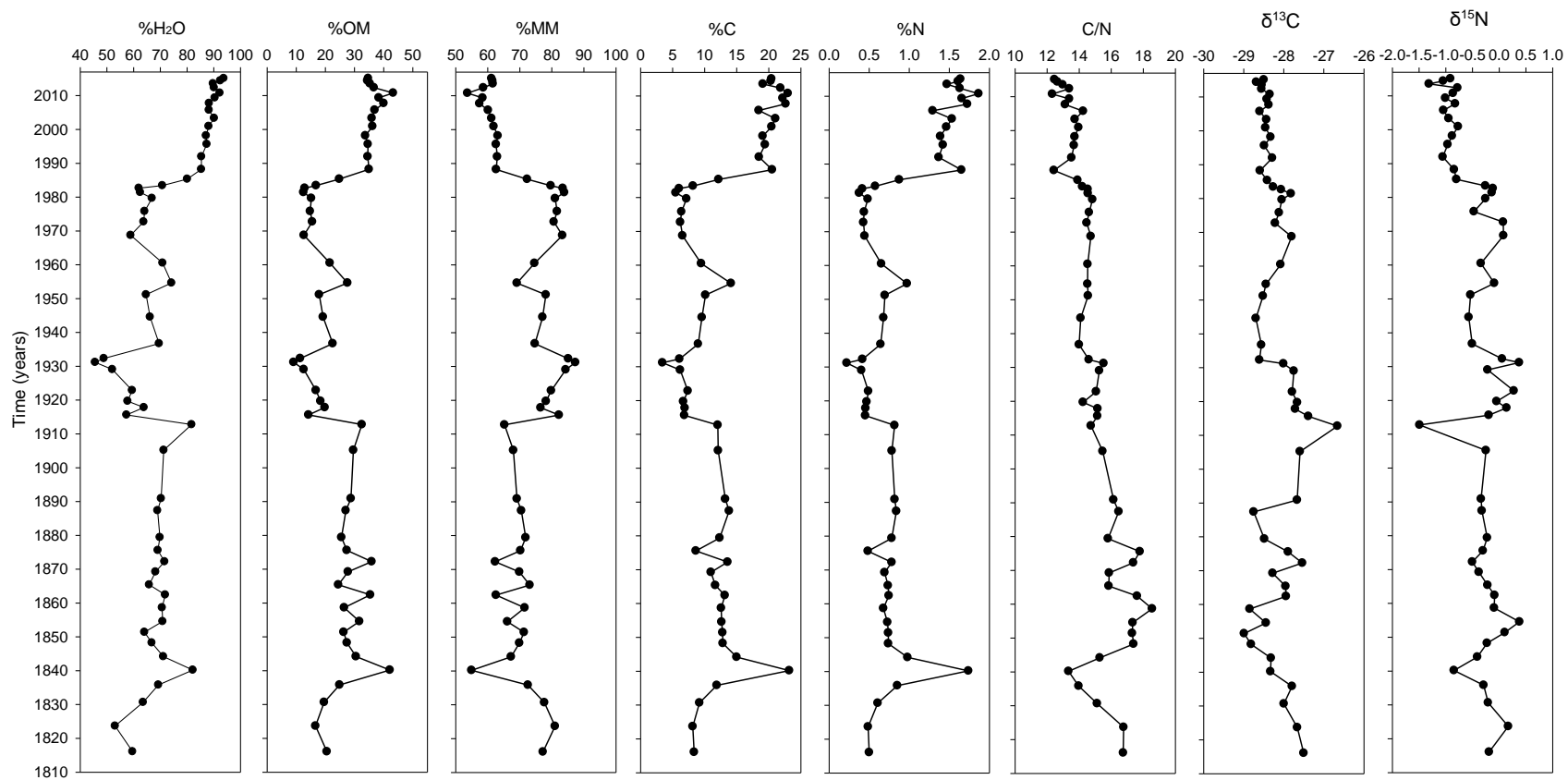


Figure B3. Stratigraphies for loss-on-ignition (% H₂O, OM & MM) and organic carbon and nitrogen elemental and isotopic composition (%C, %N, C/N, δ¹³C, and δ¹⁵N) at lake Down 1.

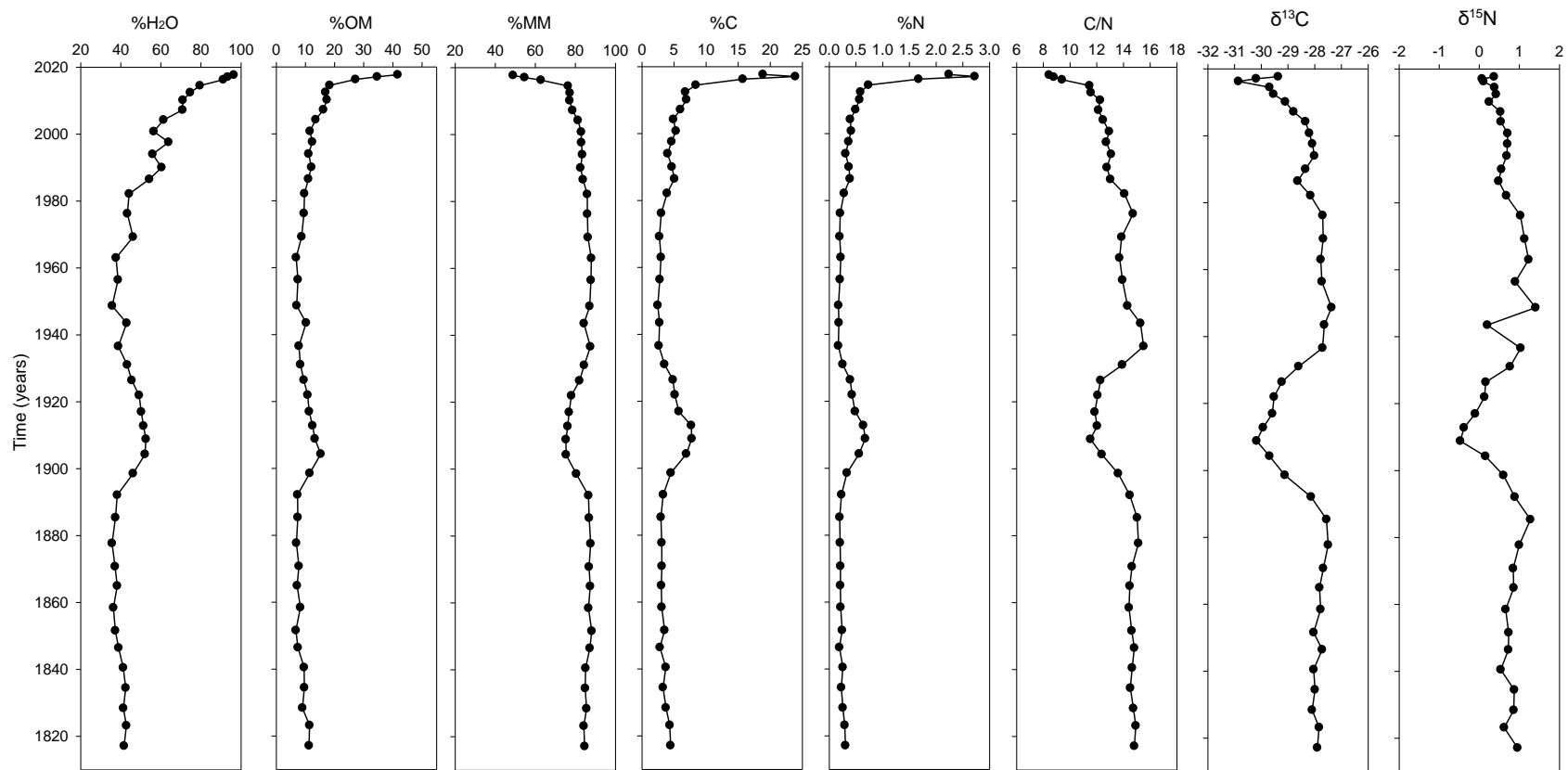


Figure B4. Stratigraphies for loss-on-ignition (% H₂O, OM & MM) and organic carbon and nitrogen elemental and isotopic composition (%C, %N, C/N, δ¹³C, and δ¹⁵N) at lake Down 26.

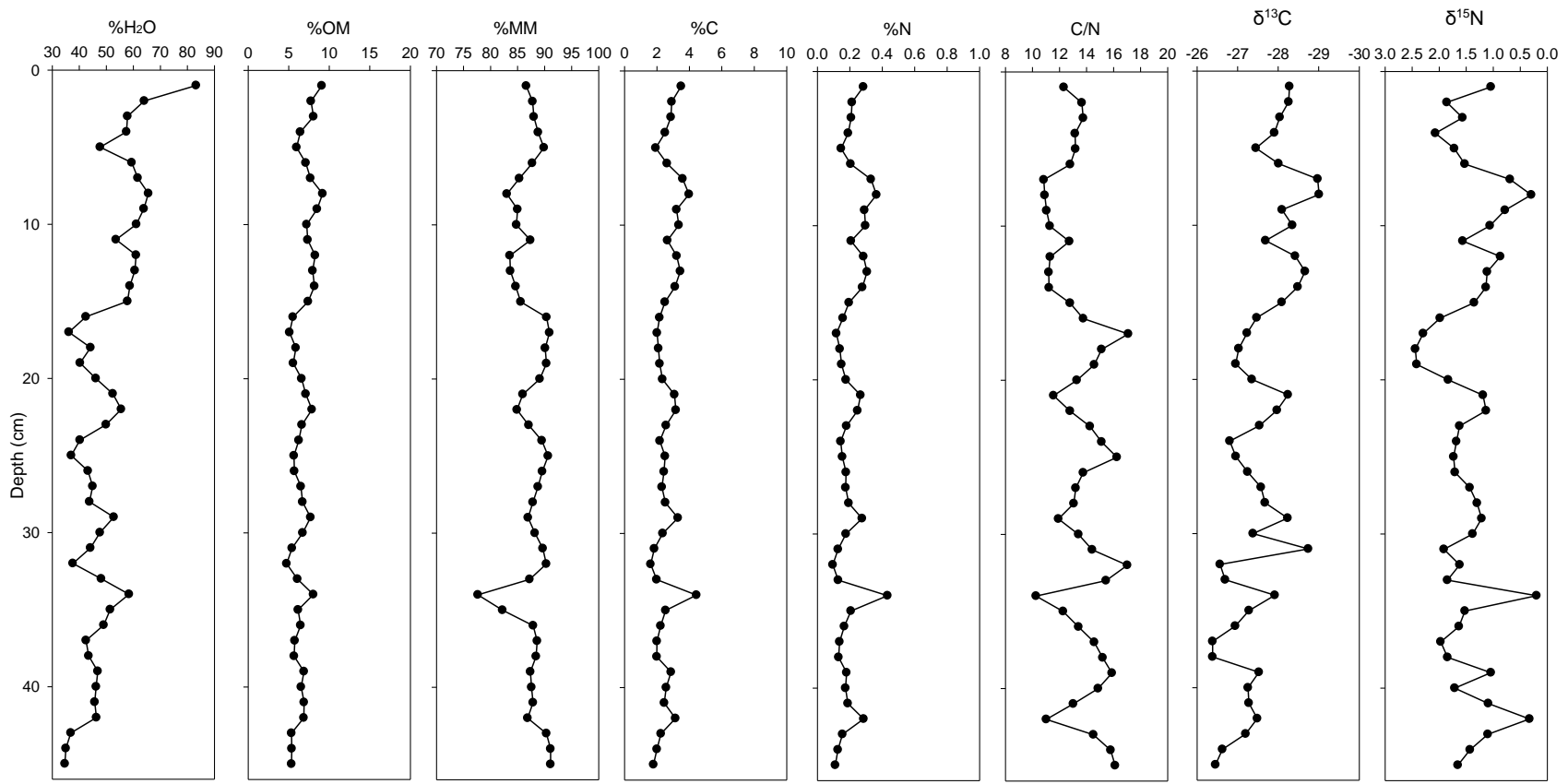


Figure B5. Stratigraphies for loss-on-ignition (% H₂O, OM & MM) and organic carbon and nitrogen elemental and isotopic composition (%C, %N, C/N, δ¹³C, and δ¹⁵N) at lake Down 58.

Table B6. RAMP (1997-2004) and JOSM (2012-2014) river-bottom and suspended sediment organic carbon data retrieved from online RAMP and JOSM databases.

Agency	Site ID	Date	Sediment type	% organic carbon
RAMP	ATR-MR-E	2004-09-20	river-bottom	1.70
RAMP	ATR-MR-W	2004-09-20	river-bottom	2.10
RAMP	ATR-DD-E	2004-09-19	river-bottom	1.40
RAMP	ATR-DD-W	2004-09-19	river-bottom	0.20
RAMP	ATR-SR-W	2004-09-18	river-bottom	0.90
RAMP	ATR-FR-W	2004-09-18	river-bottom	0.50
RAMP	ATR-SR-E	2004-09-18	river-bottom	1.60
RAMP	ATR-FR-E	2004-09-18	river-bottom	0.60
RAMP	ATR-DC-W	2004-09-17	river-bottom	0.20
RAMP	ATR-UFM	2004-09-17	river-bottom	0.60
RAMP	ATR-DC-E	2004-09-17	river-bottom	1.30
RAMP	ATR-MR-W	2003-09-17	river-bottom	1.50
RAMP	ATR-MR-E	2003-09-17	river-bottom	1.40
RAMP	ATR-FC-E	2003-09-13	river-bottom	1.60
RAMP	ATR-FR-W	2003-09-12	river-bottom	0.40
RAMP	ATR-DD-E	2003-09-12	river-bottom	1.10
RAMP	ATR-DD-W	2003-09-12	river-bottom	< 0.1
RAMP	ATR-FR-E	2003-09-12	river-bottom	< 0.1
RAMP	ATR-FC-W	2003-09-09	river-bottom	0.80
RAMP	ATR-SR-E	2003-09-07	river-bottom	< 0.1
RAMP	ATR-SR-W	2003-09-07	river-bottom	0.50
RAMP	ATR-UFM	2003-09-06	river-bottom	1.20
RAMP	ATR-DC-W	2003-09-06	river-bottom	0.60
RAMP	ATR-DC-E	2003-09-06	river-bottom	4.50
RAMP	ATR-FR-W	2002-09-13	river-bottom	1.40
RAMP	ATR-FR-E	2002-09-13	river-bottom	1.00
RAMP	ATR-DC-E	2002-09-07	river-bottom	2.80
RAMP	ATR-DC-W	2002-09-07	river-bottom	< 0.01
RAMP	ATR-UFM	2002-09-07	river-bottom	1.60
RAMP	ATR-MR-W	2002-09-06	river-bottom	1.80
RAMP	ATR-MR-E	2002-09-06	river-bottom	1.00
RAMP	ATR-SR-E	2002-09-06	river-bottom	2.10
RAMP	ATR-SR-W	2002-09-06	river-bottom	1.10
RAMP	ATR-DD-W	2002-09-05	river-bottom	0.90
RAMP	ATR-FC-E	2002-09-05	river-bottom	1.60
RAMP	ATR-DD-E	2002-09-05	river-bottom	4.70
RAMP	ATR-FC-W	2002-09-05	river-bottom	1.00
RAMP	ATR-DC-W	2001-11-02	river-bottom	< 0.01
RAMP	ATR-DC-E	2001-11-02	river-bottom	< 0.01
RAMP	ATR-SR-W	2001-11-01	river-bottom	0.60
RAMP	ATR-MR-E	2001-11-01	river-bottom	< 0.01
RAMP	ATR-SR-E	2001-11-01	river-bottom	0.20
RAMP	ATR-MR-W	2001-11-01	river-bottom	< 0.01
RAMP	ATR-FC-E	2001-10-14	river-bottom	0.80
RAMP	ATR-FC-W	2001-10-14	river-bottom	0.62
RAMP	ATR-MR-W	2000-10-04	river-bottom	0.70
RAMP	ATR-MR-E	2000-10-04	river-bottom	0.80
RAMP	ATR-FC-W	2000-10-03	river-bottom	2.70
RAMP	ATR-FC-E	2000-10-03	river-bottom	4.00

RAMP	ATR-DC-W	2000-10-02	river-bottom	0.10
RAMP	ATR-SR-W	2000-10-02	river-bottom	2.10
RAMP	ATR-SR-E	2000-10-02	river-bottom	0.50
RAMP	ATR-DC-E	2000-10-02	river-bottom	2.50
RAMP	ATR-ER	2000-09-15	river-bottom	1.10
RAMP	ATR-FC-E-D	1998-09-17	river-bottom	0.65
RAMP	ATR-FC-W-D	1998-09-17	river-bottom	2.02
RAMP	ATR-MR-E-D	1998-09-16	river-bottom	1.57
RAMP	ATR-DC-W	1998-09-16	river-bottom	0.43
RAMP	ATR-MR-W-D	1998-09-16	river-bottom	0.67
RAMP	ATR-DC-E	1998-09-16	river-bottom	0.92
RAMP	ATR-FC-CC-D	1997-10-10	river-bottom	1.67
RAMP	ATR-DC-CC	1997-10-06	river-bottom	0.67
JOSM	M3 SAND	2012-09-18	river-bottom	1.15
JOSM	M3 GRAVEL	2012-09-18	river-bottom	0.40
JOSM	M3B GRAVEL	2012-09-24	river-bottom	0.57
JOSM	M3B SAND	2012-09-24	river-bottom	0.01
JOSM	M4 GRAVEL	2012-09-20	river-bottom	0.18
JOSM	M4 SAND	2012-09-20	river-bottom	0.46
JOSM	M6 SAND	2012-09-21	river-bottom	0.03
JOSM	M6 GRAVEL	2012-09-21	river-bottom	0.55
JOSM	M7 GRAVEL	2012-09-22	river-bottom	1.78
JOSM	M7 SAND	2012-09-22	river-bottom	0.27
JOSM	M7C SAND	2012-09-22	river-bottom	0.19
JOSM	M7C GRAVEL	2012-09-23	river-bottom	4.09
JOSM	M8 GRAVEL	2012-09-25	river-bottom	0.88
JOSM	M8 SAND	2012-09-25	river-bottom	2.91
JOSM	M3 GRAVEL	2013-09-18	river-bottom	0.51
JOSM	M3 SAND	2013-09-18	river-bottom	0.07
JOSM	M3B GRAVEL	2013-09-17	river-bottom	0.63
JOSM	M3B SAND	2013-09-17	river-bottom	1.55
JOSM	M4 SAND	2013-09-19	river-bottom	1.81
JOSM	M4 GRAVEL	2013-09-19	river-bottom	1.50
JOSM	M6 GRAVEL	2013-09-22	river-bottom	1.29
JOSM	M6 SAND	2013-09-22	river-bottom	1.18
JOSM	M7 GRAVEL	2013-09-21	river-bottom	0.41
JOSM	M7 SAND	2013-09-21	river-bottom	2.01
JOSM	M7C GRAVEL	2013-09-23	river-bottom	1.71
JOSM	M7C SAND	2013-09-23	river-bottom	1.67
JOSM	M8 GRAVEL	2013-09-21	river-bottom	1.21
JOSM	M8 SAND	2013-09-21	river-bottom	1.06
JOSM	M3 GRAVEL	2014-09-21	river-bottom	0.40
JOSM	M3 GRAVEL	2014-09-21	river-bottom	0.60
JOSM	M9 GRAVEL	2014-09-21	river-bottom	2.46
JOSM	M3 GRAVEL	2014-09-21	river-bottom	0.20
JOSM	M3B GRAVEL	2014-09-21	river-bottom	1.92
JOSM	M3B SAND	2014-09-21	river-bottom	0.11
JOSM	M4 GRAVEL	2014-09-14	river-bottom	0.89
JOSM	M4 GRAVEL	2014-09-26	river-bottom	0.86
JOSM	M4 SAND	2014-09-26	river-bottom	2.06
JOSM	M6 GRAVEL	2014-09-24	river-bottom	1.70
JOSM	M6 SAND	2014-09-24	river-bottom	2.25
JOSM	M7 GRAVEL	2014-09-23	river-bottom	0.30

JOSM	M7 SAND	2014-09-23	river-bottom	0.98
JOSM	M7C GRAVEL	2014-09-22	river-bottom	1.14
JOSM	M7C SAND	2014-09-22	river-bottom	3.33
JOSM	M8 GRAVEL	2014-09-20	river-bottom	1.03
JOSM	M8 SAND	2014-09-20	river-bottom	1.72
JOSM	M0	06-2012	suspended sed.	1.32
JOSM	M0	09-2012	suspended sed.	5.77
JOSM	M2	06-2012	suspended sed.	1.92
JOSM	M2	09-2012	suspended sed.	5.54
JOSM	M3	06-2012	suspended sed.	1.75
JOSM	M3	09-2012	suspended sed.	5.53
JOSM	M9	06-2012	suspended sed.	1.77
JOSM	M9	10-2012	suspended sed.	3.78
JOSM	M0	06-2013	suspended sed.	1.56
JOSM	M0	09-2013	suspended sed.	4.70
JOSM	M0	02-2014	suspended sed.	5.43
JOSM	M2	06-2013	suspended sed.	1.38
JOSM	M2	09-2013	suspended sed.	7.78
JOSM	M2	02-2014	suspended sed.	4.90
JOSM	M3	06-2013	suspended sed.	1.60
JOSM	M3	09-2013	suspended sed.	7.57
JOSM	M4	02-2014	suspended sed.	5.58
JOSM	M9	06-2013	suspended sed.	2.04
JOSM	M0	06-2014	suspended sed.	2.45
JOSM	M0	09-2014	suspended sed.	3.96
JOSM	M2	09-2014	suspended sed.	1.97
JOSM	M3	06-2014	suspended sed.	1.81
JOSM	M3	09-2014	suspended sed.	2.27
JOSM	M9	06-2014	suspended sed.	1.87
JOSM	M9	09-2014	suspended sed.	3.23

Table B7. Organic carbon (%) for exposed river sediments, and a flood deposit, collected during this study (2016, 2017).

Site	Date	% org. C
AR* near Down 26	10-2016	1.54
AR* near Up 17	10-2016	0.97
AR* Downstream of Clearwater R.	07-2017	0.40
Fort McMurray flood deposit sed.	07-2017	1.07

*AR = Athabasca River

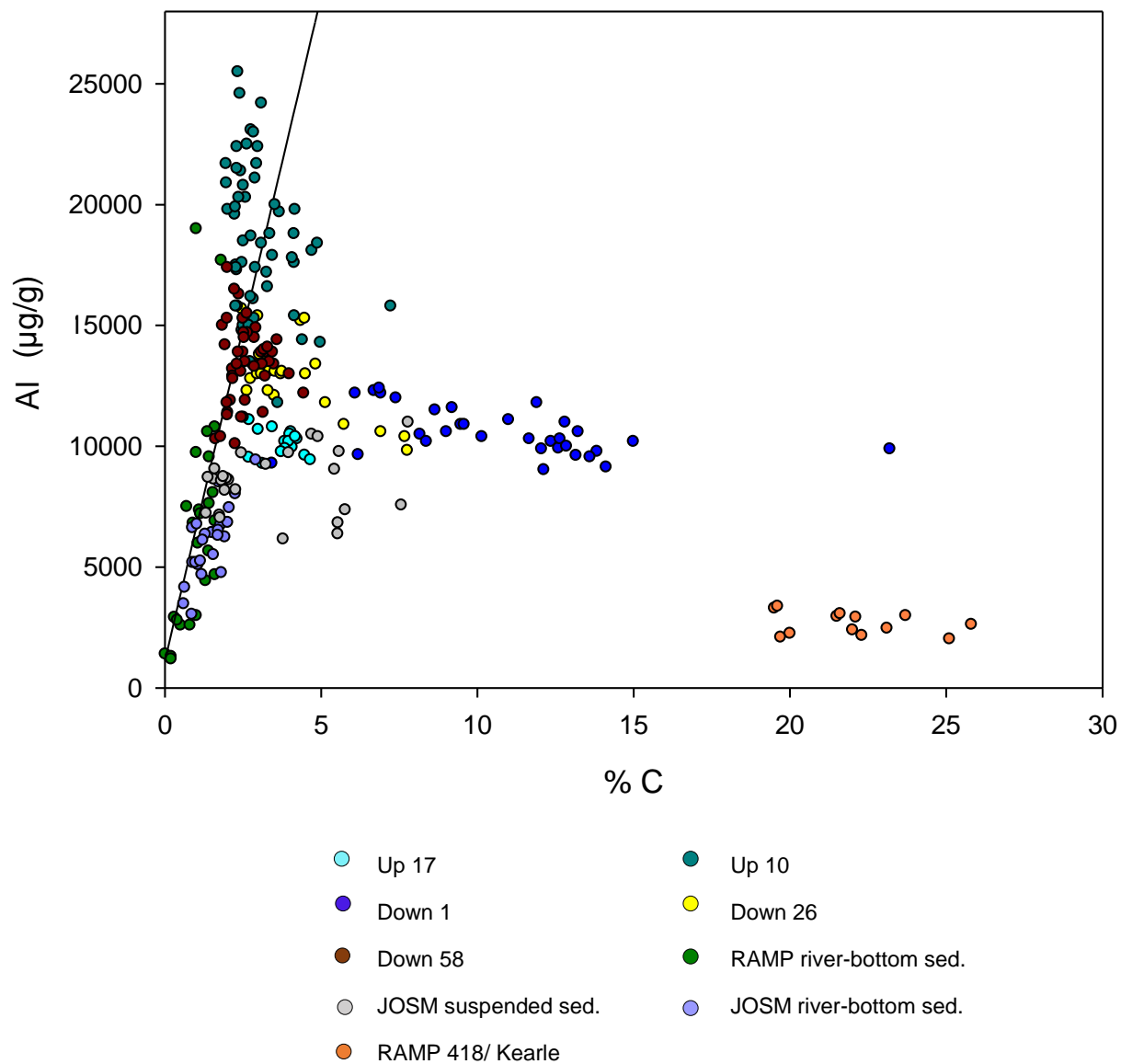


Figure B6. Pre-1967 concentrations of aluminum plotted with organic carbon content from floodplain lakes Up 17 (light blue), Up 10 (green), Down 1 (dark blue), Down 26 (yellow), post-1967 sediment from Down 58 (brown), headwater lake RAMP 418/ Kearle, and RAMP/JOSM river samples (RAMP river-bottom sediment (black), JOSM river-bottom sediment (white), and JOSM suspended sediment (grey)). The linear regression presented uses RAMP & JOSM river-bottom samples to establish the “river end member” for the lithogenic metal of interest (Al) compared to organic carbon (autochthonous, lake-generated organic matter end member).

Appendix C – Compiled metals data

Table C1. Raw values of aluminum (Al), nickel (Ni), and vanadium (V) presented in µg/g by depth and CRS-derived year at lake Up 17. Normalized values of Ni and V are presented as ratios to Al.

Depth (cm)	CRS year	Al (µg/g)	Ni (µg/g)	V (µg/g)	Ni/Al	V/Al
1	2016	5490	18.7	18.1	0.0034	0.0033
2	2016	8390	21.9	26.5	0.0026	0.0032
3	2015	8620	22	26.9	0.0026	0.0031
4	2014	10800	25	32.6	0.0023	0.0030
5	2013	11600	26.8	33.4	0.0023	0.0029
6	2012	11600	26.3	32.6	0.0023	0.0028
7	2010	11600	28.3	33.8	0.0024	0.0029
8	2009	11700	30.1	35	0.0026	0.0030
9	2007	10500	31.3	32.7	0.0030	0.0031
10	2005	10200	29.9	30.7	0.0029	0.0030
11	2003	8430	28.3	28	0.0034	0.0033
12	2001	7950	26.3	26.2	0.0033	0.0033
13	1999	8430	25.9	27.9	0.0031	0.0033
14	1997	8400	26.5	28.1	0.0032	0.0033
15	1994	9590	26.8	30.8	0.0028	0.0032
16	1992	10400	28.7	31.5	0.0028	0.0030
17	1990	9140	26.3	30.5	0.0029	0.0033
18	1987	8590	25.9	29.8	0.0030	0.0035
19	1986	8150	25.1	29.7	0.0031	0.0036
20	1984	8490	25.4	31.2	0.0030	0.0037
21	1981	7420	22.8	27.4	0.0031	0.0037
22	1979	8780	27.6	31.4	0.0031	0.0036
23	1977	10700	26.2	34.2	0.0024	0.0032
24	1975	10300	27.3	37.7	0.0027	0.0037
25	1972	9640	25.9	34.6	0.0027	0.0036
26	1970	10600	27.2	37.2	0.0026	0.0035
27	1966	10300	28.2	35.6	0.0027	0.0035
28	1963	10600	30.5	35.4	0.0029	0.0033
29	1960	10500	27.9	33.6	0.0027	0.0032
30	1957	10300	26.6	33.1	0.0026	0.0032
31	1955	9630	28.7	31.4	0.0030	0.0033
32	1951	9960	26.6	31.8	0.0027	0.0032
33	1948	9440	26.9	30.4	0.0028	0.0032
34	1946	10800	30.2	33.3	0.0028	0.0031
35	1944	10700	26.9	32.4	0.0025	0.0030
36	1939	9540	25.8	30	0.0027	0.0031
37	1928	9290	25.3	29.7	0.0027	0.0032
38	1923	11100	27.1	32.3	0.0024	0.0029
39	1918	10200	26.5	31.6	0.0026	0.0031
40	1914	10200	26.5	33	0.0026	0.0032
41	1910	10400	25.7	32.3	0.0025	0.0031
42	1905	9910	25.7	32.4	0.0026	0.0033
43	1901	9770	26.1	31.3	0.0027	0.0032

Table C2. Raw values of aluminum (Al), nickel (Ni), and vanadium (V) presented in $\mu\text{g/g}$ by depth and CRS-derived year at lake Up 10. Normalized values of Ni and V are presented as ratios to Al.

Depth (cm)	CRS year	Al ($\mu\text{g/g}$)	Ni ($\mu\text{g/g}$)	V ($\mu\text{g/g}$)	Ni/Al	V/Al
1	2016	7460	21.8	32.4	0.0029	0.0043
2	2013	16100	29	52.7	0.0018	0.0033
3	2010	10900	24.4	43.1	0.0022	0.0040
4	2005	13900	28.5	48.6	0.0021	0.0035
5	1996	13600	28.3	56.6	0.0021	0.0042
6	1990	18700	39.4	74.1	0.0021	0.0040
7	1983	18800	39	74.4	0.0021	0.0040
8	1974	22000	42.1	86.8	0.0019	0.0039
9	1963	17600	31.1	65.1	0.0018	0.0037
10	1950	18100	31.8	59.3	0.0018	0.0033
11	1940	23100	39.6	66.1	0.0017	0.0029
12	1928	15800	29.7	49.8	0.0019	0.0032
13	1911	17300	32.1	48.9	0.0019	0.0028
14	1885	19700	34.1	54.7	0.0017	0.0028
15	1867	21700	36	59.3	0.0017	0.0027
16	1850	22500	34.7	58.7	0.0015	0.0026
17	1832	22400	36.3	56.4	0.0016	0.0025
18	1818	14800	31.3	49.8	0.0021	0.0034
19	1805	15400	33.9	46.3	0.0022	0.0030
20	1779	15000	30.5	40.2	0.0020	0.0027
21	1760	16100	30.9	46.8	0.0019	0.0029
22	1739	16200	30.5	43.7	0.0019	0.0027
23	1721	17400	33.2	49.3	0.0019	0.0028
24	1705	24200	45.2	66	0.0019	0.0027
25	1687	25500	47.1	67.1	0.0018	0.0026
26	1669	20300	38.6	52.6	0.0019	0.0026
27	1651	23000	44.8	64.4	0.0019	0.0028
28	1632	24600	47.9	66.8	0.0019	0.0027
29	1610	21700	41	54.6	0.0019	0.0025
30	1592	17500	34.7	46.9	0.0020	0.0027
31	1575	15300	31.6	42.8	0.0021	0.0028
32	1557	17200	34	49	0.0020	0.0028
33	1534	13500	29	39.9	0.0021	0.0030
34	1508	11800	27.3	36.4	0.0023	0.0031
35	1492	14400	30.5	43.3	0.0021	0.0030
36	1479	14300	31.2	41.3	0.0022	0.0029
37	1468	18400	40.2	52.4	0.0022	0.0028
38	1452	17900	37.5	48.3	0.0021	0.0027
39	1432	17600	35.6	48.1	0.0020	0.0027
40	1410	17400	37.5	48	0.0022	0.0028
41	1390	20900	42.4	55.2	0.0020	0.0026
42	1368	19600	39.8	50.9	0.0020	0.0026
43	1348	19800	39.6	49.4	0.0020	0.0025
44	1329	18500	39	50.2	0.0021	0.0027
45	1311	16600	32.4	48	0.0020	0.0029
46	1294	21100	41.5	56.7	0.0020	0.0027

47	1275	18700	36	50.6	0.0019	0.0027
48	1257	18400	33.8	50.3	0.0018	0.0027
49	1241	18800	35.9	51.9	0.0019	0.0028
50	1221	18800	34.7	53.1	0.0018	0.0028
51	1204	20000	34.9	55.5	0.0017	0.0028
52	1186	22400	38.8	61.3	0.0017	0.0027
53	1165	20800	36.7	57.2	0.0018	0.0028
54	1141	19900	35.3	53.2	0.0018	0.0027
55	1117	20300	35.4	56	0.0017	0.0028
56	1093	21400	38.7	59.3	0.0018	0.0028
57	1072	15800	30.8	43.1	0.0019	0.0027
58	1047	21500	41.3	57.3	0.0019	0.0027
59	1022	15800	32.4	42.8	0.0021	0.0027
60	1001	15000	27.4	36.9	0.0018	0.0025
61	978	19800	35.5	51.5	0.0018	0.0026
62	967	17800	34	49.4	0.0019	0.0028

Table C3. Raw values of aluminum (Al), nickel (Ni), and vanadium (V) presented in $\mu\text{g/g}$ by depth and CRS-derived year at lake Down 1. Normalized values of Ni and V are presented as ratios to Al.

Depth (cm)	CRS year	Al ($\mu\text{g/g}$)	Ni ($\mu\text{g/g}$)	V ($\mu\text{g/g}$)	Ni/Al	V/Al
1	2015	6170	23.5	38.9	0.0038	0.0063
2	2014	6740	22.8	41.5	0.0034	0.0062
3	2014	5960	22.9	40.1	0.0038	0.0067
4	2012	5830	23.1	42	0.0040	0.0072
5	2011	6560	23.8	44.4	0.0036	0.0068
6	2009	6740	25	45.6	0.0037	0.0068
7	2008	6870	25.5	43.2	0.0037	0.0063
8	2006	7600	25.7	48.6	0.0034	0.0064
9	2003	6340	24.6	44.4	0.0039	0.0070
10	2001	7200	26.1	47.2	0.0036	0.0066
11	1998	7860	25.7	48.1	0.0033	0.0061
12	1996	8850	27.5	52.7	0.0031	0.0060
13	1992	8350	27.2	50.2	0.0033	0.0060
14	1988	8960	28.1	52.9	0.0031	0.0059
15	1985	8610	26.7	46.3	0.0031	0.0054
16	1983	10300	26.6	41.2	0.0026	0.0040
17	1983	10600	25	37.4	0.0024	0.0035
18	1981	10200	25.3	35.7	0.0025	0.0035
19	1980	11100	26	37.6	0.0023	0.0034
20	1976	10900	26.3	37.5	0.0024	0.0034
21	1973	11200	26.4	36.6	0.0024	0.0033
22	1969	11200	27.4	36.6	0.0024	0.0033
23	1961	10900	26.1	34.9	0.0024	0.0032
24	1955	9140	24.2	31.7	0.0026	0.0035
25	1951	10400	26	34.2	0.0025	0.0033
26	1945	10900	26.5	36.3	0.0024	0.0033
27	1937	10600	25.2	33.2	0.0024	0.0031
28	1932	12200	25.8	38.1	0.0021	0.0031

29	1931	9300	21.8	31.4	0.0023	0.0034
30	1929	9650	22.3	30.2	0.0023	0.0031
31	1923	12000	26.1	36.3	0.0022	0.0030
32	1920	12300	25.9	38.4	0.0021	0.0031
33	1918	12200	26.2	38	0.0021	0.0031
34	1916	12400	26.4	37.8	0.0021	0.0030
35	1913	9890	23.3	32.8	0.0024	0.0033
36	1905	12200	29.2	41.4	0.0024	0.0034
37	1891	10600	29.7	38.1	0.0028	0.0036
38	1887	9790	28.2	37	0.0029	0.0038
39	1879	10200	27.4	38	0.0027	0.0037
40	1876	11500	27.3	40.2	0.0024	0.0035
41	1872	9560	25.4	36.3	0.0027	0.0038
42	1869	11100	28.6	37.8	0.0026	0.0034
43	1865	10300	25.5	36.5	0.0025	0.0035
44	1862	9620	27.3	36.3	0.0028	0.0038
45	1859	9920	26	37.2	0.0026	0.0038
46	1855	10300	25.9	37.6	0.0025	0.0037
47	1851	11000	26.3	37.4	0.0024	0.0034
48	1848	10000	25.6	35.5	0.0026	0.0036
49	1844	10200	26.8	34.7	0.0026	0.0034
50	1840	9890	25.5	32	0.0026	0.0032
51	1836	11800	27	38.4	0.0023	0.0033
52	1831	11600	27.1	38.3	0.0023	0.0033
53	1824	10500	24.1	34.3	0.0023	0.0033
54	1816	10200	24.2	33.9	0.0024	0.0033

Table C4. Raw values of aluminum (Al), nickel (Ni), and vanadium (V) presented in $\mu\text{g/g}$ by depth and CRS-derived year at lake Down 26. Normalized values of Ni and V are presented as ratios to Al.

Depth (cm)	CRS year	Al ($\mu\text{g/g}$)	Ni ($\mu\text{g/g}$)	V ($\mu\text{g/g}$)	Ni/Al	V/Al
1	2018	4310	12.5	14.7	0.0029	0.0034
2	2017	2470	8.82	10	0.0036	0.0040
3	2016	4770	13.5	16	0.0028	0.0034
4	2014	11300	22.7	32.5	0.0020	0.0029
5	2012	12700	24.1	35.2	0.0019	0.0028
6	2010	12600	25	36.1	0.0020	0.0029
7	2007	12500	24.6	34.9	0.0020	0.0028
8	2004	13000	25.8	37.4	0.0020	0.0029
9	2001	12400	25.9	35.3	0.0021	0.0028
10	1998	12400	26.2	35.3	0.0021	0.0028
11	1994	13200	26.8	36.5	0.0020	0.0028
12	1990	13700	28	37.9	0.0020	0.0028
13	1986	14100	28.7	40.7	0.0020	0.0029
14	1982	15000	29.1	40.7	0.0019	0.0027
15	1976	15000	30	40.8	0.0020	0.0027
16	1969	13400	28.5	37.5	0.0021	0.0028
17	1963	15400	31.3	40.5	0.0020	0.0026
18	1956	14800	28	38.2	0.0019	0.0026
19	1949	15700	30	41.2	0.0019	0.0026
20	1943	12800	29.4	37.7	0.0023	0.0029
21	1937	12300	25.5	35.3	0.0021	0.0029
22	1931	12100	25.3	34.8	0.0021	0.0029
23	1926	13400	25.3	37.5	0.0019	0.0028
24	1922	11800	22.9	33.8	0.0019	0.0029
25	1917	10900	22.8	31.5	0.0021	0.0029
26	1913	10400	21.2	29.7	0.0020	0.0029
27	1909	9830	20.2	28.3	0.0021	0.0029
28	1904	10600	22.5	32.7	0.0021	0.0031
29	1899	13000	24.3	37	0.0019	0.0028
30	1892	13100	24.3	35.9	0.0019	0.0027
31	1885	13000	26.1	36.8	0.0020	0.0028
32	1878	13000	26.5	37.8	0.0020	0.0029
33	1871	13700	26	39.1	0.0019	0.0029
34	1865	13800	26.7	39	0.0019	0.0028
35	1858	13400	25.3	38.8	0.0019	0.0029
36	1852	13100	26.2	38.9	0.0020	0.0030
37	1846	13400	26.4	39.8	0.0020	0.0030
38	1841	13000	27.1	38.8	0.0021	0.0030
39	1834	12300	28.3	37.6	0.0023	0.0031
40	1828	13100	27.4	39.2	0.0021	0.0030
41	1823	15200	30.3	44.4	0.0020	0.0029
42	1817	15300	31.4	46.4	0.0021	0.0030

Table C5. Raw values of aluminum (Al), nickel (Ni), and vanadium (V) presented in $\mu\text{g/g}$ by depth at lake Down 58. Normalized values of Ni and V are presented as ratios to Al.

Depth (cm)	Al ($\mu\text{g/g}$)	Ni ($\mu\text{g/g}$)	V ($\mu\text{g/g}$)	Ni/Al	V/Al
1	13400	23.9	38.4	0.0018	0.0029
2	14900	24.9	40.1	0.0017	0.0027
3	14500	24.9	40.2	0.0017	0.0028
4	15300	27.4	40.8	0.0018	0.0027
5	14200	25.8	38	0.0018	0.0027
6	15500	27.7	41.6	0.0018	0.0027
7	14400	24.3	39.2	0.0017	0.0027
8	13000	24.1	36.9	0.0019	0.0028
9	12900	24.3	36.5	0.0019	0.0028
10	13500	24.3	37	0.0018	0.0027
11	14700	27	41.4	0.0018	0.0028
12	13900	24.9	38.9	0.0018	0.0028
13	13900	24.4	39.2	0.0018	0.0028
14	13400	25.6	37.8	0.0019	0.0028
15	13900	26.5	38.3	0.0019	0.0028
16	13200	27.1	37.3	0.0021	0.0028
17	11400	23.7	33.3	0.0021	0.0029
18	11900	24.8	35.5	0.0021	0.0030
19	12900	23.8	36.2	0.0018	0.0028
20	13900	25	40	0.0018	0.0029
21	13900	25.7	37.6	0.0018	0.0027
22	14000	25.6	40.1	0.0018	0.0029
23	13500	25.3	38.4	0.0019	0.0028
24	12800	26.9	38.9	0.0021	0.0030
25	11200	24.5	35	0.0022	0.0031
26	13100	24.2	36.4	0.0018	0.0028
27	13400	24.5	37.3	0.0018	0.0028
28	14700	25.1	40.7	0.0017	0.0028
29	14100	25.4	40.8	0.0018	0.0029
30	16300	28.8	43.4	0.0018	0.0027
31	15000	28	40.6	0.0019	0.0027
32	10300	22.9	30.4	0.0022	0.0030
33	11800	24.1	33.9	0.0020	0.0029
34	12200	23.8	36.8	0.0020	0.0030
35	14500	26.9	39.3	0.0019	0.0027
36	16500	30.1	43.6	0.0018	0.0026
37	17400	32.5	47.4	0.0019	0.0027
38	15300	29.8	40.7	0.0019	0.0027
39	13300	26.9	39.6	0.0020	0.0030
40	11900	26.3	35.6	0.0022	0.0030
41	11200	24.5	33.9	0.0022	0.0030
42	11400	25.5	35.2	0.0022	0.0031
43	10100	22.5	33.6	0.0022	0.0033
44	11300	22.7	34.1	0.0020	0.0030
45	10400	21.1	31.6	0.0020	0.0030

Table C6. Raw values of aluminum (Al), nickel (Ni), and vanadium (V) presented in µg/g for river-bottom sediment data from RAMP and JOSM.

Agency	Site	Date	Al (µg/g)	V (µg/g)	Ni (µg/g)
RAMP	ATR-FR-W	2002-09-13	5660	16.5	20
RAMP	ATR-FR-E	2002-09-13	2990	9.4	10.6
RAMP	ATR-DC-E	2002-09-07	2760	17.3	10.2
RAMP	ATR-DC-W	2002-09-07	1400	5.1	4.8
RAMP	ATR-UFM	2002-09-07	6910	18.3	19.6
RAMP	ATR-MR-W	2002-09-06	17700	42.1	32.6
RAMP	ATR-MR-E	2002-09-06	9740	26.6	23.1
RAMP	ATR-SR-E	2002-09-06	9020	29.7	27.2
RAMP	ATR-SR-W	2002-09-06	7360	29.2	24.6
RAMP	ATR-DD-W	2002-09-05	6820	17.8	14.4
RAMP	ATR-FC-E	2002-09-05	10800	24.9	16.9
RAMP	ATR-DD-E	2002-09-05	4720	16.3	10.2
RAMP	ATR-FC-W	2002-09-05	19000	36.7	23.8
RAMP	ATR-DC-W	2001-11-02	2600	10	8
RAMP	ATR-DC-E	2001-11-02	1300	5	5
RAMP	ATR-SR-W	2001-11-01	18600	48	22
RAMP	ATR-MR-E	2001-11-01	1200	4	4
RAMP	ATR-SR-E	2001-11-01	7500	17	11
RAMP	ATR-MR-W	2001-11-01	2800	9	7
RAMP	ATR-FC-E	2001-10-14	7200	23	14
RAMP	ATR-FC-W	2001-10-14	10600	28	17
RAMP	ATR-MR-W	2000-10-04	4440	19.1	12.6
RAMP	ATR-MR-E	2000-10-04	4680	28.8	19.4
RAMP	ATR-FC-W	2000-10-03	1850	8.9	7.9
RAMP	ATR-FC-E	2000-10-03	3440	15.9	12.9
RAMP	ATR-DC-W	2000-10-02	2920	12.1	10.7
RAMP	ATR-SR-W	2000-10-02	5160	30.4	20.2
RAMP	ATR-SR-E	2000-10-02	2600	11.4	8.8
RAMP	ATR-DC-E	2000-10-02	3920	17.6	23.9
RAMP	ATR-FC-E-D	1998-09-17	7630	20	14
RAMP	ATR-FC-W-D	1998-09-17	9440	22	20
RAMP	ATR-MR-E-D	1998-09-16	10900	28	19
RAMP	ATR-DC-W	1998-09-16	5990	18	14
RAMP	ATR-MR-W-D	1998-09-16	9560	24	17
RAMP	ATR-DC-E	1998-09-16	8080	22	13
RAMP	ATR-FC-CC-D	1997-10-10	8160	19	21
RAMP	ATR-DC-CC	1997-10-06	10700	28	16
JOSM	M3 SAND	2012-09-18	2390	11.6	7.3
JOSM	M3 GRAVEL	2012-09-18	3730	13.3	10.3
JOSM	M3B GRAVEL	2012-09-24	4450	14.6	12.7
JOSM	M3B SAND	2012-09-24	934	4.1	4.5
JOSM	M4 GRAVEL	2012-09-20	2740	10.4	8.9
JOSM	M4 SAND	2012-09-20	4290	15	16.9
JOSM	M6 SAND	2012-09-21	688	4.7	3.4
JOSM	M6 GRAVEL	2012-09-21	3510	12.9	11.3
JOSM	M7 GRAVEL	2012-09-22	6730	20.1	19.4

JOSM	M7 SAND	2012-09-22	3400	12	10.3
JOSM	M7C SAND	2012-09-22	1800	7.9	7
JOSM	M7C GRAVEL	2012-09-23	3030	10.7	23.8
JOSM	M8 GRAVEL	2012-09-25	6630	19.2	18
JOSM	M8 SAND	2012-09-25	9430	27.4	24.8
JOSM	M3 GRAVEL	2013-09-18	4110	13.6	10.2
JOSM	M3 SAND	2013-09-18	2280	8.2	8
JOSM	M3B GRAVEL	2013-09-17	4160	14.4	11.9
JOSM	M3B SAND	2013-09-17	5510	16.2	16.6
JOSM	M4 SAND	2013-09-19	4770	14.6	14.8
JOSM	M4 GRAVEL	2013-09-19	6430	19.9	17.6
JOSM	M6 GRAVEL	2013-09-22	6360	18.1	18.2
JOSM	M6 SAND	2013-09-22	4690	12.9	13.8
JOSM	M7 GRAVEL	2013-09-21	4000	12.5	11.9
JOSM	M7 SAND	2013-09-21	6850	18.2	20.1
JOSM	M7C GRAVEL	2013-09-23	6520	19.3	18.2
JOSM	M7C SAND	2013-09-23	4260	13	13.6
JOSM	M8 GRAVEL	2013-09-21	6110	16.9	17.5
JOSM	M8 SAND	2013-09-21	5100	14.6	15.5
JOSM	M3 GRAVEL	2014-09-21	2160	9.5	6.2
JOSM	M3 GRAVEL	2014-09-21	3480	12.7	9.4
JOSM	M9 GRAVEL	2014-09-21	2820	11.3	7.6
JOSM	M3 GRAVEL	2014-09-21	5400	14.6	16
JOSM	M3B GRAVEL	2014-09-21	6250	19.5	16.5
JOSM	M3B SAND	2014-09-21	1570	6.3	5.7
JOSM	M4 GRAVEL	2014-09-14	5190	16	15.1
JOSM	M4 GRAVEL	2014-09-26	3050	11	9.4
JOSM	M4 SAND	2014-09-26	7460	21.1	22.6
JOSM	M6 GRAVEL	2014-09-24	6310	19.2	17.6
JOSM	M6 SAND	2014-09-24	8030	21.4	21.6
JOSM	M7 GRAVEL	2014-09-23	4330	14.3	12.9
JOSM	M7 SAND	2014-09-23	5190	16.9	15.3
JOSM	M7C GRAVEL	2014-09-22	5250	16.8	16.3
JOSM	M7C SAND	2014-09-22	6520	21	23.1
JOSM	M8 GRAVEL	2014-09-20	6780	19.4	18.5
JOSM	M8 SAND	2014-09-20	8520	22.7	22.9

Table C7. Raw values of aluminum (Al), nickel (Ni), and vanadium (V) presented in µg/g for river suspended sediment data from JOSM.

Agency	Site	Date	Al (µg/g)	V (µg/g)	Ni (µg/g)
JOSM	M0	06-2012	7225	18.45	22.1
JOSM	M0	09-2012	7370	16	28.3
JOSM	M2	06-2012	8175	21.5	24.6
JOSM	M2	09-2012	6830	16.6	27.6
JOSM	M3	06-2012	7150	19.4	22.45
JOSM	M3	09-2012	6370	16	22.8
JOSM	M9	06-2012	7035	18.85	21.25
JOSM	M9	10-2012	6160	15.8	21
JOSM	M0	06-2013	8645	19.25	22.15
JOSM	M0	09-2013	10500	18.9	28.3
JOSM	M0	02-2014	9045	22.15	27.85
JOSM	M2	06-2013	8710	18.3	22
JOSM	M2	09-2013	11000	26.5	33.3
JOSM	M2	02-2014	10400	28.8	28.25
JOSM	M3	06-2013	9060	19.35	22.3
JOSM	M3	09-2013	7570	20.8	27.7
JOSM	M4	02-2014	9780	28.45	24.55
JOSM	M9	06-2013	8610	21.65	21.05
JOSM	M0	06-2014	9725	22	27.8
JOSM	M0	09-2014	9730	22	32.5
JOSM	M2	09-2014	8670	22.45	24.25
JOSM	M3	06-2014	8580	21.5	22.55
JOSM	M3	09-2014	8200	21.2	24.725
JOSM	M9	06-2014	8745	22.75	22.1
JOSM	M9	09-2014	9248	24.125	25.7

Table C8. Raw values of aluminum (Al), nickel (Ni), and vanadium (V) presented in µg/g for exposed river sediments collected during this study.

Site	Date	Al (µg/g)	V (µg/g)	Ni (µg/g)
AR* near Down 26	10-2016	11100	29.9	22
AR* near Up 17	10-2016	13400	31.6	24.7
AR* Downstream of Clearwater R.	07-2017	3600	12.2	9.01
Fort McMurray flood deposit sed.	07-2017	5580	18.2	15.4

*AR = Athabasca River

Table C9. Raw values of aluminum (Al), nickel (Ni), and vanadium (V) in $\mu\text{g/g}$ by depth and CRS-derived year (only pre-1967 values used in baseline creation shown) at JOSM lake NE13. Blank spaces indicate depths where metals were not measured. Data received from Colin Cooke.

Lake ID	Depth (cm)	Pre-67 Chronology	Al ($\mu\text{g/g}$)	V ($\mu\text{g/g}$)	Ni ($\mu\text{g/g}$)
NE13	11.5	1951	339	8.1	4.9
NE13	12	1946			
NE13	12.5	1942	318	8.5	5.2
NE13	13	1937			
NE13	13.5	1933	299	7.1	4.5
NE13	14	1928			
NE13	14.5	1923	281	4.8	4.2
NE13	15	1918			
NE13	15.5	1913	332	5.2	4.5
NE13	16	1908			
NE13	16.5	1903	255	3.4	3.2
NE13	17	1897			
NE13	17.5	1891	317	7.3	5
NE13	18	1886			
NE13	18.5	1880	253	6.2	4.4
NE13	19	1874			
NE13	19.5	1867	328	6.2	4.6
NE13	20	1861	311	6.8	4.9
NE13	21	1848			
NE13	22	1835			
NE13	23	1821			
NE13	24	1806			
NE13	25	1791	295	1.6	3.2
NE13	26	1775			
NE13	27	1759			
NE13	28	1743			
NE13	29	1725	234	0.65	2.8
NE13	30	1708			
NE13	31	1690			
NE13	32	1671			
NE13	33	1652			
NE13	34	1632	146	0.4	2

Table C10. Raw values of aluminum (Al), nickel (Ni), and vanadium (V) in $\mu\text{g/g}$ by depth and CRS-derived year (only pre-1967 values used in baseline creation shown) at JOSM lake NE20. Blank spaces indicate depths where metals were not measured. Data received from Colin Cooke.

Lake ID	Depth (cm)	Pre-67 Chronology	Al ($\mu\text{g/g}$)	V ($\mu\text{g/g}$)	Ni ($\mu\text{g/g}$)
NE20	15.5	1955	835	6.2	6.4
NE20	16	1953			
NE20	16.5	1951	848	5.5	6.7
NE20	17	1949			
NE20	17.5	1947	743	4.3	6.1
NE20	18	1945			
NE20	18.5	1943	808	4.6	7.4
NE20	19	1941			
NE20	19.5	1939			
NE20	20	1937	814	4.9	8.2
NE20	21	1933			
NE20	22	1928			
NE20	23	1924			
NE20	24	1919			
NE20	25	1915	832	4.2	7.7
NE20	26	1910			
NE20	27	1906			
NE20	28	1901			
NE20	29	1897	785	3.1	6.4
NE20	30	1892			
NE20	31	1887			
NE20	32	1882			
NE20	33	1877			
NE20	34	1872	727	3	6.1
NE20	35	1867			
NE20	36	1862			
NE20	37	1857			
NE20	38	1852			
NE20	39	1847	862	2.1	5.7

Table C11. Raw values of aluminum (Al), nickel (Ni), and vanadium (V) in $\mu\text{g/g}$ by depth and CRS-derived year (only pre-1967 values used in baseline creation shown) at JOSM lake RAMP 418/ Kearle. Blank spaces indicate depths where metals were not measured. Data received from Colin Cooke.

Lake ID	Depth (cm)	Pre-67 Chronology	Al ($\mu\text{g/g}$)	V ($\mu\text{g/g}$)	Ni ($\mu\text{g/g}$)
RAMP 418/Kearle	14.5	1943	2930	12.3	14.9
RAMP 418/Kearle	15	1939			
RAMP 418/Kearle	15.5	1934	2960	10.1	12.9
RAMP 418/Kearle	16	1930			
RAMP 418/Kearle	16.5	1926			
RAMP 418/Kearle	17	1921	3300	9.4	13
RAMP 418/Kearle	17.5	1916			
RAMP 418/Kearle	18	1912			
RAMP 418/Kearle	18.5	1907	2990	8	11.6
RAMP 418/Kearle	19	1902			
RAMP 418/Kearle	19.5	1897	3380	8.3	11.7
RAMP 418/Kearle	20	1892			
RAMP 418/Kearle	21	1882	3070	8.9	10.7
RAMP 418/Kearle	22	1872			
RAMP 418/Kearle	23	1861			
RAMP 418/Kearle	24	1850	2630	7.2	9.2
RAMP 418/Kearle	25	1839			
RAMP 418/Kearle	26	1827			
RAMP 418/Kearle	27	1816	2260	9.6	11.2
RAMP 418/Kearle	28	1804			
RAMP 418/Kearle	29	1792	2100	6	6.9
RAMP 418/Kearle	30	1780			
RAMP 418/Kearle	31	1768			
RAMP 418/Kearle	32	1756			
RAMP 418/Kearle	33	1743	2030	6.1	7
RAMP 418/Kearle	34	1731			
RAMP 418/Kearle	35	1719			
RAMP 418/Kearle	36	1706	2470	7.4	7.5
RAMP 418/Kearle	37	1694			
RAMP 418/Kearle	38	1681			
RAMP 418/Kearle	39	1669	2400	6.9	7.4

Appendix D – Chronology information (for developing age-depth models)

Table D1. Radioisotope values (²¹⁰Pb, ¹³⁷Cs, ²²⁶Ra in dpm/g) and CRS-inferred chronology for lake Up 17. Grey highlighted cells are extrapolated dates using the CRS model. (--) = no measurement taken; (ND) = below the detection limit and should be treated as 0.

Sediment core top depth (cm)	CRS chronology	CRS Error ± 2 sigma	²¹⁰ Pb dpm/g	²¹⁰ Pb error (1 std. dev.) dpm/g	¹³⁷ Cs dpm/g	¹³⁷ Cs error (1 std. dev.) dpm/g	²²⁶ Ra* dpm/g	²²⁶ Ra error (1 std. dev.) dpm/g
0	2016.50	0.16	6.3095	1.2327	0.3104	0.1882	1.9107	0.4660
1	2016.20	0.28	4.6195	1.0175	0.4856	0.1298	1.7793	0.3209
2	2015.32	0.42	5.6799	0.4862	0.4929	0.0661	1.8819	0.2407
4	2013.09	0.88	5.0883	0.4819	0.4633	0.0650	2.1882	0.2489
6	2010.26	1.38	5.9878	0.5397	0.1566	0.0750	2.3502	0.3096
8	2006.84	1.92	7.7947	0.5600	0.1549	0.0820	2.5471	0.3340
10	2003.36	2.54	8.2611	0.9809	0.0698	0.2180	2.0301	0.3865
12	1998.71	3.45	7.1947	0.5751	0.2355	0.0797	2.0611	0.2829
14	1994.04	4.48	5.6053	0.5795	0.2589	0.0814	1.8541	0.3072
16	1989.75	5.54	3.4968	0.4448	0.2855	0.0612	1.6950	0.2330
18	1986.00	6.51	2.8901	0.3902	0.2041	0.0549	1.8499	0.2109
20	1981.37	7.77	3.0728	0.3931	0.2108	0.0552	1.8771	0.2018
22	1976.73	9.06	3.0173	0.4040	0.2226	0.0561	2.0868	0.2261
24	1972.36	10.44	3.1736	0.4446	0.4615	0.0625	2.1021	0.2667
26	1966.46	12.51	3.2715	0.4144	1.1431	0.0627	2.2298	0.2423
28	1959.63	14.94	3.1185	0.3668	2.3770	0.0652	2.3866	0.2500
30	1954.57	17.11	2.8196	0.3343	1.6088	0.0529	2.2386	0.2311
32	1948.21	19.71	2.8427	0.3760	1.0892	0.0564	2.3065	0.2403
34	1944.15	20.26	2.5353	0.3529	0.3675	0.0495	2.3324	0.2386
36	1927.63	27.97	2.7292	0.3155	ND	ND	1.8941	0.1930
38	1918.38	--	2.5056	0.3362	ND	ND	2.3161	0.2263
40	1909.83	--	2.0914	0.3419	ND	ND	2.0502	0.2432
42	1900.58	--	2.3796	0.3427	ND	ND	1.9004	0.1922

*²²⁶Ra = weighted mean of ²¹⁴Bi and ²¹⁴Pb

Table D2. Radioisotope values (^{210}Pb , ^{137}Cs , ^{226}Ra in dpm/g) and CRS-inferred chronology for lake Up 10. Grey highlighted cells are extrapolated dates using the CRS model. (--) = no measurement taken; (ND) = below the detection limit and should be treated as 0.

Sediment core top depth (cm)	CRS chronology	CRS Error ± 2 sigma	^{210}Pb dpm/g	^{210}Pb error (1 std. dev.) dpm/g	^{137}Cs dpm/g	^{137}Cs error (1 std. dev.) dpm/g	$^{226}\text{Ra}^*$ dpm/g	^{226}Ra error (1 std. dev.) dpm/g
0	2015.72	0.50	16.7288	1.1745	0.2568	0.1271	5.0332	0.6165
1	2013.22	1.11	10.6011	1.0028	0.0100	0.0329	4.6124	0.5352
2	2010.01	1.64	10.1991	0.8401	0.1425	0.0886	3.8841	0.3885
3	2005.14	2.48	14.1155	1.2735	0.0462	0.0906	4.3345	0.5331
4	1995.97	4.25	10.1307	0.7076	0.2860	0.0793	2.7641	0.3323
5	1990.22	5.58	8.3982	0.6933	0.4377	0.0848	3.9585	0.4054
6	1982.70	7.57	6.8161	0.5845	0.5129	0.0726	3.3980	0.3104
7	1973.86	10.45	5.3673	0.4442	0.7466	0.0592	2.6887	0.2239
8	1962.86	14.82	5.0042	0.4194	1.2270	0.0611	3.0032	0.2559
9	1949.81	21.74	4.7618	0.4023	1.8727	0.0634	3.1440	0.2594
10	1940.13	25.54	3.7551	0.3650	0.6806	0.0496	3.1228	0.2800
11	1928.11	31.27	3.8823	0.3905	0.0982	0.0437	3.2280	0.2559
12	1910.85	--	2.7863	0.3523	0.0452	0.0349	2.3845	0.2306
13	1885.12	--	2.9934	0.3764	0.0346	0.0352	3.1274	0.2466
14	1866.87	--	2.8880	0.3459	ND	ND	2.8529	0.2410
16	1832.50	--	3.1451	0.4014	ND	ND	3.5410	0.3001
18	1805.06	--	2.9475	0.3835	ND	ND	2.4876	0.2246
20	1759.60	--	2.9060	0.3511	ND	ND	2.6468	0.2032

* ^{226}Ra = weighted mean of ^{214}Bi and ^{214}Pb

Table D3. Radioisotope values (^{210}Pb , ^{137}Cs , ^{226}Ra in dpm/g) and CRS-inferred chronology for lake Down 1. Grey highlighted cells are extrapolated dates using the CRS model. (--) = no measurement taken; (ND) = below the detection limit and should be treated as 0.

Sediment core top depth (cm)	CRS chronology	CRS Error \pm 2 sigma	^{210}Pb dpm/g	^{210}Pb error (1 std. dev.) dpm/g	^{137}Cs dpm/g	^{137}Cs error (1 std. dev.) dpm/g	$^{226}\text{Ra}^*$ dpm/g	^{226}Ra error (1 std. dev.) dpm/g
0	2015.093	0.16195	7.70508	0.671049	1.04700	0.093979	1.54702	0.35138
1	2014.427	0.25890	9.23562	0.684137	1.04953	0.094137	1.67917	0.317527
2	2013.559	0.38590	8.12270	0.503178	1.01518	0.071548	1.70241	0.29588
4	2010.776	0.92220	8.90909	0.795308	1.13032	0.113887	2.02139	0.43906
6	2007.716	1.42050	7.41149	0.415308	1.15030	0.061073	1.54629	0.204988
8	2003.325	2.20790	7.51882	0.46483	1.35828	0.069499	1.84616	0.258486
10	1998.15	3.27824	7.94900	0.499078	1.55803	0.075532	1.52207	0.240002
12	1991.975	4.79936	7.13162	0.450641	1.53417	0.068816	1.87323	0.249207
14	1985.326	6.78008	5.82380	0.416644	1.57179	0.066854	1.91458	0.258428
16	1982.641	7.67993	2.63243	0.322248	1.18678	0.050241	1.78041	0.208004
18	1979.659	8.75053	2.99326	0.305857	1.29265	0.047732	1.76607	0.205164
20	1972.718	10.9771	3.01570	0.315882	1.83791	0.053739	2.34584	0.248333
22	1960.527	15.7462	3.29311	0.354234	0.86721	0.050664	2.15298	0.263178
24	1951.166	20.8478	2.72947	0.314193	0.25000	0.039906	1.8921	0.205468
26	1936.726	32.1645	2.8273	0.312914	0.16161	0.040836	1.92443	0.224256
28	1931.178	36.2619	1.87157	0.261929	ND	0.035768	1.99580	0.21185
30	1922.858	42.8582	2.44717	0.323548	ND	0.042708	2.12096	0.230698
32	1917.807	43.5988	1.94628	0.276473	ND	0.022526	1.86711	0.206888
34	1912.752	41.8847	2.20217	0.415102	0.22721	0.052404	2.04820	0.23907
36	1890.885	14.5848	2.43824	0.369719	ND	0.116494	2.09137	0.282384
40	1872.258	--	2.10082	0.358699	ND	0.053478	2.09912	0.269616
44	1858.659	--	2.20189	0.34472	ND	0.035708	1.8232	0.247613
48	1844.189	--	1.69173	0.300447	ND	0.033711	1.94252	0.216895
52	1823.669	--	2.00968	0.297729	ND	0.034163	--	--

* ^{226}Ra = weighted mean of ^{214}Bi and ^{214}Pb

Table D4. Radioisotope values (²¹⁰Pb, ¹³⁷Cs, ²²⁶Ra in dpm/g) and CRS-inferred chronology for lake Down 26. Grey highlighted cells are extrapolated dates using the CRS model. (--) = no measurement taken; (ND) = below the detection limit and should be treated as 0.

Sediment core top depth (cm)	¹³⁷ Cs chronology	Error 1 std. dev.	²¹⁰ Pb dpm/g	²¹⁰ Pb error (1 std. dev.) dpm/g	¹³⁷ Cs dpm/g	¹³⁷ Cs error (1 std. dev.) dpm/g	²²⁶ Ra* dpm/g	²²⁶ Ra error (1 std. dev.) dpm/g
0	2017.681	0.0163	9.4482	2.040914	0.0277	0.117141	3.1399	0.2969
1	2017.054	0.0833	8.8297	1.019024	0.2378	0.097759	1.6877	0.2760
2	2016.276	0.1666	6.2269	0.875248	0.0825	0.075252	2.2229	0.1385
4	2012.405	0.5809	4.0735	0.563051	0.1855	0.038866	2.5904	0.0953
6	2007.195	1.1383	3.3886	0.553148	0.2404	0.038397	2.6982	0.0594
8	2000.756	1.8273	2.6192	0.472477	0.2495	0.031846	2.4704	0.0268
10	1994.003	2.5498	2.7231	0.572047	0.1763	0.034548	2.8542	0.1455
12	1986.499	3.3527	2.7714	0.582597	0.2281	0.038093	2.9012	0.1408
14	1976.212	4.4535	2.1747	0.476213	0.2741	0.028792	2.6000	0.0693
16	1963	5.8671	2.4451	0.518256	0.3263	0.033804	2.6833	0.0890
18	1948.674	7.4000	2.0767	0.572821	0.0502	0.031676	3.0545	0.0815
22	1926.404	9.7829	1.8545	0.470878	0.0479	0.033804	2.0533	0.1111
26	1908.83	11.6633	2.0019	0.46639	-0.0324	0.042916	2.0369	0.0313
30	1885.362	14.1743	1.5281	0.508948	-0.0235	0.038382	2.5943	0.0629
34	1858.457	17.0532	2.3944	0.483765	-0.0201	0.03643	2.3945	0.0940
35	1851.578	17.7892	--	--	--	--	--	--
36	1846.44	18.3390	--	--	--	--	--	--
37	1840.507	18.9739	--	--	--	--	--	--
38	1834.49	19.6177	--	--	--	--	--	--
39	1828.399	20.2694	--	--	--	--	--	--
40	1823.201	20.8255	--	--	--	--	--	--
41	1817.126	21.4756	--	--	--	--	--	--

*²²⁶Ra = weighted mean of ²¹⁴Bi and ²¹⁴Pb

Table D5. Radioisotope values (^{210}Pb , ^{137}Cs , ^{226}Ra in dpm/g) and CRS-inferred chronology for lake Down 58. Grey highlighted cells are extrapolated dates using the CRS model. (--) = no measurement taken; (ND) = below the detection limit and should be treated as 0.

Sediment core top depth (cm)	^{210}Pb dpm/g	^{210}Pb error (1 std. dev.) dpm/g	^{137}Cs dpm/g	^{137}Cs error (1 std. dev.) dpm/g	$^{226}\text{Ra}^*$ dpm/g	^{226}Ra error (1 std. dev.) dpm/g
26	2.8884	0.3242	0.2254	0.0407	2.0665	0.1785
30	2.4054	0.3082	0.0727	0.0400	2.3459	0.1802
34	2.6184	0.3342	0.2443	0.0422	1.9567	0.1807
36	3.2180	0.3457	0.1404	0.0453	1.8910	0.1785
38	2.7394	0.3703	0.2198	0.0460	2.3542	0.1990
40	2.9248	0.3292	0.2133	0.0429	1.6983	0.1697
42	1.9933	0.2968	0.1612	0.0365	2.1368	0.1761
44	2.3570	0.2977	0.1396	0.0372	1.8631	0.1639

* ^{226}Ra = weighted mean of ^{214}Bi and ^{214}Pb

Table D6. Focus factors used to calculate adjusted excess flux for lakes Up 17, Up 10, and Down 1, following method by Muir *et al.*, 2009 (*Envir. Sci. & Tech.*).

Lake	Focus factor (\pm measured error)
Up 17	1.841 (0.125)
Up 10	0.505 (0.034)
Down 1	0.875 (0.060)

Appendix E – Statistical analyses

Table E1. AICc values, change in AIC values, and model weights of a model set formulated to test the hypothesis that a linear model for aluminum best predicts vanadium concentration in the floodplain lakes in the AOSR.

Model	K	AICc	Δ AICc	Model weights
V ~ Al	3	862.45	0.00	1
V ~ logAl	3	1137.88	275.43	0

Table E2. AICc values, change in AIC values, and model weights of a model set formulated to test the hypothesis that a linear model for aluminum best predicts nickel concentration in the floodplain lakes in the AOSR.

Model	K	AICc	Δ AICc	Model weights
Ni ~ Al	3	808.55	0.00	1
Ni ~ logAl	3	942.21	133.66	0

Table E3. Breakpoints for temporally determined enrichment factors for V and Ni calculated at Down 1 using R package ‘segmented’.

	Nickel		Vanadium	
	Breakpoint 1	Breakpoint 2	Breakpoint 1	Breakpoint 2
Predicted breakpoint	1980	1990	1980	1990
Model estimated breakpoint \pm S.E.	1982 \pm 1.08	1986 \pm 1.01	1982 \pm 0.326	1986 \pm 0.509
p-value	5.74 x 10 ⁻⁵		6.63 x 10 ⁻⁵	

Table E4. Slopes for the three-segmented breakpoint analysis on V and Ni EF data at Down 1. Multiple R² of 0.8172 (Ni) and 0.9727 (V), and adjusted R² of 0.7982 (Ni) and 0.9698 (V).

Slope	Nickel	Vanadium
Segment 1 \pm S.E.	-3.55x10 ⁻⁴ \pm 2.10x10 ⁻⁴	-3.90x10 ⁻⁴ \pm 2.22x10 ⁻⁴
Segment 2 \pm S.E.	9.03x10 ⁻² \pm 4.82x10 ⁻²	2.04x10 ⁻¹ \pm 3.37x10 ⁻²
Segment 3 \pm S.E.	2.30x10 ⁻² \pm 2.06x10 ⁻³	2.60x10 ⁻³ \pm 2.11x10 ⁻³

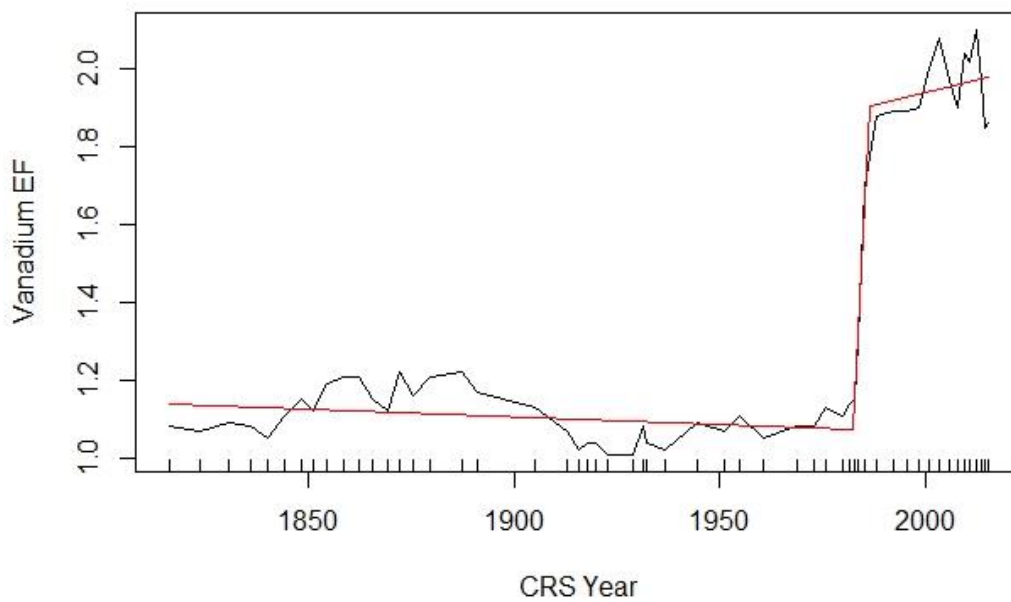


Figure E1. Three-segmented breakpoint model superimposed on a plot of the change in vanadium enrichment factor (EF) over time at lake Down 1.

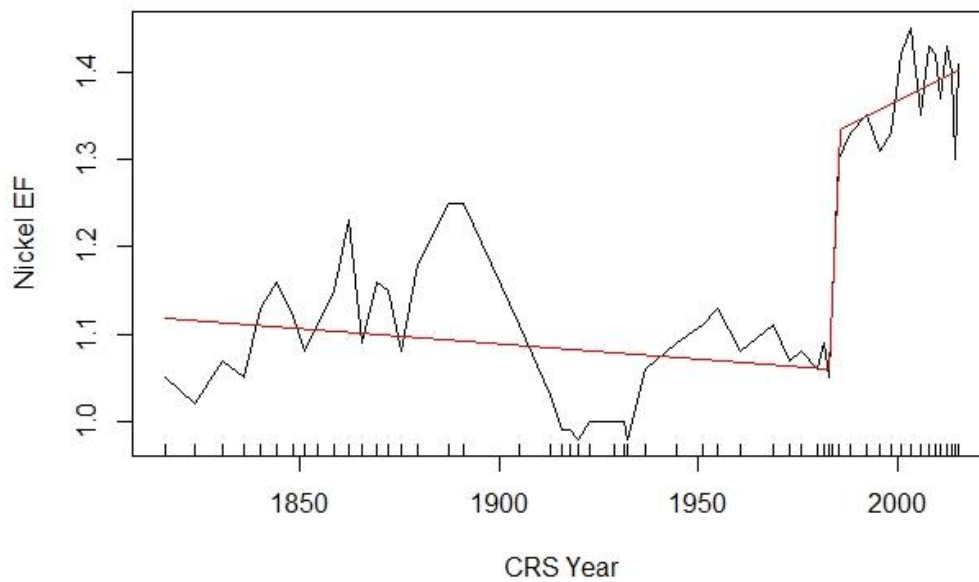


Figure E2. Three-segmented breakpoint model superimposed on a plot of the change in nickel enrichment factor (EF) over time at lake Down 1.